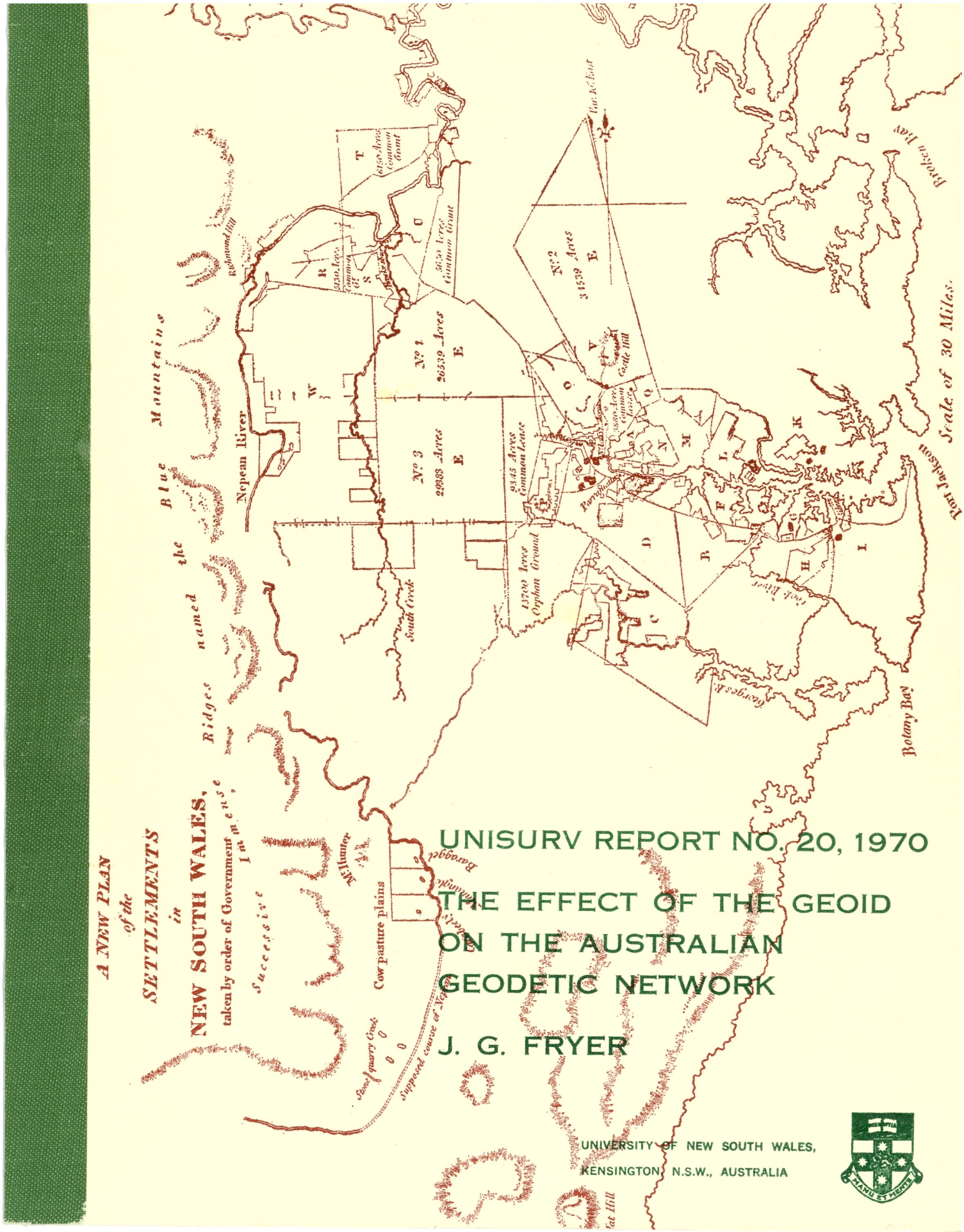

UNISURV REPORT NO. 20, 1970

THE EFFECT OF THE GEOID ON THE AUSTRALIAN GEODETIC NETWORK

J. G. FRYER

UNIVERSITY OF NEW SOUTH WALES,
KENSINGTON, N.S.W., AUSTRALIA

Reference to Districts.

A Northern Boundaries
B Liberty Plains
C Banks Town
D Parramatta
EEEE Ground reserved
for Govt. purposes
F Concord
G Petersham
H Bulanaming
I Sydney
K Hunters Hills
L Eastern Farms
M Field of Mars
N Ponds
O Toongabbey
P Prospect
Q
R Richmond Hill
S Green Hills
T Phillip
U Nelson
V Castle Hill
W Evan

The cover map is a reproduction in part of a map noted as follows:

London: Published by John Booth, Duke Street, Portland Place, July 20th, 1810

Reproduced here by courtesy of The Mitchell Library, Sydney

U N I S U R V R E P O R T NO. 20

THE EFFECT OF THE GEOID ON THE AUSTRALIAN GEODETIC NETWORK

J.G.Fryer

Received 7th July 1970

School of Surveying,
University of New South Wales,
P.O. Box 1,
Kensington, N.S.W. 2033
Australia

SUMMARY.

The relationship between the Australian Geodetic Datum and a geocentred reference spheroid of dimensions equal to those implied in Reference System 1967 is defined. The 1968 free air and the Fischer/Slutsky astro-geodetic geoid solutions for Australia are compared to produce a preliminary set of geocentric orientation parameters for the Johnston Origin of the Australian Geodetic Datum. Regions of low precision free air geoid values are delineated and, when excluded from computations, the meshing of the abovementioned geoid solutions reduces to ± 3 metres over 80% of the Australian continent.

Estimations of the indirect effect for the free air geoid are obtained on global and continental bases. A study of this effect in the Australian region with respect to the 1968 free air and astro-geodetic geoid solutions is presented. The results indicate that both the above solutions are too insensitive to detect any improvements arising from the incorporation of the indirect effect. The zero order terms relating to the complete definition of the geoid are examined in view of the global estimates of the indirect effect and the differential terrain correction. The adoption of geocentric orientation parameters for the purpose of referring control station co-ordinates to a geocentred reference spheroid is recommended.

The scale errors which arise from the neglect of the geoid spheroid separation vector in the reduction of measured distances to assumed spheroid level are investigated. The effects of scale errors on the misclosure of traverse loops and on baselines for satellite tracking purposes are formulated. These formulae are reviewed for a hypothetical case study on the Australian Geodetic Datum.

TABLE OF CONTENTS

Table of Contents (2)

Table of Contents (3)

GUIDE TO NOTATION

1. COMMONLY USED SYMBOLS.

a	Equatorial radius of reference spheroid.
a	Instrumental error of electronic distance measuring device (in cms).
A	Azimuth.
A_n	Representative of spherical harmonic coefficients.
b	Atmospheric uncertainty re electronic distance measuring (in p.p.m.).
dA, dS	Elements of surface area.
dm	Element of mass.
$d\sigma$	Element of surface area on a unit sphere.
ds	Length increment.
dz	Height increment.
e	Error estimate; where relevant, a standard deviation.
f	Flattening of the meridian ellipse.
h	Elevation.
h_d	Height anomaly.
h_n	Normal height.
h_o	Orthometric elevation.
h_s	Spheroidal elevation.
$\underline{i}, \underline{j}$	Unit vectors.
$\underline{i}$ $(i=1,3)$	Direction cosines.
k	Gravitational constant.
ℓ	Distance between adjacent control stations.

Guide to Notation (2)

m	Order of surface harmonic.
$\underline{m}$	Misclosure vector.
$M\{x\}$	Mean value of x.
n	Degree of surface harmonic.
$\underline{n}$	Normal vector to a curve.
N	Geoid Spheroid separation.
P	Computation or fixed point.
r	Distance of a general variable point from the computation point.
r_o	Radius of an inner zone around the computation point.
R, R_m	Radius of curvature in normal section of reference spheroid; where relevant, the mean radius of the earth.
s	Distance.
t, T	Scale error.
U	Potential on the reference system.
V_d	Disturbing potential.
W	Potential of the existent earth.
x_i $(i=1,3)$	A general rectangular cartesian co-ordinate system.
x, y	Rectangular two dimensional axes system.
z	Variable height.
α	Azimuth.
γ, γ_m	Normal gravity; where relevant, the mean value of normal gravity over the reference spheroid.
Δg	Gravity anomaly.
$\Delta\xi_o, \Delta\eta_o, \Delta N_o$	Geocentric orientation parameters at the origin of a geodetic datum.

Guide to Notation (3)

η, (ξ_2)	Prime vertical component of the deflection of the vertical.
λ	Longitude, positive east.
ξ, (ξ_1)	Meridian component of the deflection of the vertical.
π	3·1415926....
ρ	Density.
ρ	Radius of curvature on a spheroid in the meridian.
ν	Radius of curvature on a spheroid in the prime vertical.
ϕ	Latitude, positive north.
ϕ	Potential.
ψ	Angular distance on unit sphere.
$\underline{\nabla}$	$= \sum_{i=1}^{2} \frac{\partial}{\partial x_i} \underline{i}$

2. SUBSCRIPTS.

a	Astronomically determined values; astro-geodetic values.
c	Refers to differential terrain correction (Δg_c).
d	Disturbing value.
f	Refers to free air geoid, free air anomalies.
g	Gravimetric values.
G	Evaluation at geoid; referring to geodetic values.
i,in	Evaluation of an inner zone.
o	Referred to origin; evaluation outside inner zone.
p	Evaluation at the fixed point P.
S	Evaluation at spheroid.

Guide to Notation (4)

3. GENERAL ABBREVIATIONS.

A.G.D.	Australian Geodetic Datum.
A.N.S.	Australian National Spheroid.
I.A.G.	International Association of Geodesy.
p.p.m.	Parts per million.
R.S. 1967	Reference System 1967.

CHAPTER 1.

INTRODUCTION AND DEFINITIONS.

1.1 Introduction.

The basic problem in physical geodesy is the relating of a physical reality of unknown position to a reference system of assumed size, shape and location which unfortunately has no physical reality, being only a mathematical device onto which observations made on the existent earth are reduced. The most suitable reference system is an oblate spheroid if the physical reality to be mapped is the geoid. This has always been the problem in "classical geodesy", but in recent years this fundamental problem of physical geodesy may be solved by the adoption of the telluroid as the reference system and the earth's surface as the physical reality *(Moritz, 1965)*.

This thesis deals specifically with the geoid-spheroid case, although many of the methods employed and conclusions reached should have analogous counterparts in the telluroid-earth's surface system which for the sake of completeness has been defined in this Chapter. For the geoid-spheroid system, the discrepancies of the real equipotential surface from the spheroidal model are the variations which have to be mapped. These discrepancies are due to irregular variations of the equipotential surfaces of the earth's gravitational field arising from both local and regional mass anomalies. These undulations of the geoid cannot be readily evaluated. Calculation of a first approximation,

the free air geoid, are given and then the latter half of this work involves an estimation of the difference (so-called indirect effect) between the free air geoid and geoid itself on a global scale. Since all geodetic observations are made with respect to the local vertical (direction of "gravity" at that point), an obvious approach to the mapping of these physically real surfaces is to relate their irregularly changing verticals to the spheroidal normals of known direction on the reference system. The relationships between the local verticals and spheroidal normals are called the deflections of the vertical. These deflections of the vertical can be manipulated to produce geocentric orientation parameters for an arbitrarily oriented triangulation spheroid so that its earth space location can be defined with respect to the earth's centre of mass. The methods of obtaining these geocentric orientation parameters and the resultant effects on the geodetic control network are two areas of investigation that are dealt with in following Chapters.

1.2 Definitions.

To facilitate an understanding of the following Chapters, the definitions below are given. A consideration of figures (1.1), (1.2) and (1.3) may be of assistance;

Geop.

A geop is an equipotential surface of the actual earth's gravitational field. The curvature characteristics of a family of geops will tend to be irregular due to variations in the earth's density

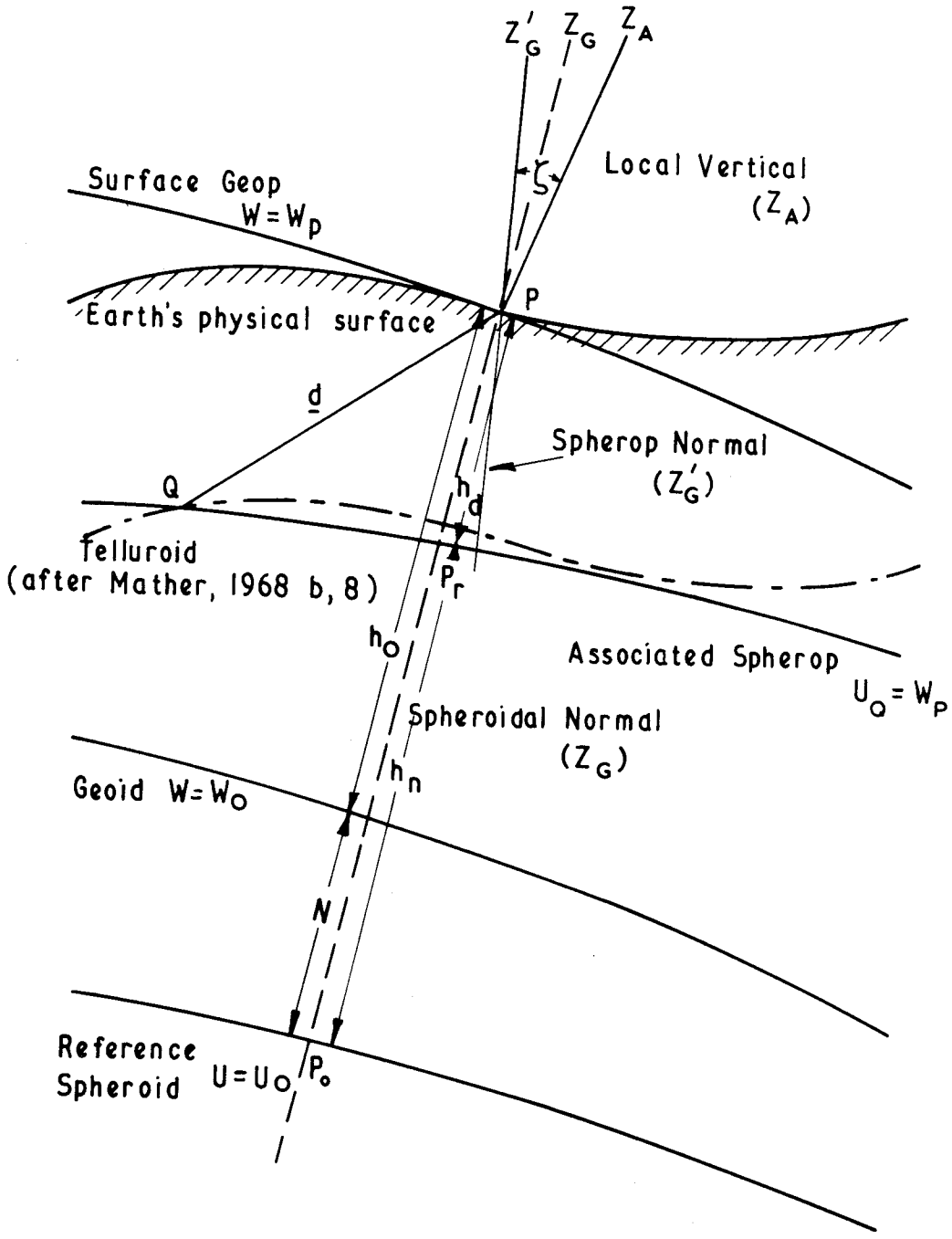
Z'_G
Z_G
Z_A
ζ
Local Vertical
(Z_A)
Surface Geop
$W = W_P$
P
Earth's physical surface
d
Spherop Normal
(Z'_G)
Q
h_d
Telluroid
(after Mather, 1968 b, 8)
P_r
h_o
Associated Spherop
$U_Q = W_P$
Spheroidal Normal
(Z_G)
h_n
Geoid $W = W_O$
N
Reference
Spheroid $U = U_O$
P_o

FIGURE 1.1

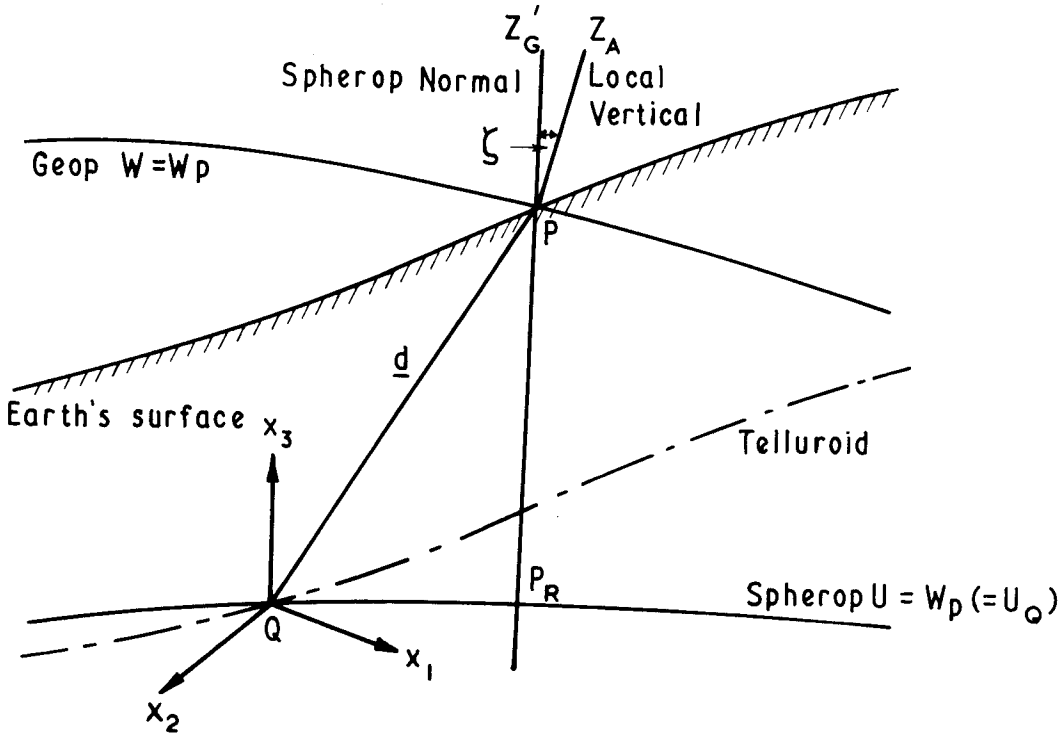

FIGURE 1.2

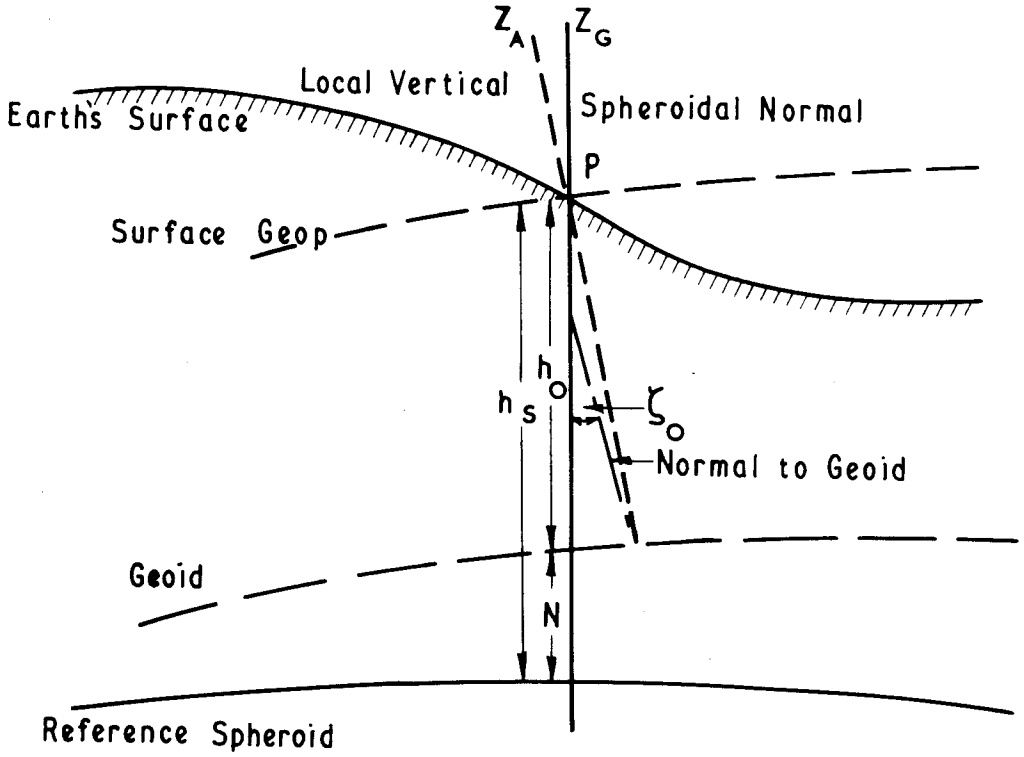

FIGURE 1.3

distribution. The geoid is probably the most important member of the family of geops.

Geoid.

The geoid can be readily defined over ocean areas as the free surface of the ocean if the latter were free from tidal, wind and wave motion effects. In fact it is this equipotential surface that is referred to as mean sea level and is used as a datum for elevations, although the "elevations" derived from ordinary levelling are not the required spheroidal heights h_s but orthometric heights h_o, figure (1.3). Unfortunately the geoid does not have a physical counterpart of the ocean over land areas and is in fact generally located below the land surface. Since the geoid is an equipotential surface it is quite susceptible to local and regional mass anomalies and thus its shape is dependent on the stratification of matter within the earth's crust.

Until recently, solutions for the geoid using Stokes' integral equation (equation (1.1)) required the removal or transfer of the topography exterior to the geoid so that the conditions of Stokes' integral could be satisfied. Such solutions are called regularised geoids, although in fact Stokes' integral only gives a solution for a co-geoid and correction terms (indirect effect) must be added to give the desired value of geoid spheroid separation N.

Recent advances in theory have enabled the solution for non-regularised geoids where such mathematical manoeuvres are unnecessary.

The most suitable gravity anomaly to be used in such solutions is the free air anomaly, the resultant geoid being called the free air geoid. Although the free air geoid is only a co-geoid, it is claimed to be the best direct approximation to the geoid obtainable and the only co-geoid of real geodetic importance *(Mather, 1968b, p.47)*.

Free air anomalies are the differences between observed gravity values, corrected for the elevation of the observation point, and the expected value of gravity (normal gravity) at that point. Using free air anomalies, the free air geoid spheroid separation value, N_f, is given by

$$N_f = \frac{R_m}{4\pi\gamma_m} \int_{\sigma=0}^{\sigma=4\pi} f(\psi)\ \Delta g_f\ d\sigma \qquad \ldots\ldots(1.1)$$

where R_m is the mean radius of the earth,

γ_m is the global mean value of normal gravity,

Δg_f is the free air anomaly representing the element of surface area $d\sigma$ on a unit sphere which is at an angular distance ψ from the computation point,

$f(\psi)$ is Stokes' function, conventionally represented as follows,

$$f(\psi) = \operatorname{cosec}\tfrac{1}{2}\psi + 1 - 5\cos\psi - 6\sin\tfrac{1}{2}\psi - 3\cos\psi \log\left(\sin\tfrac{1}{2}\psi\ (1+\sin\tfrac{1}{2}\psi)\right) \qquad \ldots\ldots(1.2)$$

The free air geoid described above assumes that no zero or first order terms exist in the solution. The first assumption is equivalent

to adopting a zero value for the global mean of the free air anomalies and the second implies the setting of the reference spheroid, on which normal gravity was calculated, at the centre of mass of the earth. If the former assumption is not satisfied, a more complete expression for the free air geoid *(ibid, p.25)* is,

$$N_f = \frac{W_o - U_o}{\gamma_m} - \frac{R_m\, M\{\Delta g_f\}}{\gamma_m} + \frac{R_m}{4\pi\gamma_m} \int_{\sigma=0}^{\sigma=4\pi} f(\psi)\ \Delta g_f\ d\sigma \qquad .....(1.3)$$

where W_o is the potential of the geoid and U_o that of the reference spheroid. $M\{\Delta g_f\}$ refers to the mean global free air anomaly value. The assumption of a zero value for the first term in equation (1.3) is equivalent to assigning the value of the potential on the reference spheroid to the geoid.

As ψ tends to zero, the surface integrals in the above equations become indeterminate. However the contribution N_{fi} of the innermost region (often called zone) can be evaluated by the expression *(Mather, 1968a, p.264)*,

$$N_{fi} = \frac{\Delta g_f}{\gamma_m}\, r_o \left(1 + \frac{r_o}{R_m}\right) \qquad .....(1.4)$$

where r_o is the radius of the inner zone assumed to be circular and Δg_f is the local free air anomaly.

Spherop.

A spherop is an equipotential surface of the earth's reference system (i.e. oblate spheroid). The curvature of a family of spherops

is more regular than the corresponding curvature of a family of geops. Spherops converge towards the poles such that the normals at the same parallel of latitude on different spherops have different orientations in space, giving rise to the so-called "curvature of the vertical" *(Bomford, 1962, p.410)*. This curvature is concave towards the axis of rotation and is taken into consideration when comparing astro-geodetic and gravimetric deflections of the vertical.

Reference Spheroids.

To define any reference spheroid in space, the definition of seven parameters is involved. These parameters can be subdivided into three groups, viz.,

(i) The size and shape of the spheroid, usually designated by a and f, the semi-major axis length and the flattening respectively;

(ii) The positioning of the origin of the reference system requires four parameters; a three dimensional rectangular cartesian system plus a fourth parameter to determine the direction of one of the axes of this cartesian system in space;

(iii) The seventh parameter relates the rotation axis to one of the reference system axes.

Ideally the reference axes system should be centred at the earth's centre of mass but this is not always the case in practice, as shall be seen later with the Australian Geodetic Datum. The other

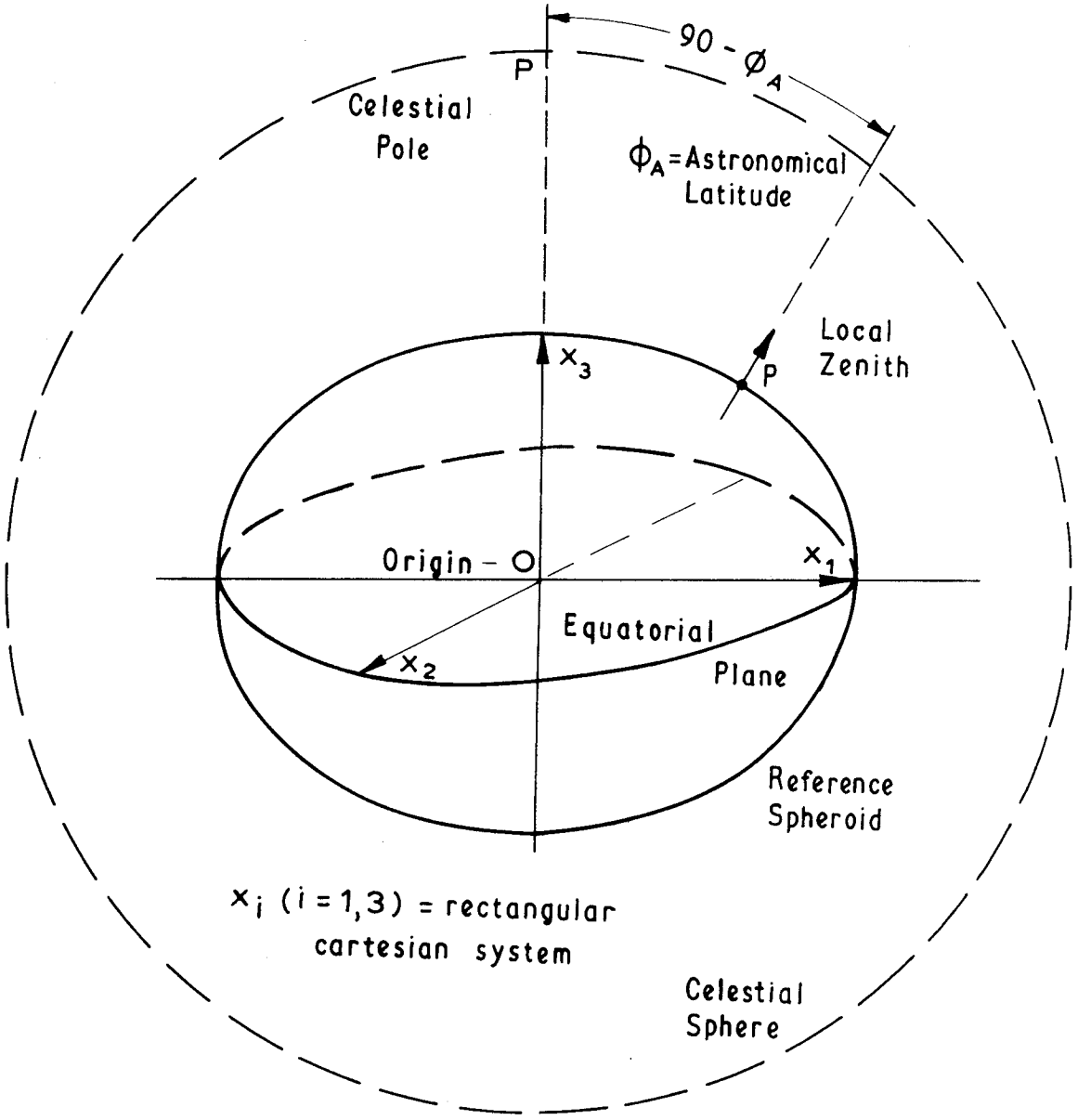
90 - Ø_A
P
Celestial
Pole
Φ_A = Astronomical
Latitude
Local
Zenith
P
x_3
Origin - O
x_1
Equatorial
Plane
x_2
Reference
Spheroid
x_i (i = 1,3) = rectangular
cartesian system
Celestial
Sphere

FIG. 1.4

requisites above are satisfied by the adoption of the celestial pole as being fixed in space. If the prolongation of the semi-minor axis is made to pass through it, then astronomical determinations of latitude at any point on the reference spheroid are given by the complement of the intercept on the great circle arc between the prolonged local zenith and the celestial pole. These relationships are displayed in figure (1.4).

Many different spheroids have been adopted throughout the world as reference systems for geodetic control networks and, in general, geodetic data obtained on these networks is not readily applicable to other datums because of differences in size, shape and orientation. An internationally respected system must be adopted so that large volumes of gravity anomaly data, etc., are available for use by geodesists and scientists everywhere without recourse to tedious correction formulae. The International Spheroid system fulfills this need and it has parameters,

$$a = 6{,}378{,}388 \text{ (= semi-major axis).}$$
$$f = 1/297.0 = 3.367 \times 10^{-3} \text{ (= flattening)} \qquad \ldots\ldots(1.5)$$

This spheroid was adopted by the International Association of Geodesy in Madrid in 1924 and it forms the basis of the International Gravity Formula. This international spheroid, by definition, possesses the following qualities;

(i) Same mass as the existent earth,

(ii) Common centre of mass with the existent earth,

(iii) The potential of its equipotential bounding surface is the same as the potential of the geoid,

(iv) There are no masses exterior to this bounding surface,

(v) Same rotational characteristics (potential) as the existent earth.

Complete lists of the numerical values of all quantities commonly used by geodesists (e.g. bounding potential U_o, equatorial gravity γ_e, etc.,) are readily obtainable *(e.g. Heiskanen and Moritz, 1967, p.79)*. These values and associated formulae have been used since 1930 but because the International Spheroid could no longer be considered the closest approximation of the earth by a spheroid, a revision has taken place and the new *(1967)* values are,

$$a = 6{,}378{,}160 \text{ metres}$$

$$f = 1/298.25$$

$$kM = 3.98603 \times 10^{20} \text{ cm.sec}^{-2} \qquad \ldots\ldots(1.6)$$

These values give rise to the 1967 International Gravity Formula which will eventually replace the former one. It is interesting to note that the values of a and f in equation (1.6) above are those presently used for the Australian Geodetic Datum and are those adopted by the International Astronomical Union at Hamburg in 1964 *(Fricke et al., 1965)*. A certain amount of conflict exists between the interests of geodesists and astronomers regarding the size and shape of the spheroid which best approximates the actual earth. The

astronomer constantly wants the best-fitting spheroid possible whereas the geodesist needs a *permanent* reference surface that is reasonably close to the best-fitting figure so that his large amount of numerical data does not have to continually undergo small corrective changes. Pleas for such a permanent reference figure are to be found in several references, notably *(Heiskanen and Moritz, 1967, p.111)* and *(Mather, 1968c, p.348)*.

Telluroid.

Considering figure (1.1) let the spheroid have potential $U = U_o$; let the geoid have potential $W = W_o$; let the geop passing through the point P on the physical surface have potential $W = W_p$, then the spherop with potential $U = W_p$ has the same potential on the reference system as the geop through P has on the real system.

If a point Q on the reference system is defined such that

$$\begin{aligned} U_Q &= W_p \\ \phi_Q &= \phi_{ap} \\ \lambda_Q &= \lambda_{ap} \end{aligned} \qquad \ldots\ldots(1.7)$$

where the suffix a refers to astronomic values, then the point Q is fixed without ambiguity if W_o is known since,

$$W_p = W_o - \Delta W \qquad \ldots\ldots(1.8)$$

and it may be assumed ΔW can be determined by levelling procedures.

If P_r is the point where the normal through P intersects the spherop through Q, then the locus of the points P_r is defined as the telluroid, *(Hirvonen, 1960, p.40)*. PP_r is called the height anomaly = h_d.

The above definition assumes, however, that W_o is known and is equal to U_o. W_p cannot be defined unless W_o is known. As this is unknown, U_o cannot be assigned a value either. Thus a more practical definition of the telluroid was suggested *(Mather, 1968b, p.8)*, and it is an adaptation of the "normal surface" *(Moritz, 1965, p.12)*. This new definition defines the points P_r (figure (1.1)) as those on the reference system having the same difference in potential with respect to U_o (i.e. with respect to the spheroid) as the difference in geopotential (ΔW) between P and the geoid. Thus a telluroid of complete definition would be the locus of the points Q defined by

$$\phi_Q = \phi_{ap}$$

$$\lambda_Q = \lambda_{ap}$$

$$U_Q - U_o = W_p - W_o \qquad \ldots\ldots(1.9)$$

Relationships between Surfaces.

To completely define the relationship between equivalent points on reference and irregular, physically real surfaces, the use of a three dimensional vector $\underline{d}$ (= PQ in figures (1.1), (1.2)) is most convenient. This vector is defined by three parameters; h_d, the separation between the surfaces, and ξ and η, the deflections of the vertical in the meridian and prime vertical directions

respectively. From a consideration of figure (1.2), it can be seen that the vector $\underline{d}$ can be represented by

$$\underline{d} = R\,\xi\,\underline{1} + R\,\eta\,\underline{2} + h_d\,\underline{3} \qquad \ldots\ldots(1.10)$$

where R is the mean radius of curvature of the spherop at Q (for practical purposes, it is assumed to be equal to the mean radius of the earth); $\underline{i}$, $(i = 1,3)$ are the direction cosines of a local three dimensional rectangular cartesian system with the x_3 axis coincident with the local spherop normal and the x_1 and x_2 axes in the horizontal plane, being oriented north and east respectively.

If the telluroid is adopted as the reference surface, the three parameters of the vector $\underline{d}$ are

(a) the height anomaly, h_d,

(b) the angle ζ between the surface vertical and the normal to the associated spherop resolved into the meridian and prime vertical directions (see figure (1.1)).

If the reference surface is the spheroid then the parameters are

(a) the geoid spheroid separation N,

(b) the angle ζ_o between the geoid and spheroid normals resolved into the meridian and prime vertical directions.

Clearly, ζ_o and ζ are not equal, their difference varying according to the topography, being larger in mountainous regions.

The use of the free air geoid is believed to provide close approximations to both angles *(Mather, 1968b, p.47)*. The results of comparisons between gravimetric deflections of the free air geoid for Australia and astro-geodetic deflections on the Australian Geodetic Datum (corrected for curvature of the vertical) should therefore be of interest to persons studying either system of reference.

CHAPTER 2.

DEFLECTIONS OF THE VERTICAL.

2.1 Astro-geodetic Deflections.

The astro-geodetic deflections of the vertical are the components in the meridian and prime vertical directions of the angle between the normal to the surface geop and the spheroidal normal. These astro-geodetic deflections, when based on a geocentred reference spheroid, vary by only a small amount from the gravimetric deflections of the vertical mentioned last Chapter.

Let the point P in figures (1.3), (2.1) and (2.2) represent a point on a geodetic control network which has geodetic co-ordinates ϕ_G, λ_G. Assuming astronomical observations have been performed at P, giving astronomical co-ordinates ϕ_A, λ_A, a consideration of the local vertical zenith Z_A, the spheroidal normal zenith Z_G and the celestial pole N gives the discrepancy ξ in astronomical latitude as,

$$\begin{aligned} \xi &= NZ_G - NZ_A \\ &= MZ_A \\ &= 90 - \phi_G - (90 - \phi_A) \\ &= \phi_A - \phi_G \end{aligned} \qquad \ldots\ldots(2.1)$$

If the local outward vertical is north of the spheroidal normal then ξ, known as the deflection of the vertical in the meridian direction, is considered positive.

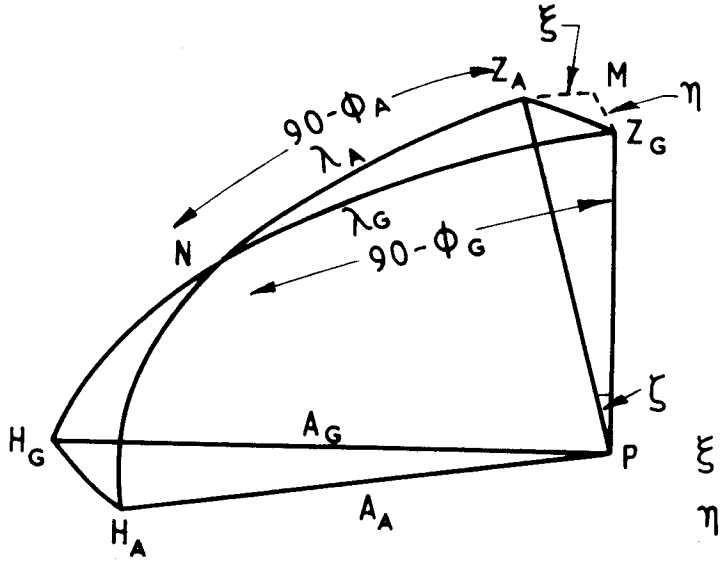

$\xi = \Phi_A - \Phi_G$

$\eta = (\lambda_A - \lambda_G)\cos\Phi$

FIG. 2.1

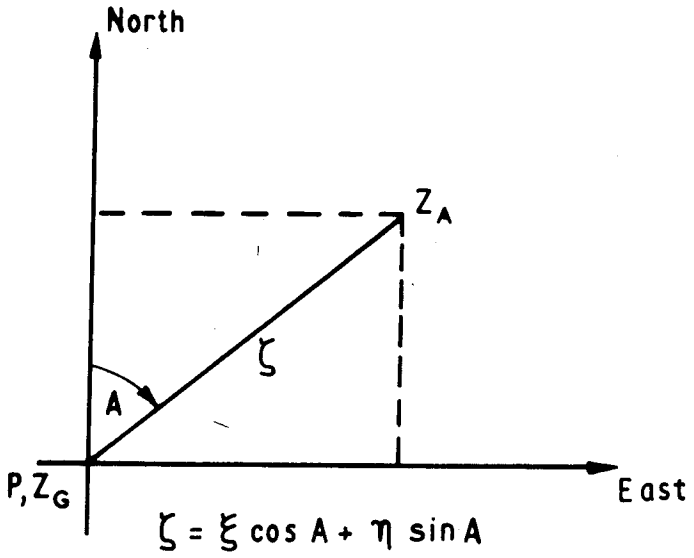

$\zeta = \xi \cos A + \eta \sin A$

FIG. 2.2

The discrepancy η in the prime vertical direction, from a consideration of figure (2.1) is given by,

$$\begin{aligned} \eta &= MZ_G \\ &= Z_A NZ_G \cos\phi \\ &= (\lambda_A - \lambda_G) \cos\phi \end{aligned} \qquad \ldots\ldots(2.2)$$

If the local outward vertical is east of the spheroidal normal then η, known as the deflection of the vertical in the prime vertical direction, is considered positive.

The angle $Z_A PZ_G$ (ζ) may be referred to the deflections of the vertical in the meridian and prime vertical directions by the following relationship,

$$\zeta = \xi \cos A + \eta \sin A \qquad \ldots\ldots(2.3)$$

where A is the azimuth (positive if clockwise from north) of the plane $Z_G PZ_A$ (see figure (2.2)).

It should be remembered that ϕ_G, λ_G are not absolute quantities and depend upon both the dimensions and orientation of the reference spheroid. This means that the astro-geodetic deflections of the vertical are also entirely dependent on the reference spheroid model and its orientation.

The presence of these deflections has virtually no effect on methods of horizontal angle measurement and the resulting geodetic control. Any point may be fixed uniquely in space using a three dimensional reference system such as spheroidal co-ordinates.

Latitude and longitude have been discussed briefly above and do not pose any difficulties once the reference spheroid has been defined. It is the third co-ordinate, elevation above the datum surface, that must be considered in some detail.

The required elevation is the length of the spheroidal normal (h_s, figure (1.3)) between the spheroid and the point in question. However, it is not possible to obtain this quantity directly in the field, the values obtained by the usual levelling process representing differences in orthometric height (h_o). From a consideration of figure (1.3), it can be seen that the spheroidal elevation h_s is given by,

$$h_s = h_o + N \qquad \ldots\ldots(2.4)$$

where N is the geoid spheroid separation. For the sake of completeness it can be seen from figure (1.1) that in the case of the telluroid system,

$$h_d + h_n = N + h_o \qquad \ldots\ldots(2.5)$$

where h_d is the height anomaly and h_n is termed the normal height. h_d is approximately equal to N, with any differences usually being less than one or two metres and arising from density variations. Thus to completely define a point on the earth's surface with respect to a reference surface, astronomical latitude and longitude, orthometric elevation, N, ξ and η need to be known. For the case of a geocentred reference spheroid N, ξ and η can be evaluated from global considerations of gravity anomalies. The establishment of comprehensive

gravity surveys on a world-wide basis is essential if all control datums are to become geocentred. Most land areas have some gravimetric surveys which provide a coverage of anomaly values over continents, but values for ocean areas, which constitute approximately 70% of the total surface area, are practically non-existent. The only available data over such areas is that afforded by satellite solutions which, while being the best available, are only generalised solutions which cannot detect the large positive and negative anomalies which occur in some small areas. The result is a series of smoothened anomaly mean values. The nature of these solutions is such that this cannot be avoided with the result that some uncertainty will exist in any gravimetric solution for N, ξ and η.

2.2 Astro-geodetic Levelling.

Astro-geodetic levelling is a means of mapping the geoid spheroid separation along a chain of geodetic control stations where astronomical determinations for latitude and longitude have been carried out. The process consists of determining successive values of N by utilising the astro-geodetic deflections of the vertical (ξ,η) at each control station after an initial value of N has been adopted. The spacing between the stations must be kept to a length such that any variations from an assumed linear rate of change of the deflection values will not be large enough to cause the values of N obtained to be significantly different from the actual changes in the geoid spheroid separation *(Bomford, 1962, p.321)*.

It is most unfortunate that in recent years many maps of geoidal undulations have been produced which fail to have at any control station (including the origin of the geodetic control network), a gravimetrically obtained geoid spheroid separation value. Instead, these maps have only an assumed value of N as datum for the calculations involved in their astro-geodetic geoid determination. The reference spheroids of these geodetic control networks are not geocentred, with the result that these geoid maps, while internally consistent, need to be corrected for their incorrect orientation before they can be combined together for the eventual production of a world-wide geoid map. Of course, each of the reference spheroids for the geodetic control networks must be of the same size and shape, although differences between them will be small and correction formulae are simple *(e.g. Mather, 1968a, pp.285 et.seq.)*.

Astro-geodetic geoidal variation maps possessing an arbitrary value of N at the origin do serve one very useful purpose. They allow the reduction of measured distances directly to the reference spheroid by the combination of the orthometric height with the value of astro-geodetically determined N in the reduction to spheroid level correction. This enables internal scale errors on the local geodetic network to be minimised (see Chapter 7).

The essentials of astro-geodetic levelling are displayed in figure (2.3), where, on adopting the sign convention of the previous Section for ζ, it can be seen that,

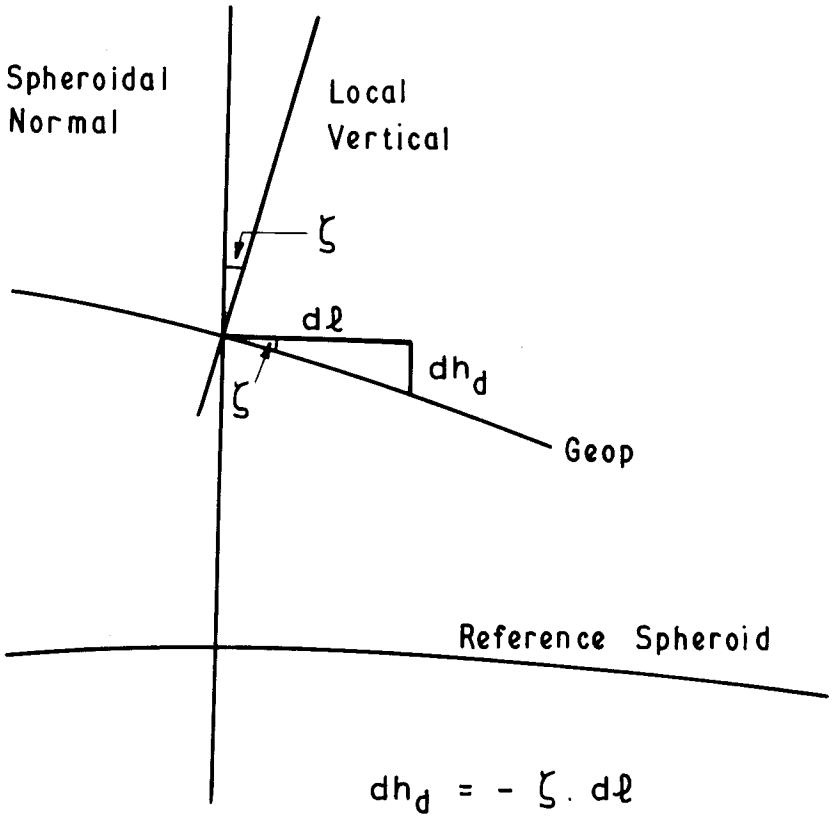
Spheroidal
Normal
Local
Vertical
ζ
dℓ
dh_d
ζ
Geop
Reference Spheroid
dh_d = - ζ . dℓ

FIGURE 2.3

$$dh_d = -\zeta \, d\ell \qquad \ldots\ldots(2.6)$$

where dh_d is the increment in surface separation over an increment in length $d\ell$.

Incorporating equation (2.3),

$$dh_{d_{i,i+1}} = -d\ell \, (\xi \cos A + \eta \sin A) \qquad \ldots\ldots(2.7)$$

where A is the azimuth of the line from the station (i) with a known surface separation h_{d_i} to the station (i+1) whose surface separation $h_{d_{i+1}}$ will be,

$$h_{d_{i+1}} = h_{d_i} + dh_{d_{i,i+1}} \qquad \ldots\ldots(2.8)$$

In equation (2.7), the values of ξ and η used in practice will be the average values of ξ and η at stations (i), (i + 1). The above formulae are only "working" formulae, since in the strictest sense the difference in separation should be the integral sum over the line, viz.,

$$dh_{d_{i,i+1}} = -\int_{i}^{i+1} \zeta \, d\ell \qquad \ldots\ldots(2.9)$$

If the stations (i), (i+1) are less than 50 km apart, it is generally considered that the use of formula (2.7) is valid since over such distances it is assumed that the rate of change of the deflections of the vertical is linear and thus the geoid shape can be faithfully reproduced. While this situation may be valid for flat topography, it would be difficult to set any value for the maximum

station spacing distance in mountainous regions as the deflections of the vertical are believed to change rapidly in these areas.

2.3 Gravimetric Deflections of the Vertical.

Surface deflections of the vertical in gravimetry are defined by the angle $Z_G P Z_A$ (figure (1.1)). This is the angle between the local vertical and the normal to the associated spherop and can be resolved into the meridian and prime vertical directions to give the desired deflection of the vertical components. The deflections of the vertical defined here are for the case of the telluroid-earth's surface system; those for the geoid-spheroid system being the components of the angle between the normal to the geoid and the spheroidal normal resolved as previously (see figure (1.3) and relevant discussion Section 1.2).

The gravimetric deflections of the vertical ξ_i, (i=1,2) may be written as,

$$\xi_i = \left(\frac{\partial h_d}{\partial x_i}\right)_{U=U_Q} , \quad i = 1,2 \qquad \ldots\ldots(2.10)$$

where ξ_1 is the deflection in the meridian; ξ_2 $(=\eta)$ is the deflection in the prime vertical; the x_1, x_2 axes are oriented north and east respectively and h_d refers to the height anomaly previously discussed (Sections 1.2, 2.1 and 2.2). Equation (2.10) states that the surface deflections of the vertical at any point are a function of the rate of change of the separation between the geop and the

associated spherop, and the differential is evaluated at the spherop where the potential on the reference system equals U_Q ($=W_p$) (figure (1.1)).

The purpose of this thesis is not to continue to develop fully the theory required to obtain an evaluation of ξ_i, (i=1,2) for the cases of the earth's surface-telluroid and the geoid-spheroid systems. If the reader is desirous of finding such theoretical developments they are referred to *(Mather, 1968b, pp.32 et.seq.)* and *(Mather, 1968a, pp.210 et.seq.)*, respectively. Since extensive use is made of gravimetric deflections of the vertical in later Chapters of this thesis, the formula used for their calculation is included and it may be expressed as follows,

$$\xi_i^{(sec)} = \frac{206265}{4\pi\gamma_m}\int_{\sigma=0}^{\sigma=4\pi} \frac{\partial(f(\psi))}{\partial\psi} \cos\alpha_i \, \Delta g_f \, d\sigma, \quad i = 1,2 \qquad \ldots\ldots(2.10a)$$

where $\xi_1 = \xi$; $\xi_2 = \eta$

$$\alpha_1 = A \; ; \quad \alpha_2 = \frac{\pi}{2} - A \qquad \ldots\ldots(2.10b)$$

and A is the azimuth from the computation point to the element of surface area $d\sigma$ whose mean free air anomaly is Δg_f. The above equation becomes indeterminate at $\psi = 0$ and in a manner analogous to equation (1.4) (the innermost zone contribution to N_f), the inner zone contributions (ξin_i, i=1,2) to ξ_i are given by Sollins' formula *(Sollins, 1947, p.282)*,

$$\xi_{in_i}^{(sec)} = -\frac{206265}{2\gamma_m} r_o \frac{\partial\Delta g_f}{\partial x_i}\left(1+\frac{3r_o}{4R_m}\right), \quad i=1,2 \qquad \ldots\ldots(2.10c)$$

where the x_1 and x_2 axes are oriented north and east respectively and r_o is the radius of the inner zone which is assumed to be circular.

A further discussion of the inner zone effect occurs in Chapter 4 where the results obtained from the use of the above formula for calculations over the Australian continental extent are reviewed.

2.4 Comparison of Astro-geodetic and Gravimetric Deflections of the Vertical.

Introduction.

In order to compare astro-geodetic and gravimetric deflections of the vertical, corrections must be applied for differences between the sizes, shapes and orientation conditions of the reference spheroids on which the two sets of data have been obtained. A small correction for curvature of the vertical must also be applied. Corrections for differences in the orientation conditions of the two reference spheroids will hereafter be referred to as geocentric orientation parameters, i.e. parameters which when applied to the origin of the geodetic control network will enable all co-ordinates on that network to be referred to the geocentred reference spheroid on which the gravimetric deflections of the vertical were calculated.

In the case of the Australian Geodetic Datum both the astro-geodetic and the gravimetric values of N, ξ and η have been calculated on a spheroid which is that one presently adopted by the I.A.G. as a basis for Reference System 1967. Thus only curvature of

the vertical and geocentric orientation parameters have to be applied in order to prepare the data for comparisons. The formulae relating to change of spheroid size has been quoted in this Section for the sake of completeness.

Curvature of the Vertical.

The curvature of a family of spherops and their resultant convergence towards the pole gives rise to the phenomenon of curvature of the spheroidal normal (usually referred to as curvature of the vertical). This convergence towards the pole means that at the same parallel of latitude on different spherops the normals have different orientations in space. Since astro-geodetic deflections are related to the normal at the spheroid and gravimetric deflections to the normal of the associated spherop, the angular difference between these two directions is the quantity that is termed the correction of curvature of the vertical. To determine the size of this correction consider figures (2.4) and (2.5) and let gravity at $X = \gamma$; gravity at $Y = \gamma - d\gamma$; difference in latitude $X - Y = d\phi$ and difference in potential between the reference spheroid and the associated spherop = dU, then,

$$dU = -\gamma h \quad \text{... at X normal}$$

$$= -(\gamma - d\gamma)(h + dh) \quad \text{... at Y normal}$$

$$\text{Thus } \gamma h = \gamma h - h\, d\gamma + \gamma\, dh - 0\{dh\, d\gamma\}$$

$$\text{i.e. } dh = \frac{h\, d\gamma}{\gamma} \qquad \text{.....(2.11)}$$

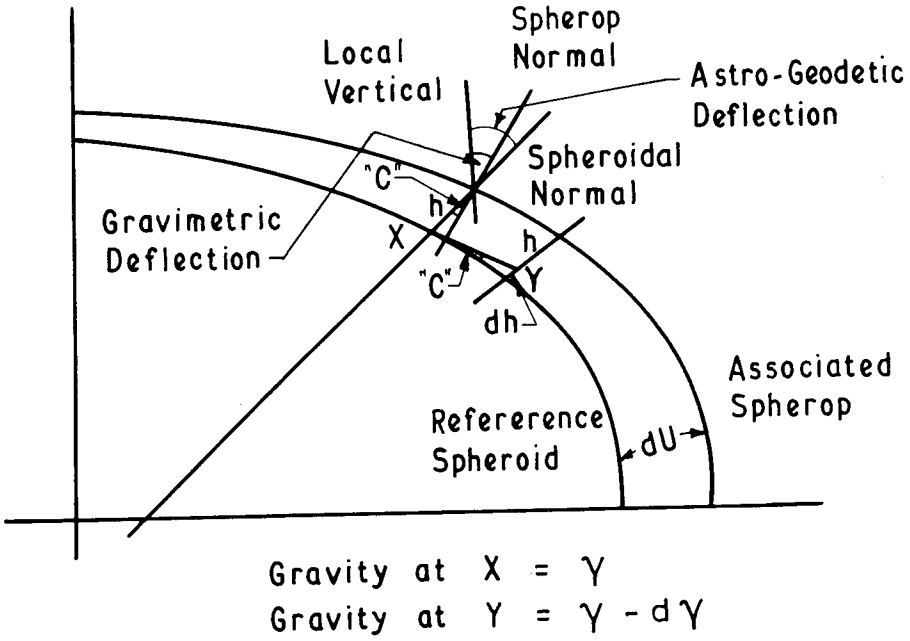

Gravity at X = γ

Gravity at Y = $\gamma - d\gamma$

FIG. 2.4

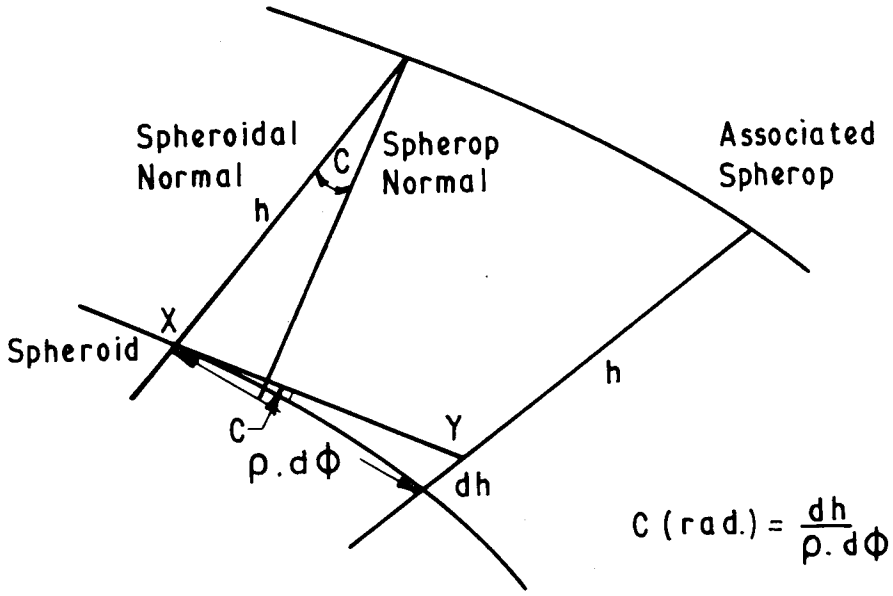

$$C\,(rad.) = \frac{dh}{\rho . d\Phi}$$

FIG. 2.5

where h is the length of the normal between the spheroid and the associated spherop at X and $(h + dh)$ the corresponding length at Y. From the well referenced formula for gravity at any point on the International Spheroid (the International Gravity Formula), a simple differentiation with respect to latitude gives,

$$d\gamma = \gamma_e \beta \sin 2\phi \, d\phi + 0\{\text{order } f^2\} \qquad .....(2.12)$$

Substitute equation (2.11) into equation (2.12) and,

$$dh = h \beta \sin 2\phi \, d\phi \qquad .....(2.13)$$

The correction angle (c) of figure (2.5) can be represented by,

$$c^{(\text{rad.})} = \frac{dh}{\rho \, d\phi} \qquad .....(2.14)$$

where ρ is the radius of curvature in the meridian. It should be noted that this correction only applies to the meridian direction and has no component in the prime vertical. By combining equations (2.13) and (2.14) and making the substitutions $\rho = 6371.2$ km (the mean value of earth radius), $\beta = 0.005288$ and the conversion of c from radians to seconds of arc, the correction is,

$$c^{(\text{sec})} = 0.00017 \, h \sin 2\phi \qquad .....(2.15)$$

where h (metres) is the height of a geodetic control station where a comparison is to be made of astro-geodetic and gravimetric meridian deflections. The sign of this correction is such that it must be subtracted from the astro-geodetic deflection ξ to make that deflection comparable with the gravimetric deflection of the vertical in the meridian.

Geocentric Orientation Parameters.

Suppose the difference in position between the centre of mass of the earth (the centre of the spheroid upon which gravimetric deflections are based) and the centre of the geodetic control spheroid (basis for astro-geodetic deflections) can be represented by a vector whose three linear components in the x_i (i=1,3) axes are dx_i (i=1,3). The values of dx_i can be expressed as changes $\Delta\xi, \Delta\eta$ and ΔN to the deflections of the vertical in the meridian and prime vertical directions and to the value of the geoid spheroid separation, respectively, at some convenient control station on the geodetic network.

Assuming that the x_i axes are orthogonal and the x_3 axis is oriented parallel to the rotational axis of the earth, let the x_1 axis be oriented such that it intersects the meridian through P_o (ϕ_o, λ_o), the origin of the geodetic control network, in the equatorial plane. At any point P (ϕ, λ) (see figure (2.6)) in the control network, the linear changes (dN,dE) in position in the north and east directions respectively, due to the above changes in the deflections of the vertical, conventionally signed as previously (Section 2.1), are given by,

$$dN = - \Delta\xi \, (\rho + h) \qquad \ldots\ldots (2.16)$$

$$dE = - \Delta\eta \, (\nu + h) \qquad \ldots\ldots (2.17)$$

where ρ and ν are the radii of curvature in the meridian and

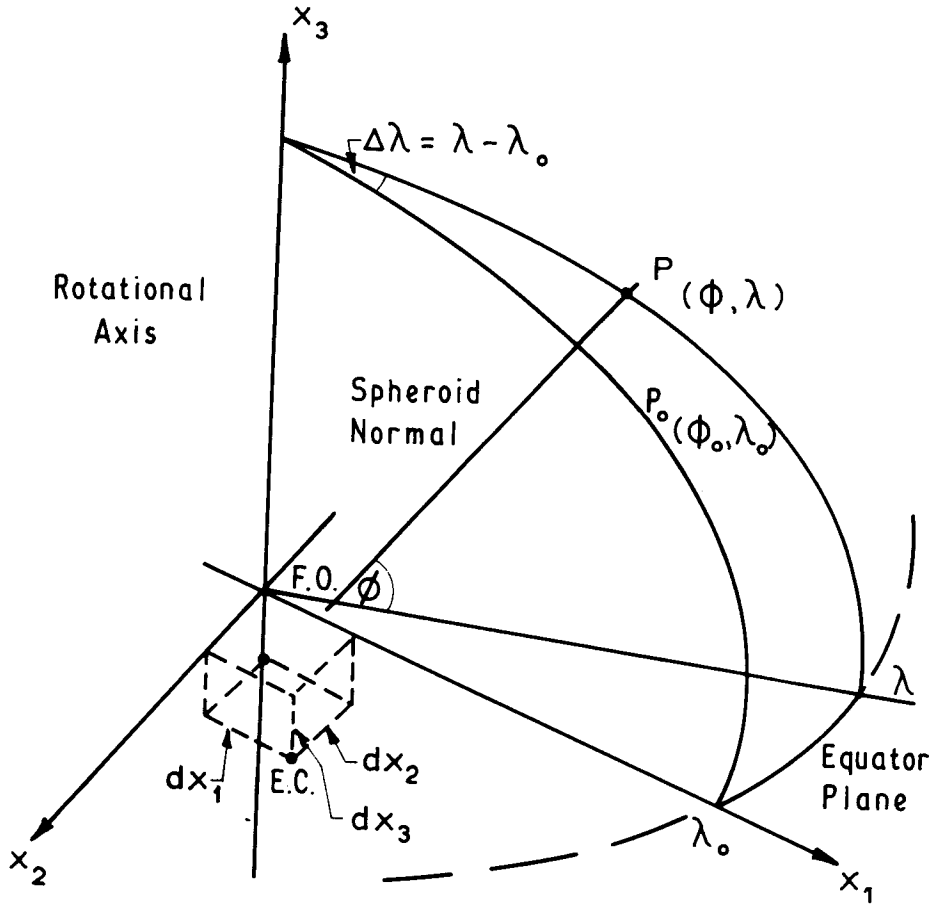

F.O. = False Origin
E.C. = Earth Centre
dx_i $(i = 1,3)$ = Orientation parameters

FIG. 2.6

prime vertical directions respectively and h is the height of the station P.

These changes are related to dx_i (i=1,3) by the following equations *(Vening meinesz, 1950, pp.33 et. seq.)*,

$$- \Delta\xi\ (\rho + h) = dx_3 \cos\phi - dx_1 \sin\phi \cos(\lambda-\lambda_o) + dx_2 \sin\phi \sin(\lambda-\lambda_o) \quad .....(2.18)$$

$$- \Delta\eta\ (\nu + h) = - dx_1 \sin(\lambda-\lambda_o) - dx_2 \cos(\lambda-\lambda_o) \quad .....(2.19)$$

$$\Delta N = dx_3 \sin\phi + dx_1 \cos\phi \cos(\lambda-\lambda_o) - dx_2 \cos\phi \sin(\lambda-\lambda_o) \quad .....(2.20)$$

Evaluating the above three equations at the origin of the geodetic control network and using the suffix $_o$ to indicate these terms,

$$- \Delta\xi_o\ (\rho_o+h_o) = dx_3 \cos\phi_o - dx_1 \sin\phi_o \quad .....(2.21)$$

$$- \Delta\eta_o\ (\nu_o+h_o) = - dx_2 \quad .....(2.22)$$

$$\Delta N_o = dx_3 \sin\phi_o + dx_1 \cos\phi_o \quad .....(2.23)$$

From these three equations, solutions for the dx_i (i=1,3) can be readily obtained as,

$$dx_1 = \Delta\xi_o\ (\rho_o+h_o) \sin\phi_o + \Delta N_o \cos\phi_o \quad .....(2.24)$$

$$dx_2 = \Delta\eta_o\ (\nu_o+h_o) \quad .....(2.25)$$

$$dx_3 = - \Delta\xi_o\ (\rho_o+h_o) \cos\phi_o + \Delta N_o \sin\phi_o \quad .....(2.26)$$

Substitution of the above values of dx_i (i=1,3) into equations (2.18) to (2.20) gives,

$$\begin{aligned} - \Delta\xi\ (\rho+h) = &- \Delta\xi_o\ (\rho_o+h_o)\ (\cos\phi_o \cos\phi + \sin\phi_o \sin\phi \cos\Delta\lambda) \\ &+ \Delta\eta_o\ (\nu_o+h_o) \sin\phi \sin\Delta\lambda \\ &+ \Delta N_o\ (\sin\phi_o \cos\phi - \cos\phi_o \sin\phi \cos\Delta\lambda) \end{aligned} \quad .....(2.27)$$

$$-\Delta\eta\ (\nu+h) = -\Delta\xi_o\ (\rho_o+h_o)\ \sin\phi_o\ \sin\Delta\lambda - \Delta\eta_o\ (\nu_o+h_o)\ \cos\Delta\lambda - \Delta N_o\ \cos\phi_o\ \sin\Delta\lambda \quad .....(2.28)$$

$$\Delta N = \Delta\xi_o\ (\rho_o+h_o)\ (-\sin\phi\ \cos\phi_o + \sin\phi_o\ \cos\phi\ \cos\Delta\lambda) - \Delta\eta_o\ (\nu_o+h_o)\ \cos\phi\ \sin\Delta\lambda + \Delta N_o\ (\sin\phi\ \sin\phi_o + \cos\phi_o\ \cos\phi\ \cos\Delta\lambda) \quad .....(2.29)$$

where $\Delta\lambda = \lambda - \lambda_o$. These three equations give the changes in the values of the deflections of the vertical and the value of N at any point in a geodetic control network for specific values of $\Delta\xi_o$, $\Delta\eta_o$ and ΔN_o at the origin. In the following Chapters of this thesis, this set of formulae is adapted for use as observation equations for a least squares solution to determine the geocentric orientation parameters ($\Delta\xi_o$,$\Delta\eta_o$ and ΔN_o) for the Johnston Origin of the Australian Geodetic Datum. The differences between astro-geodetic and free air geoid gravimetric values of ξ, η and N over Australia are used as the data source. Applying the observation equations to the values available at 540 Laplace stations in Australia 1620 equations possessing the three orientation unknowns are obtained. The time factor in the manufacture of data and the period of computation is a problem worthy of closer examination. Upon investigation, two facts emerge;

(1) The astro-geodetic values of N have been computed from the available astro-geodetic values of ξ and η using equation (2.7), and (2) The gravimetric values of ξ, η and N are interrelated

since in the calculation of N, Stokes' function $f(\psi)$ is used while the calculation of ξ and η involves the derivative of $f(\psi)$.

From the above observations, it is logical to assume a definite interconnection must exist between equations (2.27), (2.28) and (2.29). If this interconnection does exist, then it may be unnecessary to calculate geocentric orientation parameters using all three observation equations. The relationship between the three equations is obtained by utilising the definition of deflections given by equation (2.10),

$$\xi_i = - \left(\frac{\partial h_d}{\partial x_i}\right)_{U=U_Q} , \quad i = 1,2 \qquad .....(2.10)$$

Differentiation of equation (2.29) with respect to x_1 (north direction) gives,

$$\frac{d(\Delta N)}{dx_1} = \frac{\partial(\Delta N)}{\partial\phi} \frac{d\phi}{dx_1} \qquad .....(2.30)$$

$$= \frac{1}{(\rho+h)} \left(\Delta\xi_o \, (\rho_o+h_o) \, (-\cos\phi \, \cos\phi_o - \sin\phi_o \, \sin\phi \, \cos\Delta\lambda)\right.$$

$$+ \Delta\eta_o \, (\nu_o+h_o) \, \sin\phi \, \sin\Delta\lambda$$

$$\left. + \Delta N_o \, (\sin\phi_o \, \cos\phi - \cos\phi_o \, \sin\phi \, \cos\Delta\lambda)\right)$$

$$= - \Delta\xi \text{ (i.e. equation (2.27))} \qquad .....(2.31)$$

Similarly,

$$\frac{d(\Delta N)}{dx_2} = \frac{\partial(\Delta N)}{\partial(\Delta\lambda)} \frac{d(\Delta\lambda)}{dx_2}$$

$$= \frac{1}{(\nu+h) \, \cos\phi} \left(-\Delta\xi_o \, (\rho_o+h_o) \, \cos\phi \, \sin\phi_o \, \sin\Delta\lambda\right.$$

$$- \Delta\eta_o \, (\nu_o+h_o) \, \cos\phi \, \cos\Delta\lambda$$

$$\left. - \Delta N_o \, \cos\phi \, \cos\phi_o \, \sin\Delta\lambda\right)$$

$$= - \Delta\eta \text{ (i.e. equation(2.28))} \qquad .....(2.32)$$

The relationship existing between equations (2.27), (2.28) and (2.29) has therefore been defined. Note that the differentiation of equation (2.29) provides a method for checking the derivation of all three equations.

A choice is provided for the observation equations to be used in a solution for geocentric orientation parameters. Either equations (2.27) and (2.28) or equation (2.29) can be used and all results should be identical. In practice, difficulties arise in the choice of method of solution. While the astro-geodetic values of ξ and η are fundamental quantities in an astro-geodetic geoid solution, from the nature of the gravimetric geoid determination, it seems preferable to use N values for comparison purposes. The gravimetric values of ξ and η are dependent, to the order of one to two seconds of arc, on the inner zone calculation. In a geoid determination over a continental extent like Australia it was not possible to sample sufficient inner zone values of gravity to obtain an accuracy in the computed values of ξ and η approaching that of their astro-geodetic counterparts.

Data was prepared for astro-geodetic values of N, ξ and η at all the available (1968) Laplace stations on the Australian Geodetic Datum. The gravimetric values of N, ξ and η were computed on a one degree grid basis across Australia. The techniques used for comparisons between grid based gravimetric values and Laplace station values of N, ξ and η are developed in later Chapters.

As previously mentioned, the correction to be applied if the deflections to be compared are from spheroids of different size and shape will be quoted. A derivation of the formula, which once again only applies to the meridian (no prime vertical effect), may be found in *(Mather, 1968a, pp.285-292)*. The correction $\Delta\xi_D$ which must be added to the astro-geodetic deflection ξ to make that deflection comparable with the gravimetric deflection at the same point is,

$$\Delta\xi_D^{(rad.)} = - df \sin 2\phi - f \frac{da}{a} \sin 2\phi + df \frac{h}{a} \sin 2\phi - f\, df \sin 2\phi \cos^2\phi \quad \ldots\ldots (2.33)$$

where da, df are changes in a (equatorial radius) and f (flattening), the parameters of the reference spheroid. The terms neglected from equation (2.33) will not amount to more than one-hundredth of a second of arc.

2.5 Least Squares Solutions.

Later Chapters of this thesis deal with the results obtained from least squares solutions utilising equations (2.27), (2.28) and (2.29) as observation equations for the determination of $\Delta\xi_o$, $\Delta\eta_o$ and ΔN_o for the Johnston Origin of the Australian Geodetic Datum. To facilitate the understanding of later Chapters a short description of the method of least squares solutions is included at this stage.

A least squares solution is, in general, preferable to other forms of solution because it is a standard form of solution and any particular conclusion may be readily reached (solution checked) by an independent worker. The assumptions made in the solutions are not

unreasonable and for the case where more observations equations are available than unknowns (the case in this thesis), the condition imposed is that the sum of the squares of the weighted residuals is a minimum,

$$\text{i.e.} \quad \sum_{i=1}^{n} w_i \, r_i^2 = \text{minimum} \qquad \ldots\ldots(2.34)$$

where n is the number of observation equations; w_i is the weight assigned to each equation (proportional to $\frac{1}{\sigma^2}$ where σ is the standard deviation of the observation) and r_i is the residual in the observation equation i after the solutions for the unknowns are substituted back into the original equation. This condition implies that the r_i $(i=1,n)$ are normally distributed and that the solutions give the most probable values for the unknowns. Matrix notation is the most suitable form to express these solutions and the following is intended to represent a complete set of observations equations expressed in this manner,

$$A\,X - L = R \qquad \ldots\ldots(2.35)$$

where, for the solutions in this thesis, A is the matrix of coefficients and is of size $(n,3)$; X is the vector of unknowns (contains $\Delta\xi_o$, $\Delta\eta_o$ and ΔN_o) and is of size (3); L is the vector of constants (= the data, astro-geodetic values of N, ξ and η minus the corresponding gravimetric ones) and is of size (n) and R is the vector of residuals, size (n). If W, size (n,n) is the weight matrix then equation (2.34) can be re-expressed as,

$$R^T W R = \text{minimum} \qquad .....(2.36)$$

Substituting equation (2.35) into (2.36), differentiating and solving gives,

$$X = (A^T W A)^{-1} A^T W L \qquad .....(2.37)$$

It is quite simple to prepare equation (2.37) for a computerised solution, the only difficulty being the large size of the weight (W) matrix. If no co-variance between observations is assumed, the weight matrix becomes a simple diagonal matrix and arithmetic operations concerning it may be performed in a computer program quite easily (without worry of exceeding storage) by considering it as a vector, viz., a (n,1) matrix. Since the weights are proportional to the inverse of the variance of the observations, the matrix of constants may contain data of different dimensions, e.g. angles and distances. When dissimilar quantities are to be used in a composite solution, the statistical laws of normal populations are only satisfied by this system of weighting.

CHAPTER 3.

AN ASTRO-GEODETIC ORIENTATION OF THE AUSTRALIAN GEODETIC DATUM.

3.1 Introduction.

The major geodetic control network that extends over the whole of the Australian mainland and some adjacent islands has been computed on a datum titled the Australian Geodetic Datum (A.G.D.) which was formally defined in the Commonwealth Gazette (1966). Most computations of a geodetic nature prior to 1963 were based on the Clarke 1858 reference figure which had the Sydney Observatory as its origin. After investigations by the Division of National Mapping which involved an examination of all available determinations of figures of the earth since 1900, a spheroid of equatorial radius a and flattening f given by,

$$a = 6{,}378{,}165 \text{ metres}; \quad f = 1/298.3$$

was adopted as a preliminary figure for the initial geodetic control network adjustment *(Lambert, 1962, p.184)*.

The Maurice trigonometrical station in South Australia was used as a preliminary origin in order that a set of homogeneous geodetic co-ordinates could be computed for all points on the network. The reference spheroid was provided with a spatial orientation with respect to the earth by comparing this set of initial co-ordinates with astronomically determined values at 150 Laplace stations widely spaced over the continent. The resulting mean values of the deflections of the

vertical, after correction for isostasy, were -1.01 sec in the meridian and -0.93 sec in the prime vertical. These were applied as corrections to the geodetic co-ordinates at the Maurice origin with consequent revision of values for the entire geodetic network. A "Central Origin" was then defined in terms of the trigonometrical station Grundy in order that the origin would occupy a central position with respect to the continent *(Bomford, 1964, pp.97 et.seq.)*.

The reference spheroid was changed after April, 1965 to the International Astronomical Union spheroid whose parameters were *(Fricke et.al.,1965)*:

a = 6,378,160 metres; f = 1/298.25

and called the Australian National Spheroid (A.N.S.). This spheroid, for all practical purposes, has the same dimensions as Reference Ellipsoid 1967 which was adopted by the International Association of Geodesy (I.A.G.) at the 1967 General Assembly at Lucerne *(I.A.G. Resolutions 1967, p.367)*.

The number of Laplace stations which had been observed on the A.G.D. had increased to 533 by early 1966. The deflections of the vertical at these points were re-examined in order to determine whether any corrections were necessary to the values of the geodetic co-ordinates at the origin *(Bomford, 1967a, p.57)*. After a study of the pattern of distribution of these deflections, it was decided not to change the co-ordinate values of this central origin but rather

to define it in terms of the Johnston Geodetic Station *(Lambert, 1968, p.93)*. This station, referred to hereafter as the Johnston Origin has been assigned zero geoid spheroid separation because of lack of information to the contrary *(Bomford, 1967a, p.58)*. The geodetic datum defined by the combination of the set of co-ordinates adopted for the Johnston Origin and the Australian National Spheroid is called the Australian Geodetic Datum.

The complete adjustment of the A.G.D. in 1966 gave co-ordinate values to approximately 2500 control stations and it was expected that the accuracy between adjacent stations would be of the order of 3 or 4 parts per million *(ibid, p.69)*. Apart from some uncertainty in the accuracies quoted arising from the use of orthometric instead of spheroidal heights for the reduction to spheroid level of measured distances, considerable doubt was placed on the relative accuracy between adjacent stations in a paper presented to a Conference on Electronic Distance Measurement in Sydney in November, 1968 *(Bobroff, 1968)*. When MRA 4 tellurometers were used to re-measure some major control routes, surveyors from the Division of National Mapping found discrepancies which were occasionally as large as plus or minus 15 parts per million between the distances measured with these instruments and the distances as both originally measured and as adjusted. In some sections not specifically shown in the paper, the measurements gave comparison figures as high as 30 parts per million *(ibid, p.248)*.

These discrepancies were obtained from the sections of loop traverses that were farthest from the intersections with other loops. The national adjustment was performed by obtaining bearings and distances for 161 sections between loop intersection points and then obtaining adjustments for each of these sections simultaneously *(Bomford, 1967a, p.62)*. The adjusted figures will tend to be stronger near to the loop intersection stations since after the simultaneous adjustment, the re-adjustment of each section will cause the stations farthest from loop intersections to obtain the largest amounts of re-adjustment.

Notwithstanding that such poor agreements could be related to unknown quantities of the MRA 4 tellurometers used, serious doubt must exist about using the present Australian Geodetic Datum for purposes of setting out long baselines (of the order of 2000 km) for satellite tracking purposes. The original intention of the geodetic survey of Australia was to provide a control network for map making, with scientific pursuits having a secondary role. The primary aim has been admirably achieved in the present Australian Geodetic Datum, but a geodetic datum which possibly contains large random and systematic errors is of doubtful value for scientific endeavours. A scheme for re-measuring sections where scientific interest centres (e.g. between satellite tracking stations) to a high degree of precision using MRA 4 tellurometers and laser geodimeters is presently in operation.

3.2 Methods of Spheroid Orientation.

There are three distinct methods for effecting the orientation of the reference spheroid of a geodetic control network. These methods can be summarised as,

(i) An absolute orientation is provided using both gravimetric and astronomic observations. In this solution the deflections of the vertical at the origin are determined gravimetrically and when used in conjunction with the astronomic values of latitude and longitude, geodetic co-ordinates for the origin are obtained. In practice, it is more satisfactory to obtain the corrections to be applied to the astronomic values at the origin from a least squares solution of comparisons between astro-geodetic and gravimetric deflections of the vertical at several control stations widely spaced around the datum. This practical refinement has the effect of minimising errors that may have occurred in the calculation of the values of the gravimetric deflections at the origin due to insufficient sampling of the gravity field in the "inner zone" region.

(ii) An orientation is sometimes provided, where there is no available gravimetric solution, by assuming that the deflections of the vertical at the origin are zero. The astronomically determined co-ordinates are directly adopted as the geodetic co-ordinates of the origin.

(iii) An orientation may be provided by adopting method (ii) above as an intermediate solution. On the basis of the astronomic

co-ordinates of the origin being placed equal to the geodetic values there, the control stations are assigned geodetic co-ordinates. Comparisons are then made between astronomic co-ordinates at selected Laplace stations (distributed as widely and as evenly over the entire network as possible) and their newly calculated geodetic co-ordinates. Assuming that the correct values of the geodetic co-ordinates at the origin will give rise to a normally distributed population of differences between astronomic and geodetic co-ordinates, corrections can be obtained for the present geodetic values at the origin to ensure that this criterion is satisfied.

A procedure of the type described in method (iii) above was used on the Australian Geodetic Datum at the Johnston Origin. This method has been the most popular form of spheroid orientation in the past due to the small amount of gravity data and the limited computation facilities available. With solutions involving satellite perturbations capable of providing good estimates of gravity anomalies over ocean areas and Government authorities, such as the Australian Commonwealth Bureau of Mineral Resources, Geology and Geophysics providing detailed gravity data over land areas, method (i) above has become a feasible proposition for a large survey organisation where high speed computers are becoming commonplace items of capital equipment.

3.3 An Astro-geodetic Orientation.

The spatial orientation of the Australian Geodetic Datum has been derived from National Mapping Council Resolutions 287 and 293. As it is fundamental to the investigation in this Chapter, Resolution 293 has been reproduced below,

Resolution 293: The Council recommends that the origin of the National Geodetic Survey of Australia be determined from the mean value of the available astronomic deflections. The Council will later express this in terms of an adopted latitude and longitude value for Johnston Station.

The imposition of the condition that the mean of the deflections of the vertical over the datum should determine the values at the origin, has aligned the A.G.D. approximately parallel to the mean geoid slope across Australia. A spheroid of reference oriented in relation to the local geoid in the Australian region does not coincide with one whose centre is at the centre of mass of the existent earth. This is due to the continent being situated on a uniformly sloping section of the geoid rising to the well defined geoidal high situated off New Guinea *(e.g. Rapp, 1969, pp.58-61)*. Thus the A.G.D. will possess an unknown spatial orientation with respect to an earth centred reference spheroid until the relationship between the local geoid and the latter has been established.

In an age of high speed computation facilities, the direct

adoption of the mean value of the deflections of the vertical as the basis of the reference spheroid orientation when a large set of data was available appeared to be a crude expediency. A review of publications showed that in 1962 *(Lambert, 1962, Sec.2.12, p.179)*, the Director of National Mapping had indicated that a least squares calculation would be made "to give the most probable changes required in the origin and the reference ellipsoid in order to give a best fitting new ellipsoid". Although no such least squares calculation was ever published by the Division of National Mapping, a calculation which "minimised the geoidal separations for an optimum fit across the mainland, holding the zero separation at Johnston by definition," was performed in 1967 *(Fischer and Slutsky, 1967, p.331)*. Only geoid spheroid separations, derived from an astro-geodetic geoid solution *(ibid, p.328)* were used in this calculation and so it became the intention of the author to perform a series of orientation solutions using not only the derived separation values, but also the original deflections themselves. These solutions were intended to test the validity of the National Mapping Council Resolution 293. The deflections of the vertical were suitably weighted to take into account the type of instrument and procedure used in their determination so that a composite solution was meaningful.

The explanation offered by the Division of National Mapping for not performing a least squares solution was found in *(Bomford, 1967a, p.57-58)*. Briefly, the decision not to alter the 1966 geodetic values

of the origin was made because using various combinations of astro-geodetic stations around Australia, the mean values of the deflections of the vertical were never larger than 0.2 sec in the meridian and 0.4 sec in the prime vertical. Although various combinations of astro-geodetic stations were tried, the decision not to alter the values of the origin was based mainly on the mean values obtained from 275 well spaced stations, whose astronomic values had been determined in accordance with the National Mapping requirements for precise astronomic determinations *(Bomford, 1965)*.

Astro-geodetic orientation solutions, as proposed by the author, will align the reference spheroid parallel to the general direction of the geoid in the area covered by the astro-geodetic stations under consideration. These solutions will not, unless the geoid in this region is coincident with a geocentred spheroid, give the local spheroid an earth centred orientation. Hence such an orientation solution appears to be of limited practical value by itself.

An astro-geodetic orientation solution does provide, however, a means for a useful check on the two types of gravimetric orientation solutions that it is possible to perform. An explanation of the conditions which require these different types of solutions for geocentric orientation parameters appears in Section 5.2 of Chapter 5. The formulae used to perform the astro-geodetic orientation consisted of equations (2.27), (2.28) and (2.29). The values of $\Delta\xi, \Delta\eta$ and ΔN in these equations were represented by the available astro-geodetic

deflections of the vertical and the Fischer/Slutsky solution values of N respectively. This set of formulae represents a specific case of the general formulae derived by Vening Meinesz *(1950, pp.33-51)*, relating to the corrections to be applied to latitude and longitude when transferring co-ordinates between reference spheroids of different shape, size and spatial orientation. The formulae as used are equivalent to the Vening Meinesz formulae with the terms concerning changes in equatorial radius and flattening held fixed at zero.

A check on the results obtained was provided by the use of the formulae published by Vincenty *(1965, pp.128-133)*. These formulae provide solutions for dx_i (i=1,3), the rectangular cartesian separation distances between the centres of the reference spheroids (see figure (2.6)). These formulae allowed an independent least squares minimisation to be made, the results of which were directly converted to give the orientation parameters in terms of $\Delta\xi_o$, $\Delta\eta_o$ and ΔN_o after the application of formulae such as that derived in Section 2.4.

Data for these calculations was provided by courtesy of A.G. Bomford, Division of National Mapping, Canberra. For the purpose of these calculations only weighting cards had to be produced because the computer cards containing information about latitude, longitude, the deflections of the vertical, the astro-geodetic value of N, station height and name had already been prepared for use in connection with the project involving a gravimetric orientation of the A.G.D. at the Johnston Origin.

3.4 Weighting Systems.

After studies which compared the astronomic determinations of latitude and longitude made at Laplace stations by various instruments with different observers at different times, discussions were held with the abovementioned A.G. Bomford and G.G. Bennett, a Senior Lecturer in Astronomy at the University of New South Wales. The results of these investigations were the various standard deviation estimates displayed in Table 3.1. The inverses of all variances have been reduced by a factor of ten in this Table for matters of computational convenience.

The accuracy of the Fischer/Slutsky astro-geodetic geoid solution has been estimated at ± 1 metre *(Mather, 1969a, p.31)* and all astro-geodetic values of N were correspondingly given a weight coefficient of 0.1.

Solutions were also obtained with all weight coefficients equal to 1.0, so that the magnitude of the difference in results, if any, could be examined in the light of the weight differences. In fact, as Table 3.2 shows, the differences in solution are numerically very small, due to the original values adopted at the Johnston Origin being very close to those obtained from least squares solutions. This makes an evaluation of the weighting system difficult and one can only conclude that a system of weight coefficients such as those in Table 3.1 should generally be employed so that the conditions of least squares solutions are satisfied.

A SYSTEM FOR WEIGHTING ASTRONOMICAL OBSERVATIONS ON THE AUSTRALIAN GEODETIC DATUM

INSTRUMENTS and METHODS USED		LATITUDE		LONGITUDE	
		Standard Deviation (")	Corresponding Weight	Standard Deviation (")	Corresponding Weight
WILD T4	Impersonal micrometer	0.22	2.00	0.40	0.70
KERN DKM3a	Impersonal micrometer	0.25	1.60	0.45	0.50
KERN DKM3a	Stopwatch	0.40	0.70	0.70	0.20
WILD T3	Stopwatch	0.60	0.30	1.00	0.10
GEODETIC TAVISTOCK	Stopwatch or Chronograph and tappet	0.45	0.50	1.00	0.10
WILD T3 Position Lines obs. in Australia		2.00	0.03	3.00	0.01
WILD T3 Position Lines obs. in New Guinea		1.20	0.07	1.50	0.04

TABLE 3.1

RESULTS OF AN ASTRO-GEODETIC ORIENTATION OF
THE AUSTRALIAN GEODETIC DATUM

DATA SET	WEIGHTING SYSTEM Table 3.1	AVERAGE VALUES OVER NETWORK			ORIENTATION PARAMETERS		
		N met.	ξ sec.	η sec.	ΔN_o met.	$\Delta\xi_o$ sec.	$\Delta\eta_o$ sec.
274	Variable	4.34	0.14	0.30	4.30	-0.04	0.28
274	Unity	4.34	0.14	0.30	4.31	-0.11	0.30
541	Variable	3.50	0.15	0.57	3.42	-0.18	0.46
541	Unity	3.50	0.15	0.57	3.44	-0.11	0.57

TABLE 3.2

This is particularly important when the solution contains quantities of different dimensions (e.g. metres and seconds) because unless the weight coefficients are proportional to the inverse of the variances of the observed quantities, the results obtained may be misleading.

3.5 Results and Conclusions.

During the preparation of data for the astro-geodetic orientation solutions, it was found that only 274 and not 275 stations, as had been widely quoted in various publications, were used for the determination of the mean value of the deflections of the vertical. Thus one set of solutions used 274 stations and the other consisted of all available data (541 stations). The results from the 274 data set are preferable to those from the 541 set due to the more uniform spacing arrangement of the 274 Laplace stations. The 541 data set has some areas of very close station spacing which is likely to place a systematic strain on the results.

The values in Table 3.2 illustrate that the orientation parameters are quite small and are very close to the mean values. Thus the National Mapping Council Resolution 293 was valid for the case of the Johnston Origin. If the magnitude of the mean values of the deflections of the vertical had been of the order of a few seconds of arc, the adoption of the mean deflection values may not have been a sufficiently accurate method of solution to the problem of providing an orientation for the Australian Geodetic Datum.

The difference between the results obtained from the use of the Vening Meinesz and Vincenty formulae was less than 1% in every case. Another check on the results was provided by holding the value of N fixed at zero metres at the Johnston Origin and comparing the subsequent results for $\Delta\xi_o$ and $\Delta\eta_o$ with those obtained by Fischer and Slutsky. As quoted in Section 3.3 they minimised the geoidal separations which were calculated from (mainly) the 541 data set of deflections. They could employ no weighting system and their orientation parameters at the Johnston station only differ by 0.05 and 0.01 seconds in the meridian and prime vertical directions respectively to those shown in Table 3.2. The accuracy of the astro-geodetic orientation parameters in Table 3.2 can be estimated to be within ± 0.2 seconds when the volume of data used and the reliability of the check calculations are considered.

This study has defined the position that the Australian Geodetic Datum occupies in space with respect to the geoid. This location can now be investigated with respect to a geocentred spheroid by using a free air geoid solution. The least squares solution method has several distinct advantages over the direct adoption of the mean. The deflections of the vertical at different stations are given varying weights in the matrix of coefficients depending on their distance from the origin. Each observation receives a weight coefficient according to the type of instrument used and the method of astronomical observation employed. The system of weight coefficients

devised and displayed in Table 3.1 is considered to be sufficiently representative of actual field observations that it could be used in other contexts with a high degree of reliability.

CHAPTER 4.

THE PRELIMINARY 1968 FREE AIR GEOID FOR AUSTRALIA.

4.1 Introduction.

A full definition of a free air geoid is provided in Section 1.2, but basically it is the co-geoid which is obtained by using free air anomalies in Stokes' integral (see equation (1.1)). It differs from a complete geoid solution by an amount called the indirect effect, which includes both global variations and a zero order term. An estimation of the indirect effect for the free air geoid is presented in Chapter 6.

In 1967 a free air geoid determination was produced for the state of South Australia *(Mather, 1968a, pp.323-327)* using as gravity data for regions farther than 20^{o} from the computation point the $5^{o} \times 5^{o}$ free air anomaly data set compiled by Kaula *(1966)*. The areas closer to the computation point used gravity anomalies based on surface gravimetry only. Another set of $5^{o} \times 5^{o}$ free air anomaly means was produced by Rapp *(1968)* using a modified approach for combining satellite and terrestrial gravity data. Both of these sets of data were used in combination with surface data for the region of Australia and New Guinea to produce preliminary solutions for the free air geoid in Australia. These solutions are described in Section 4.3, where preliminary results of comparisons between the solutions obtained and the astro-geodetic geoid determination for Australia *(Fischer and Slutsky, 1967)* are presented.

If a more detailed account of the free air geoid in Australia (1968) is required, the reader is referred to *(Mather, 1969)*. This Chapter includes a condensation of those sections of that work which are relevant to later Chapters of this thesis.

4.2 Gravity Data Used.

The introduction has outlined the sets of free air anomaly data that were used to calculate N_f, the free air geoid spheroid separation value. Section 1.2 defines the formulae used to perform this calculation. The following technique was adopted for introducing free air anomaly values into the free air geoid equation and are based on a study of the variation of $f(\psi)$ with ψ. Table 4.1 sets out the type of gravity data used in the calculations, the ranges of ψ adopted being dependent on,

(a) the extent of gravity data available, noting that the gravity field over large areas of Australia has been established by helicopter traverses with a station spacing of approximately one tenth of a degree;

(b) the accuracy with which a chosen anomaly can represent an area of a particular size *(e.g. Hirvonen, 1956, p.3)*;

and (c) the linearity of the function $f(\psi)$ over the region represented by the area mean.

In regions where no gravity data was obtainable, the available gravity field was extended using a two dimensional trigonometrical

GRAVITY DATA USED IN CALCULATIONS

RANGE OF ψ	SOURCE	GRAVITY DATA USED
$\psi < 0.1^{o}$	Surface Gravity	Individual readings
$0.1^{o} < \psi < 1.5^{o}$	Surface Gravity	0.1^{o} x 0.1^{o} sq. values
$1.5^{o} < \psi < 5^{o}$	Surface Gravity	0.5^{o} x 0.5^{o} sq. means
$5^{o} < \psi < 20^{o}$	Surface Gravity	1^{o} x 1^{o} sq. means
$20^{o} < \psi$	Combined Satellite data and Surface Gravity	5^{o} x 5^{o} sq. means

TABLE 4.1

series after allowing for topographic variations *(Mather, 1967, pp.132-137)*. These extensions proved to be quite reliable when obtained by interpolation but under conditions of extrapolation into ocean areas, the accuracy of the extensions decreased rapidly as the distance from the well defined land areas increased.

Tests of Gravity Data.

The two sets of 5^{o} x 5^{o} free air anomaly means due to Kaula and Rapp which were used to represent the range $\psi > 20^{o}$, were tested against each other and found to be considerably different, *(Mather, 1969, pp.11-23)*. The sets showed no global correlation, the standard deviation of the comparisons for each quarter of the earth's surface area being of similar magnitude, ranging from

± 11.4 mgal to ± 14.2 mgal. The global mean standard deviation of ± 12.5 mgal is about half the magnitude of Hirvonen's estimate of the error of representation of a 5^{o} x 5^{o} square by a single reading.

Comparisons of these combined data sets were also made with the available 5^{o} x 5^{o} free air anomaly means for Australia and its environs. As tenth degree squares were represented by a single reading in the latter sample, the maximum number of readings possible in a five degree square was 2500. No significant difference could be found in the statistical parameters defining the comparisons in each case considered. The standard deviation of the comparisons increased from a minimum of ± 5.2 mgal in the case where the terrestrial samples were well represented to a maximum of ± 10.2 mgal when the latter included squares in which there were as few as 50 readings. This is significant because it can be expected that comparisons with poorly represented surface samples would have greater standard deviations if the combined solutions were truly representative of the earth's gravity field. Such assessments of the reliability of data sets obtained from combined solutions are of great importance as this technique affords the only means of providing an adequate representation of large sections of the global gravity field in the foreseeable future.

Any gravity data which was referred to the International Gravity Formula was converted to Gravity Formula 1967 using a set of correction formulae *(e.g. Mather, 1968c)*. A correction of - 14 mgal to the Potsdam

datum gave the final free air anomalies to be used in the computations *(I.A.G. Resolutions 1967, p.383)*.

4.3 Calculation of the Free Air Geoid.

The free air geoid was calculated over the Australian mainland region at the corners of a one degree (1^{o}) grid. The inner zone was considered to be the four tenth degree squares comprising the area immediately around the computation point. The values of Δg_f and $\partial \Delta g_f / \partial x_i$ for use in equations (1.4) and (2.10c) were computed from the four values of the free air anomaly representing these squares. The inner zone contribution to N_f seldom exceeded 20 cm but the values of ξ_{in_i} were quite often as large as 1 second. It can be concluded that the magnitude of the deflections of the vertical can be significantly affected by the approximate technique used for the evaluation of the inner zones in this set of computations.

Due to the approximations introduced in evaluating the inner zones in the current determination and the inherent variability of deflections of the vertical over limited regions, it was decided that maps of the deflections would provide a more representative picture if the inner zone effects were omitted. Improved values of the deflections of the vertical could be obtained by further sampling the inner zone gravity field and combining the results with the deflections calculated from the other zones.

The computer programs used were revised versions of those

previously published in the report on the calculation of the South Australian free air geoid *(Mather, 1968a, p.232 et.seq.)*. The geoid potential adopted for the calculations was 6,263,703 kgal metres, a value which is equivalent to adopting the 1967 Gravity Formula for the calculation of normal gravity and assuming that W_o is equal to U_o. The zero order term for the free air geoid has not been included because it is constant for all values of N_f and therefore similar to a datum shift. The zero order term for the Kaula set is + 8.4 metres and for the Rapp set it is - 3.2 metres. As can be seen from equation (1.3) this zero order term is merely dependent on the global mean free air anomaly value.

Although there were variations in outer zone data sets, the free air geoids calculated from them had basically the same trends. Upon finding geocentric orientation parameters from either solutions (see Section 4.4), differences in the orientation parameters $\Delta\xi_o$ and $\Delta\eta_o$ were never greater than 0.2 seconds while the ΔN_o parameter from the Kaula solution was between 4.7 metres and 5.5 metres larger than the corresponding Rapp ΔN_o value. This ΔN_o is akin to a simple datum shift in a vertical sense.

4.4 Preliminary Comparisons between the 1968 Free Air and Astro-Geodetic Geoid Solutions for Australia.

Comparisons between the 1968 free air and the Fischer/Slutsky astro-geodetic geoid solutions for Australia can be performed if,

(a) the reference spheroids used in both solutions are of the same size and shape (i.e. geometrically identical),
and (b) both spheroids have coincident locations in space.

The requirements of (a) above are satisfied since the preliminary free air geoid has been calculated using gravity anomalies relating to the 1967 Gravity Formula which has as its basis Reference Ellipsoid 1967. This ellipsoid is the same shape and size as the Australian National Spheroid which is the reference figure for the Australian Geodetic Datum (A.G.D.). The spatial orientation of the A.G.D. has been obtained by aligning the datum along an estimate of the mean geoid slope across Australia (see Chapter 3).

The requirement (b) can be satisfied by applying three geocentric orientation parameters ($\Delta\xi_o$, $\Delta\eta_o$ and ΔN_o) to the co-ordinates at the Johnston Origin of the A.G.D. so that co-ordinates on the Australian National Spheroid can be related to equivalent locations on an earth centred spheroid, i.e. the free air geoid reference figure. The derivation of the formula used to obtain these origin orientation parameters appears in Chapter 2. Equation (2.29) is used in conjunction with a least squares minimisation procedure to find preliminary values of ΔN_o, $\Delta\xi_o$ and $\Delta\eta_o$.

The Fischer/Slutsky astro-geodetic geoid was based on approximately 600 astro-geodetic stations around the A.G.D. with the assumption that the geoid spheroid separation value at the Johnston Origin was zero metres. The distribution pattern of these stations is

illustrated in *(Bomford, 1967a, fig.1)*. While the distribution pattern is not one that is totally desirable, it was estimated that the geoid undulations derived in the Fischer/Slutsky solution would, in general, be accurate to ± 1 metre at any point. This estimate was derived after a consideration of the following information,

(i) an error of one second of arc in astronomical determinations of position will give rise to an error of half a metre in the value of N over a length of 100 km

and (ii) only 600 stations are used to cover an area of over six and a half million square kilometres, i.e. each station per 12,000 sq. km should be representative of the deflections of the vertical in that area. Unfortunately the station spacing noted above is a very conservative estimate for the areas represented by some stations.

The data used in the solution for geocentric orientation unknowns consists of the differences between the gravimetric and the astro-geodetic values of N at corners of a one degree grid over the Australian continent. This is not the best method of obtaining orientation parameters since only N values are compared at arbitrary points. A better method of solution (as performed in Chapter 5), compares gravimetric and astro-geodetic values of N, ξ and η at specific control stations situated over the continental extent and uses various weighting techniques so that observations performed with superior instruments are given greater importance in the least squares solution. For the problem of determining if the

preliminary 1968 free air geoid is reasonably representative of the actual geoidal undulations across Australia, however, the former method described above should be quite sufficient.

A free air geoid solution with good gravity data coverage for the region within 20^{o} of the computation point and acceptable satellite data for outer zone areas should give free air geoid values of N to approximately ± 1 metre (the formula used is correct to ± 30 cm). For the majority of Australia these conditions did not exist. Most computation points had good terrestrial gravity data for the 5 to 10 degrees immediately surrounding them but the remainder of their intermediate zones consisted of interpolated and extrapolated values. Some computation points did not have gravity observations in the inner zones and these points relied heavily on interpolated values. It was therefore expected that for some regions of Australia, the free air geoid solution would have considerable unreliability. One of the aims of the preliminary comparisons with the Fischer/Slutsky solution was to detect regions of weakness so that before any future free air geoid calculations took place, these areas could have their gravity anomaly values suitably strengthened.

The method of determining areas of weakness in the free air geoid was to obtain geocentric orientation parameters for the Johnston Origin as outlined previously and then to calculate, using equation (2.29), values of ΔN at each one degree corner over Australia. These ΔN values were added to the Fischer/Slutsky

astro-geodetic N values to give an astro-geodetic geoid solution that was on an earth centred reference figure. The differences between the geocentred astro-geodetic and the free air geoid solutions were calculated and the standard deviation of these differences obtained. The difference in N values at each point was examined and where this difference was two or more times greater than the standard deviation, reasonable grounds for suspicion of the free air geoid existed.

A standard deviation of ± 5.2 metres was obtained when 701 comparison points (i.e. all available data) were used in the type of solution discussed above. After an examination of the differences between the geocentred astro-geodetic and the free air geoid values of N, the following regions were delineated as regions of lower precision,

(i) Regions west of meridian 120° East longitude,

(ii) Regions north of parallel 15° South latitude,

(iii) The Officer Basin area of north and west South Australia,

and (iv) All regions within 1° of the coastline.

After the regions detected above were eliminated the solution for geocentric orientation parameters at the Johnston Origin was re-computed using 566 comparison points. Again the Fischer/Slutsky astro-geodetic values of N were given a geocentred orientation and compared with the free air geoid solution. The resultant standard deviation was ± 3.0 metres.

The geocentric orientation parameters did not change a great deal in the re-calculation, and the values of,

$$\Delta\xi_o = -4.7 \text{ sec}$$

$$\Delta\eta_o = -4.5 \text{ sec}$$

$$\text{and } \Delta N_o = 14.1 \text{ metres} \qquad \ldots\ldots(4.1)$$

seem to be good preliminary estimates of the orientation parameters to be applied to the Johnston Origin in order to relate the A.G.D. to a geocentred location. The values in equation (4.1) are those computed using the Rapp set of data for outer zones, the Kaula outer zone data set giving similar (within ± 0.2 sec) values for $\Delta\xi_o$ and $\Delta\eta_o$ and a ΔN_o value 4.7 metres larger at 18.8 metres. The comparison tests with terrestrial data over Australia did not show either set of data to be superior, although the studies undertaken by Rapp *(1968, pp.2-5)* conclude that the approach he uses to combine terrestrial and satellite data is more exacting than Kaula's.

The regions listed above as those excluded from the second solution were originally suspect because of their limited state of gravity control. These regions had relied mostly upon interpolated values with large distances between gravity control stations and, in the case of the west coast region of Western Australia, extrapolations into the large anomalous regions of the Timor Sea. Whilst some terrestrial gravity data existed for the New Guinea regions *(St. John, 1967)*, the anomalies in this region were very large. More detailed observations of gravity must take place before the free air

geoid solution north of 15^{o} South latitude will approach the precision of the solution in the remainder of Australia. The Officer Basin area of South Australia is a region of rapidly varying free air anomalies and has a poor gravimetric coverage. The astro-geodetic geoid solution will probably be of lower precision in this area also, as comparatively few Laplace stations have been established there.

4.5 Conclusions.

From the studies undertaken with the preliminary 1968 free air geoid in Australia, some conclusions were made, even though the nature of the indirect effect was not known. Free air geoids computed for the Australian region using sets of $5^{o} \times 5^{o}$ free air anomaly means obtained by the combination of satellite data and surface gravimetry for the representation of distant zones, appeared to be satisfactory estimates of the geoid itself, provided the intermediate and inner zone gravity fields were adequately sampled. The method of sub-division adopted for the gravimetric computations was suitable for the Australian region (see Table 4.1).

The 1968 free air geoid meshed quite well with the Fischer/ Slutsky astro-geodetic solution (standard deviation ± 3.0 metres) when regions of poor gravity coverage were eliminated. The meshing was expected to improve when the nature of the indirect effect was determined. The results of Chapter 6 and the conclusions in Chapter 8 show that the Fischer/Slutsky astro-geodetic and the 1968 free air

geoid solutions were not sufficiently precise, however, to detect any slight improvements arising from the incorporation of the indirect effect computation. The 1970 free air geoid *(Mather, 1970a)* and an improved astro-geodetic solution are briefly discussed in these Chapters and it is believed that these may be sensitive to the indirect effect.

Preliminary estimates for geocentric orientation parameters for the Johnston Origin of the A.G.D. were obtained in this Chapter and although more exacting methods for obtaining these values are presented in Chapter 5, the values presented in equation (4.1) appear likely estimates of the parameters which can define the relationship between the A.G.D. and a geocentred reference figure. The geocentric orientation parameters derived by Mather *(ibid)* are within 0.5 seconds for $\Delta\xi_o$ and $\Delta\eta_o$. A zero order term has been included in the value of ΔN_o in the 1970 solution reducing it to + 7.2 metres.

CHAPTER 5.

A GRAVIMETRIC ORIENTATION OF THE AUSTRALIAN GEODETIC DATUM.

5.1 Introduction.

The Australian Geodetic Datum is a geodetic control network composed of triangulation, trilateration and tellurometer traverses. The earth space orientation of the Australian National Spheroid is approximately parallel to the mean position of the geoid across the Australian continent. This spheroid orientation is based on the 1963 Division of National Mapping decision to adopt the mean values of the deflections of the vertical over Australia as those for the Johnston Origin. An examination of this decision has been undertaken in Chapter 3 where it was shown that the decision to use mean values has aligned the Australian National Spheroid to within 0.5 secs of the mean geoid position across the continent.

For the purposes of establishing a global geodetic network, a geocentred reference spheroid is desirable. The main objective of the Australian Geodetic Datum was for topographic mapping, in which case the spheroid orientation parallel to the mean geoid position across the continent provided an effective means for limiting scale errors in the geodetic control network. The Australian Geodetic Datum was not originally intended for high order scientific research work (e.g. satellite baselines and tracking station operations), but the present situation is that sections of the Datum are being re-measured with a view to such research. For the purposes of connections

to other large geodetic datums, it is desirable that the relationship between the local geodetic datum and an earth centred reference figure be defined. The definition of the relationships existing between geodetic datums is fundamental to the establishment of evidence for large scale geophysical investigations into continental drift theories, sea-floor spreading, etc. Datum inter-connections can only be significant if all geodetic networks have a common earth space orientation, or if the parameters defining the relationships between these different systems and a common geocentric orientation are known. The most suitable orientation in earth space that a reference spheroid can have is an earth centred one. This Chapter is devoted to obtaining geocentric orientation parameters ($\Delta\xi_o$ in the meridian, $\Delta\eta_o$ in the prime vertical and ΔN_o in the normal direction) for the Johnston Origin of the Australian network so that the relationship between the Australian Geodetic Datum and an earth centred reference spheroid will be defined.

5.2 Types of Solutions for Geocentric Orientation Parameters.

Most of the larger geodetic datums in the world have several control stations at which astronomic values for latitude and longitude have been obtained. The general procedure in recent years has been to give an arbitrary geoid spheroid separation value to one of the major stations in the network and then to calculate the geoidal undulations over the network using the available values of the deflections of the vertical. For example, both the Johnston Origin

for the Australian Geodetic Datum and Meades Ranch for the North American Datum *(Fischer, 1966, p.4905)* have been arbitrarily assigned a value of zero metres for the geoid spheroid separation. The variation of the geoid spheroid separation over the network will depend on the nature of the spheroid orientation as well as on the distribution pattern of the deflections of the vertical.

If the mean values of the deflections of the vertical over the region have been adopted as those for the origin, then the spheroid will be very close to the mean geoid position across the network. The resulting geoid spheroid separations will be relatively small (e.g. the Fischer/Slutsky astro-geodetic geoid determination for Australia) and will oscillate about the geoid spheroid separation value adopted for the origin. If this method of spheroid orientation has not been used then the geoid spheroid separations may tend to increase systematically.

Geodetic co-ordinates for control stations on most geodetic networks are obtained by the use of orthometric heights for the reduction of measured distances to spheroid level as spheroidal heights are not available. Systematic errors are consequently introduced into the values of the computed co-ordinates. These co-ordinates can be reduced to spheroid level by using the astro-geodetic geoid determination in conjunction with the orthometric heights. The type of solution required is one which will define the geocentric orientation vector in terms of the origin of the network so that the local

spheroid can be located with respect to the earth's centre of mass. The data to be compared in such an orientation calculation are the astro-geodetic and gravimetric values of N, ξ and η (see figure 5.1).

If an astro-geodetic geoid determination has not been used to reduce the control station co-ordinates to spheroid level, then the type of solution required for the geocentric orientation parameters would use only the gravimetric values of N, ξ and η as data. This solution would provide orientation parameters which would relate the control station co-ordinates to equivalent positions on an earth centred spheroid.

For the case of the Australian Geodetic Datum the choice of solution requires further discussion. Although no corrections have been made to control station co-ordinates using the astro-geodetic geoid solution, any such corrections would be very small since the average geoid spheroid separation is approximately 4 metres. As the main purpose of the Australian Geodetic Datum was for topographic mapping, such small corrections are not warranted.

The Division of National Mapping is presently strengthening the astro-geodetic geoid solution by observing long chains of closely spaced Laplace stations. From a strengthened astro-geodetic geoid solution this authority could provide the corrections to spheroid level necessary for the control lines of scientific interest (e.g. satellite baselines or distances between tracking stations). Thus the most suitable solution for geocentric orientation parameters for

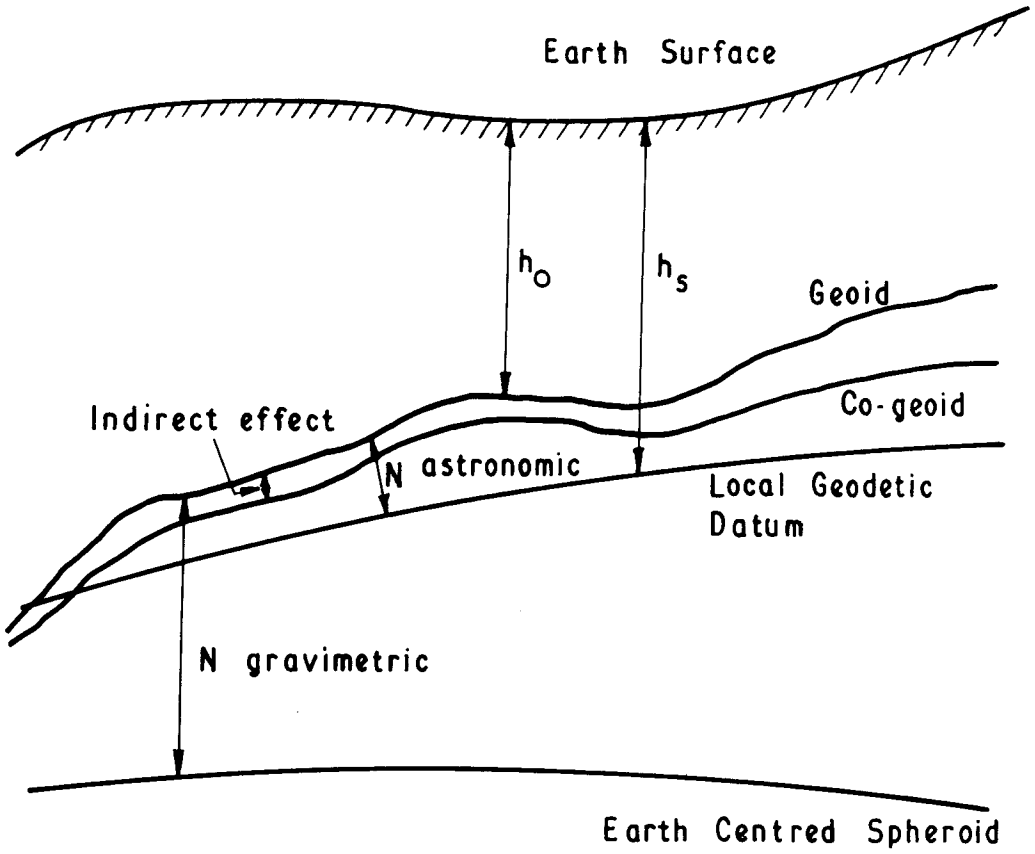
Earth Surface
h_o
h_s
Geoid
Co-geoid
Indirect effect
N astronomic
Local Geodetic Datum
N gravimetric
Earth Centred Spheroid

FIG. 5.1

the Australian Geodetic Datum would contain comparisons of astro-geodetic and gravimetric values of N, ξ and η.

If the geodetic co-ordinates of control stations on the Australian network, derived by the use of orthometric heights for the reduction of measured distances to spheroid level, are assumed to refer to the Australian National Spheroid, the maximum error from this source is approximately ± 0.1 seconds of arc. This estimate was determined by considering a line between the Johnston Origin and a control station in the region near Perth, Western Australia, where the astro-geodetic geoid solution reaches a maximum value of 18 metres. The astro-geodetic values of the deflections of the vertical therefore contain a maximum error of ± 0.1 seconds *from this source*.

5.3 The Computations.

One method of calculating geocentric orientation parameters for the Johnston Origin of the Australian Geodetic Datum was outlined last Chapter (Section 4.4). Briefly, it consisted of comparing the 1968 free air geoid with the Fischer/Slutsky astro-geodetic geoid values of N at each one degree corner over the Australian continental extent. A least squares solution gave the required geocentric orientation parameters ($\Delta\xi_o$, $\Delta\eta_o$ and ΔN_o) for the Johnston Origin. The solution to find the most probable values of the geocentric orientation parameters excluded those regions detected last Chapter as being of low precision. The most probable geocentric orientation parameters were calculated from comparisons at 566 grid corners and

the values obtained were $\Delta\xi_o$ = - 4.7 sec, $\Delta\eta_o$ = - 4.5 sec and ΔN_o = 14.1 metres.

The method outlined above makes no allowance for a consideration of the differences between the values of the gravimetric and astro-geodetic deflections of the vertical. As the values of N from the astro-geodetic solution are only derived quantities and have undergone various adjustments before their final presentation in map form *(Fischer and Slutsky, 1967, p.329)*, it was decided to investigate other solutions for obtaining geocentric orientation parameters that used composite sets of data consisting of the deflections of the vertical and N values. The conditions of least squares solutions can be maintained provided each observation equation is weighted proportionally to the inverse of the variance of the particular observation which is used as data in that equation (see Section 2.5 for the theory of least squares adjustments). The systems of weight coefficients used are determined in Section 5.4 of this Chapter and are of a similar nature to those used in the calculations of Chapter 3.

In order to include the values of the deflections of the vertical, solutions were performed in this Chapter with comparisons of free air and astro-geodetic geoid values of N, ξ and η (in varying combinations), at specific Laplace stations throughout the continent. The astro-geodetic values of ξ and η were provided by courtesy of the Division of National Mapping and the astro-geodetic

N values were derived from the Fischer/Slutsky astro-geodetic geoid solution.

As described last Chapter, the 1968 free air geoid values of N, ξ and η were computed at the corners of a one degree grid over the Australian continent. For the calculations in this Chapter, the method of Besselian interpolation to the second order was used to derive values of N, ξ and η at specific Laplace stations. This meant a total of sixteen grid points were involved in the obtaining of each interpolated value *(Clark, 1964, Vol.2, p.32)*. The decision to use Besselian second order interpolation was based on some preliminary hand calculations which showed that errors of the order of $\pm$ 1 metre in N and $\pm$ 1 second in ξ and η could be made if only a first order (planar) interpolation was used.

Formulae Used.

Following the approach to the calculations in Chapter 3, two different sets of formulae were utilised so that all results obtained were provided with a check computation from an independent least squares minimisation. The formulae derived in Section 2.4 (viz., equations (2.27), (2.28) and (2.29)) were programmed on the University of New South Wales' I.B.M. 360/50 computer to provide results for $\Delta\xi_o$, $\Delta\eta_o$ and ΔN_o. These values were checked by a solution using the Vincenty formulae *(Vincenty, 1965, pp.128-133)* which produced results for dx_i (i=1,3). The values of dx_i were converted into values

of $\Delta\xi_o$, $\Delta\eta_o$ and ΔN_o, the geocentric orientation parameters for the Johnston Origin of the Australian Geodetic Datum.

Features of these computer programs were that as well as a composite solution using observation equations for N, ξ and η, three solutions using only the observation equations of each of N, ξ and η were performed. A solution using both ξ and η observation equations was also obtained, making a total of five separate solutions for the geocentric orientation parameters each time the programs operated.

The orientation parameters were substituted back into the original observation equations to obtain the vectors of residuals for N, ξ and η in order to establish which set of calculations gave the most probable solution. The means and standard deviations of these residuals were calculated and the assumption was made that the most representative solution, viewed with respect to the regions that were used for the data, would have the lowest standard deviations for the residuals. Most attention was paid to the standard deviation of the N residuals because it is with these values that one is primarily concerned in attempting to correctly reduce observations to spheroid level. A low standard deviation of a set of N residuals should be accompanied by relatively low standard deviations of ξ and η residuals. The relationship between N and ξ and η has already been illustrated in Section 2.4, equations (2.31) and (2.32).

Weighting Systems.

The probable errors in the Fischer/Slutsky astro-geodetic and the 1968 free air geoid solutions were discussed in Section 4.4. It appears that on the average, the Fischer/Slutsky solution could have a standard deviation of ± 1 metre at any point, with the proviso that this is a rather conservative estimate in some areas where the spacing of the Laplace stations is sparse.

The 1968 preliminary free air geoid values for N should also possess variable standard deviations, depending on the density of sampling of the gravity anomaly field in the near and inner zones. Areas close to the coastline were immediately suspect due to the extrapolation of gravity anomaly values from the land regions into ocean areas. These extrapolations were especially suspect in the northern areas of Australia due to the large anomalous regions of the Timor Sea and New Guinea. The Officer Basin area of north and west South Australia also had very few gravity readings and the gravimetric values of N, ξ and η were expected to be of lower precision in this region.

Areas of low precision free air geoid values were detected by examining the size of the residuals upon back substitution of the geocentric orientation parameters into the original observation equations. Once these regions were delineated the gravimetric N values were assumed to possess a standard deviation of ± 1 metre. The differences between free air geoid and astro-geodetic N values

were accordingly assigned a standard deviation of ± 1.4 metres.

For some of the calculations the differences between the gravimetric and astro-geodetic values of ξ and η were assigned a standard deviation of ± 1.4 seconds. This is not an unreasonable estimate as the values of the astro-geodetic deflections of the vertical, on the average, should have standard deviations of approximately ± 0.6 seconds (see Table 3.1). The gravimetric deflections, acknowledging their dependence on the inner zone contribution, were thought to have standard deviations in the vicinity of ± 1.5 seconds. For some of the calculations, a convenient standard deviation of ± 1.4 seconds was therefore assigned to the differences between the astro-geodetic and free air geoid values of ξ and η. This allowed a weighting system of {1.0, 1.0 and 1.0} to be used for some calculations for the differences in values of N, ξ and η respectively as the data for N was in metres and for ξ and η in seconds of arc.

A more refined set of weight coefficients was constructed after studying the results of the calculations with the above weighting set. The regions delineated as being of low precision were excluded and, observing that the gravimetric N values were not exceedingly dependent on the inner zone contribution, the standard deviation of ± 1.4 metres was retained for N value comparisons.

The weight coefficients for ξ and η were thoroughly reviewed and it seemed that the previous estimates were too conservative,

especially for the η comparisons. The astro-geodetic values of η definitely have larger standard deviations than the corresponding values of ξ, presumably due to the precision required with timing mechanisms for longitude observations. From the preliminary results for the free air geoid, the same trend was detected with their gravimetric counterparts. A possible explanation could be the weaknesses existing in the gravity fields to the east and west of Australia. In the north-south direction, some values for New Guinea and the Timor Sea were available to strengthen calculations for ξ. The standard deviations of the η residuals were generally about 0.5 seconds larger than those for ξ when continent-wide solutions for geocentric orientation parameters were undertaken. The inner zone effect for gravimetric values of ξ and η is quite considerable (sometimes greater than one second) and on these premises, standard deviations of $\pm$ 2.0 and $\pm$ 2.5 seconds for the differences between gravimetric and astro-geodetic values of ξ and η respectively were assigned.

The resulting weight coefficients, after multiplication of the inverse of each variance by a factor of six for convenience, were 3.0, 1.5 and 1.0 for comparisons of N, ξ and η respectively. After comparing the results of computations using these weight coefficients with those using the initial set of {1.0, 1.0 and 1.0}, it was decided that further refining of the weighting system would be unnecessary. Differences in results arising from the two sets of

weight coefficients were of the order of 1% in $\Delta\xi_o$ and $\Delta\eta_o$ and less than 0.2% in ΔN_o. For example, the results from calculations using 144 well spaced Laplace stations situated across Australia in regions of good gravimetric coverage changed as below when firstly the {1.0, 1.0 and 1.0} set and then the {3.0, 1.5 and 1.0} set of weight coefficients were used,

ΔN_o : from + 13.78 to + 13.76 metres

$\Delta\xi_o$: from - 4.64 to - 4.68 seconds

$\Delta\eta_o$: from - 4.38 to - 4.41 seconds

Since similar results occurred every time the weighting system was modified, it was concluded that any reasonable set of weight coefficients of the style derived above would give acceptable results. It is very advisable to study the weighting systems to be used quite thoroughly before deciding on a particular set of weight coefficients, especially when quantities of different dimensions are being used in a composite solution. One must check that the units of the expected standard deviations correspond with those of the data sets being used, e.g. if a standard deviation of ± 1 metre was expected for comparisons of values of N and the observation equations weighted accordingly, then the data set used must be in terms of metres. If the data set inadvertently contained values of N in centimetres, then the weight given to the values of N in this particular computation would be a factor of 10^4 too large. Other data, e.g. comparisons of values of ξ and η, would be completely overshadowed in such a solution. All

computations in this thesis had data values of N in metres and ξ and η in seconds of arc.

5.4 Results.

Several different solutions with varying amounts of data were used to obtain the geocentric orientation parameters for the Johnston Origin that will define the earth space location of the Australian Geodetic Datum with respect to a geocentred spheroid. The largest set of data used all the available astro-geodetic stations on the Australian mainland that were covered by the 1968 free air geoid solution (Solution Code 2, Table 5.1). There were 506 of these stations and the values of $\Delta\xi_o$, $\Delta\eta_o$ and ΔN_o from this calculation as well as those obtained from the other calculations are given in Table 5.1. The standard deviations of the residuals are also given in this Table and it is in conjunction with these standard deviations that the residuals were reviewed so that regions of poor meshing of the astro-geodetic and gravimetric geoids could be delineated.

The 506 stations were not well spaced around the network, being grouped together along the long chains of tellurometer traverses and triangulation. Since these stations covered the entire mainland the suspected regions of low precision free air geoid values detected last Chapter (see Section 4.4) were included in the data. The standard deviation of the N residuals of this solution was $\pm$ 5.6 metres.

Another solution was performed using 252 stations (Solution Code 3)

SUMMARY OF GEOCENTRIC ORIENTATION PARAMETERS

No. of comparisons	Solution Code	Orientation Parameters			Standard Deviation of Residuals		
		ΔN_o (m)	$\Delta \xi_o$ (sec)	$\Delta \eta_o$ (sec)	N (m)	ξ (sec)	η (sec)
701	1	15.9	-4.61	-3.97	±5.6	-	-
506	2	14.8	-4.48	-3.95	±5.6	±3.0	±3.7
252	3	16.1	-4.48	-3.81	±6.1	±3.1	±3.7
566	4	14.1	-4.69	-4.46	±3.0	-	-
144	5	13.8	-4.68	-4.41	±2.7	±2.7	±3.1
42	6	10.6	-6.09	-4.91	±2.0	±3.2	±3.0
33	7	7.8	-4.74	-5.52	±1.6	±2.8	±2.3

TABLE 5.1

Key to Solution Code

1 N values only at corners of one degree grid - Australia-wide

2 Irregularly spaced Laplace stations - Australia-wide

3 Evenly spaced Laplace stations - Australia-wide

4 N values only on one degree grid, excluding regions west of meridian 120°E, north of -15°N and the Officer Basin, S.Aust.

5 Well spaced Laplace stations - region as at 4

6 Laplace stations in the region bounded by meridians (128°E, 144°E) and parallels (-20°N, -26°N)

7 Laplace stations in N.S.W. and regions within one degree of its borders

which were selected on the bases of even spacing and the precision of their astronomic observations. These Laplace stations were well spaced over the entire continent and hence included the regions of lower precision free air geoid determination. The geocentric orientation parameters $\Delta\xi_o$ and $\Delta\eta_o$ were very similar to those of Solution Code 2 while the ΔN_o parameter differed by 1.3 metres. The standard deviation of the N residuals was slightly larger at ± 6.1 metres than that for the previously mentioned solution, but this is understandable when the relative numbers of stations in the regions of lower precision free air geoid values are considered. The values of the geocentric orientation parameters obtained by Mather *(1969a, p.29)*, when only values of N at one degree corners were used (Solution Code 1), were within 0.2 seconds for $\Delta\xi_o$ and $\Delta\eta_o$ and 1.1 metres for ΔN_o for both sets of results described above.

A decision was made to isolate those regions where the residuals of the observation equations upon back substitution of the orientation parameters were more than twice as large as their standard deviations, in order to see if these areas corresponded with those detected last Chapter. In this Chapter comparisons of astro-geodetic and gravimetric values of N, ξ and η have been made at specific Laplace stations whereas previously, only values of N at each degree corner were used. Even with these differences in approach, the same regions as those detected last Chapter were found to have the largest residuals, viz.,

(i) Areas west of meridian $120^{o}E$,

(ii) Areas north of latitude $15^{o}S$,

(iii) The Officer Basin of South Australia

and (iv) Areas within 1^{o} of the coastline.

A further solution was performed at 144 well spaced Laplace stations which excluded the regions delineated as being of lower precision (Solution Code 5). The results of this solution are very similar to those which were decided upon last Chapter as being the most likely (see Solution Code 4). These two sets of results differ by less than 0.05 seconds in $\Delta\xi_o$ and $\Delta\eta_o$ and by 0.2 metres in ΔN_o. The standard deviation of the N residuals was relatively low at ± 2.7 metres and illustrates the good meshing of the astro-geodetic and free air geoid solutions over 80% of the Australian mainland area.

Two other solutions for geocentric orientation parameters were performed using small numbers of control stations in relatively small areas (Solution Codes 6 and 7). The first area used was rectangular in shape and was enclosed by the meridians $128^{o}E$ and $144^{o}E$ and the parallels $20^{o}S$ and $26^{o}S$. This region across Northern Territory and north-western Queensland contained 42 stations and gave results for the orientation parameters which differed considerably from those previously obtained. The second small area was composed of 25 well spaced stations in New South Wales plus 8 stations within 1^{o} of its borderline. Again the results were quite different from those previously obtained and the reason for these differences was that

the geoidal characteristics in areas of limited extent were not representative of the average geoidal characteristics across the whole continent. However, in both cases of the smaller areas, the geoid was quite uniform within the region considered (i.e. internally consistent) as the standard deviations of the N residuals were only ± 2.0 metres and ± 1.6 metres respectively.

Five least squares solutions were performed each time the computer program operated and the combinations of observation equations used have been described earlier (see Section 5.3). The two solutions which used only observation equations in ξ or η were of little value, with the results obtained for $\Delta\xi_o$ and $\Delta\eta_o$ respectively being almost equal to the mean of the data values used. The results for the other orientation parameters were up to 20 seconds and 100 metres in error due to the insensitiveness of these observation equations towards the other parameters.

The solution which used only observation equations in N gave results for all three geocentric orientation parameters that agreed with the composite solution values to within 1%. This close comparison of results shows the reliability of both the calculations for the free air geoid values of the deflections of the vertical and the calculations involved in obtaining the astro-geodetic N values.

The solution which used the observation equations for both ξ and η provided good estimates (within ± 0.2 seconds) of the values of $\Delta\xi_o$ and $\Delta\eta_o$. The value of ΔN_o was not realistic as these

observation equations are insensitive with respect to values of N.

The two sets of formulae employed provided results to well within 1% of each other when the same data was used. Since different observation equations were used in these programs, different matrices were manipulated in the adjustment procedures, and this degree of comparison was satisfactory. The set of geocentric orientation parameters derived from the geoid map of Lambeck *(1968a)* was not of any consequence as a means of independently verifying the results as only satellite data had been used for this geoid determination. The results for orientation parameters differed by up to 2 seconds in $\Delta\xi_o$ and $\Delta\eta_o$ and 15 metres in ΔN_o from the figures in Table 5.1. Solutions which use only satellite data cannot detect any local or even small regional geoidal variations as their method of computation precludes this possibility.

5.5 Conclusions.

From a study of the results in this Chapter, no significant differences were obtained in the values computed for the geocentric orientation parameters $\Delta\xi_o$, $\Delta\eta_o$ and ΔN_o when data at either the corners of a regular grid or at unevenly spaced Laplace stations was used, provided the same regions were covered by both solutions.

Although it was expected that the indirect effect would be small, either method of effecting comparisons was thought to be adequate for the verification of the indirect effect formulae. The standard

deviation of the residuals in N were expected to decrease when the corrected free air geoid was compared with the astro-geodetic solution. The results of Chapter 6 and the conclusions in Chapter 8 show that the Fischer/Slutsky astro-geodetic and the 1968 free air geoids were not sufficiently precise to detect the small indirect effect in Australia. The 1970 free air geoid *(Mather, 1970a)* has a standard deviation of N residuals of only ± 2.5 metres for Australia-wide comparisons with the Fischer/Slutsky solution. A revised astro-geodetic geoid solution should be available in 1971 and the indirect effect derivation may be verified after comparisons between it and the 1970 free air geoid. The 1968 free air geoid and the Fischer/Slutsky solution meshed together with a standard deviation of ± 3 metres over regions of adequate gravity coverage which included 80% of the area examined.

Geocentric orientation parameters for the Australian Geodetic Datum derived from the calculations in this Chapter are given by,

$$\Delta\xi_o = -4.7 \text{ sec}$$
$$\Delta\eta_o = -4.4 \text{ sec}$$
$$\Delta N_o = 14.0 \text{ metres} \qquad \text{.....(5.1)}$$

The geocentric orientation parameters derived by Mather *(ibid)* differ by 0.5 seconds for $\Delta\xi_o$, 0.1 seconds for $\Delta\eta_o$ and 6.8 metres for ΔN_o (includes a zero order term). These parameters, when applied to the Johnston Origin, can be used to relate station co-ordinate values on the Australian Geodetic Datum to equivalent representations

on a geocentred spheroid with the dimensions of Reference Ellipsoid 1967. The best representation of the geoid at present would be one using the astro-geodetic values of N added to the ΔN values computed from equation (2.29) utilising the above geocentric orientation parameters. Such a geoid, called a geocentred astro-geodetic geoid, is shown in figure (5.2).

The following conclusions can be drawn from the previous Section where the nature of the comparisons between the free air and astro-geodetic geoids was discussed. The exact system of weight coefficients used was of marginal significance when observation equations of the three types set out in equations (2.27), (2.28) and (2.29) were solved simultaneously, once a reasonable set of weight coefficients was defined. Since solutions using comparisons of N values only gave results within 1% of those obtained from solutions combining comparisons of values of N, ξ and η, the problem of assigning weight coefficients could have been avoided.

It is not advisable to use only restricted areas for comparisons of geoid solutions since the results obtained cannot be extrapolated and considered to be representative of large continental areas unless the intermediate zone gravity field is *completely defined*. Geoidal characteristics are essentially of a regional nature. This was illustrated where the standard deviation of the residuals was quite small for determinations restricted to areas of the order of one million square kilometres, but the geocentric orientation parameters computed

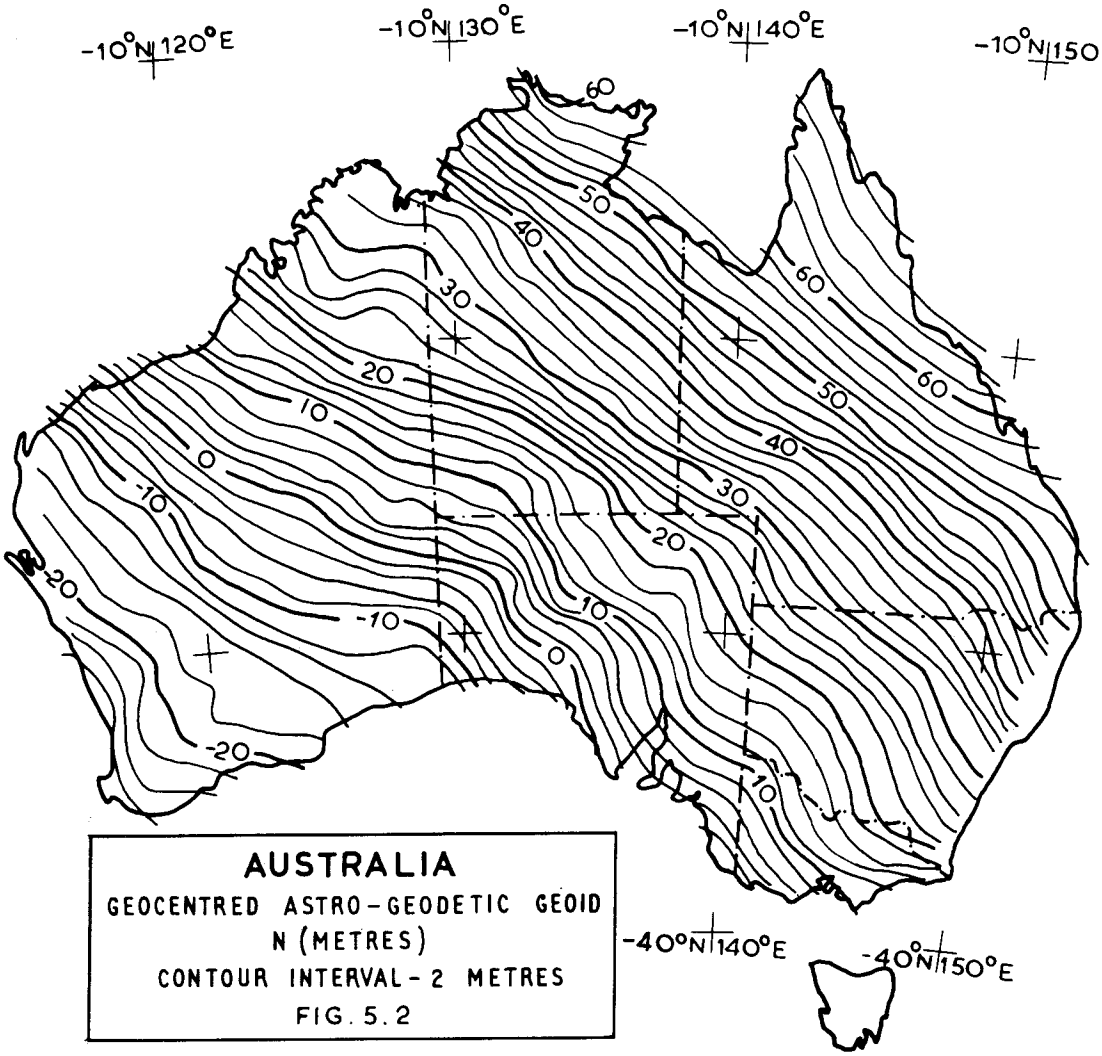

AUSTRALIA

GEOCENTRED ASTRO-GEODETIC GEOID N (METRES)

CONTOUR INTERVAL - 2 METRES

FIG. 5.2

differed significantly from those obtained after a continent-wide solution. This illustrates the need for comparisons between astro-geodetic and gravimetric values over as much of the datum as is possible when computing geocentric orientation parameters for the origin of a control network.

The close meshing of the free air and astro-geodetic geoids indicated that the Vening Meinesz formulae for the computation of gravimetric deflections of the vertical and the system of gravity data input (see Table 4.1) were satisfactory. The standard deviations of the residuals in ξ and η were expected to reduce if the inner zone anomaly field was more completely represented as these regions contributed in excess of 1 sec to the magnitude of the deflections of the vertical.

The geocentric orientation parameters given by equation (5.1) seem to be the most probable from the combination of the 1968 free air and the Fischer/Slutsky astro-geodetic geoid solutions. These geocentric orientation parameters are capable of several improvements, e.g. the sampling of gravity values in the areas of weak gravity anomaly fields and the calculation of the indirect effect. The former of these has been incorporated into the 1970 free air geoid solution with the result that the standard deviations of the N residuals reduced to ± 2.5 metres from a continent-wide solution with the Fischer/Slutsky astro-geodetic geoid. The strengthening of the astro-geodetic solution by the observation of a north-south

chain of closely spaced Laplace stations will also help to provide improved geocentric orientation parameters for the Johnston Origin of the Australian Geodetic Datum. The strengthened astro-geodetic geoid solution should be available in 1971.

CHAPTER 6.

THE INDIRECT EFFECT FOR THE FREE AIR GEOID.

6.1 Introduction.

The complete definition of the geoid over a continental extent requires solutions for a co-geoid and it's indirect effect. The formulae and method of computation of the free air geoid have been fully discussed in Chapters 1 and 4. This Chapter deals firstly with the formulae for the indirect effect and then discusses the results of its computation both globally and in Australia. The magnitude of this effect depends solely on the topography exterior to the geoid. Ocean areas do not contribute to the indirect effect of the free air geoid in any way.

The derivation of the indirect effect for the free air geoid developed in Section 6.2 stems directly from *(Mather, 1968b, p.10 et.seq.)* where the general form of a non-regularised geoid solution is presented. The indirect effect possesses, in addition to a zero order term, both a potential dependent term and one which is Stokesian in character *(ibid, p.32; see also Heiskanen and Moritz, 1967, p.145)*. The potential term is non-Stokesian in character. The approach to the derivation of the indirect effect in this Chapter is similar to the well-known terrain (or topographic) correction approach *(e.g. Molodenskii et.al, (1962), Moritz (1968a) and Pellinen (1962))*, with the following changes in emphasis,

(a) a model representative of the earth's actual topography was used where possible,

(b) the final formulae should be capable of a computerised solution,

(c) with respect to (b) above, the derived formulae should be compatible with the available data, viz., $0.1^{o} \times 0.1^{o}$ mean heights over Australia and $1^{o} \times 1^{o}$ and $5^{o} \times 5^{o}$ mean heights on a global basis,

(d) only the corrections to the free air geoid values of N were to be computed as the amount of data preparation necessary for the near zones to provide corrections to free air geoid values of the deflections of the vertical over a continental extent would have been prohibitive and, in Australia, the results probably would have been insignificant,

(e) where possible, the formulae were derived in "closed form" expressions, as preliminary calculations with series expansions showed that in regions of high topography, some of the terms in $\frac{h}{r}$ were slowly convergent.

It was originally proposed to compute the indirect effect for Australia on a grid with a 1^{o} interval and to obtain a global estimation on a $5^{o} \times 5^{o}$ grid. The world-wide computation was necessary so that the magnitude of the zero order term could be evaluated. Unfortunately these small grid intervals were found to be practically

unsuitable because of the computer time involved and were subsequently modified to 5^{o} x 5^{o} and 15^{o} x 15^{o} grids respectively.

Two studies of the non-Stokesian and Stokesian terms were carried out in mountainous regions using a relatively dense control of height values (see Section 6.3). These calculations were performed along a 17^{o} profile in the Himalayas and a 7^{o} profile across the Snowy Mountains in Australia. The experience gained in these calculations was utilised to provide a basis for approximation in the solutions of continental and global extents.

The non-Stokesian and Stokesian terms were both calculated in two different ways. The former was calculated directly by numerical integration and also by the use of a spherical harmonic analysis. The numerical integration method was expected to provide a more exacting solution as the near zone effects could be evaluated in a more rigorous manner than was possible with a fairly low order harmonic analysis. The spherical harmonic analysis does provide a better indication of the zero order term however. A check on the magnitude of the non-Stokesian term in the Himalayan region was provided from a consideration of the Airy-Heiskanen theory of isostasy *(Heiskanen and Moritz, 1967, p.136)*. A topographic model was constructed and investigated with formulae relating to the potential of such a model *(ibid, pp.127-130)*.

The Stokesian term was more difficult to calculate on a large scale as the differential terrain correction (Δg_c) was exceedingly

dependent on the undulations of the topography in the vicinity of the computation point. The values obtained for Δg_c can only be regarded as likely estimates and for the global and Australian solutions were used in both the classical Stokesian formula and an equivalent spherical harmonic analysis. The spherical harmonic solution was expected to provide the most probable value of the zero order term while the Stokesian formula solution was expected to provide more detailed information regarding the variability of the effect. One check on the Stokesian term results was afforded by comparing the spherical harmonic analysis values for Δg_c with those proposed by Pellinen *(1962, p.63)*.

6.2 Formulae for the Indirect Effect.

Introduction.

A derivation of the indirect effect for the free air geoid is presented below. This derivation stems directly from *(Mather, 1968b, p.10 et.seq.)*, where the general form of a non-regularised geoid solution, including the appropriate indirect effect, was formulated.

The non-regularised geoid solution is given by the expression,

$$N_p = \frac{W_o - U_o}{\gamma_m} + \frac{2\phi_{res}}{\gamma_m} - \frac{R\, M\{\Delta g_{oc}\}}{\gamma_m} + \frac{1}{4\pi\gamma_m R}\iint f(\psi)\ \Delta g_{oc}\ dS \quad .....(6.1)$$

where W_o is the potential of the geoid,

U_o the potential of the reference spheroid,

R the mean radius of the earth,

γ_m the mean value of normal gravity,

$f(\psi)$ is Stokes' function (equation (1.2)),

dS the element of surface area,

N_p the separation between the geoid and spheroid at P,

and $M\{\ \}$ refers to the global mean value.

The gravity anomaly Δg_{oc} is given by,

$$\Delta g_{oc} = \Delta g_f + \left(\frac{\partial \phi e}{\partial h}\right)_S - \left(\frac{\partial \phi e}{\partial h}\right)_G + 2\left(\frac{\partial \phi ei}{\partial h}\right) + \frac{4\phi ei}{R} \qquad .....(6.2)$$

where Δg_f is the free air anomaly,

ϕ_e the potential due to matter exterior to the geoid, the subscripts S and G referring to evaluation at the earth's surface and the equivalent point on the geoid respectively,

and h is the elevation.

The quantity ϕ_{ei} is defined by the equation,

$$\phi e_p = \iint \frac{\tau}{r}\, dS + \phi ei_p \qquad .....(6.3)$$

where τ is a set of surface harmonics and r is the distance of dS from the point P, on the geoid, at which ϕ_e, ϕ_{ei} are evaluated.

ϕ_{res} in equation (6.1) can be represented as,

$$\phi_{res} = \phi_e - \frac{1}{4\pi} \iint \frac{1}{r} \left(2\left(\frac{\partial \phi ei}{\partial h}\right) + \frac{\phi ei}{R}\right) dS \qquad .....(6.4)$$

The indirect effect for the free air geoid is given by,

$$N_{ip} = \frac{W_o - U_o}{\gamma_m} - \frac{R\, M\{\Delta g_{oc}\}}{\gamma_m} + \frac{2\phi_{res}}{\gamma_m} + \frac{1}{4\pi R \gamma_m} \iint f(\psi)\, \Delta g_c\, dS \qquad .....(6.5)$$

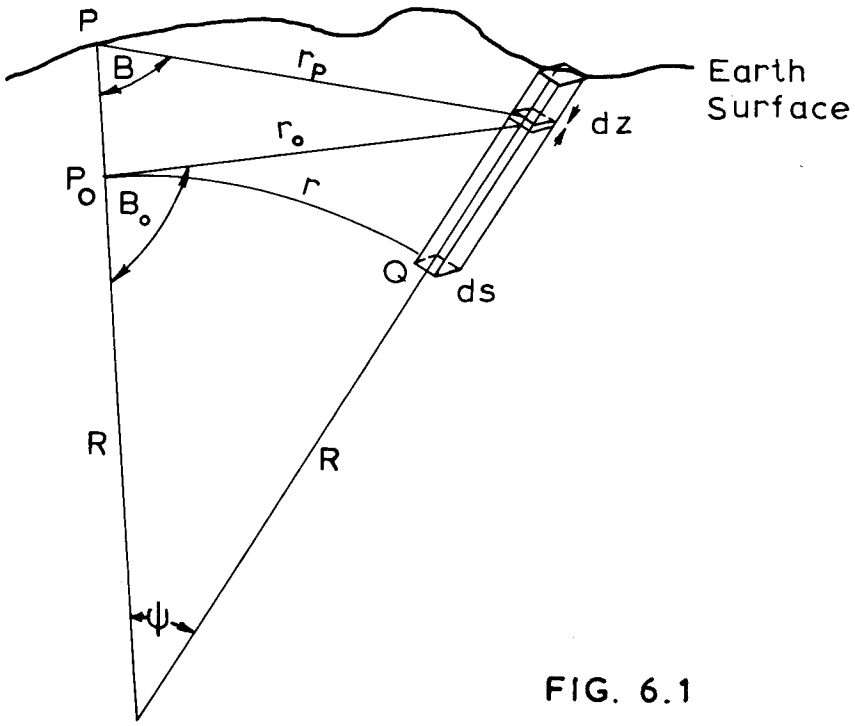
P
B
r_p
Earth
Surface
dz
r_o
P_o
B_o
r
Q
ds
R
R
ψ

FIG. 6.1

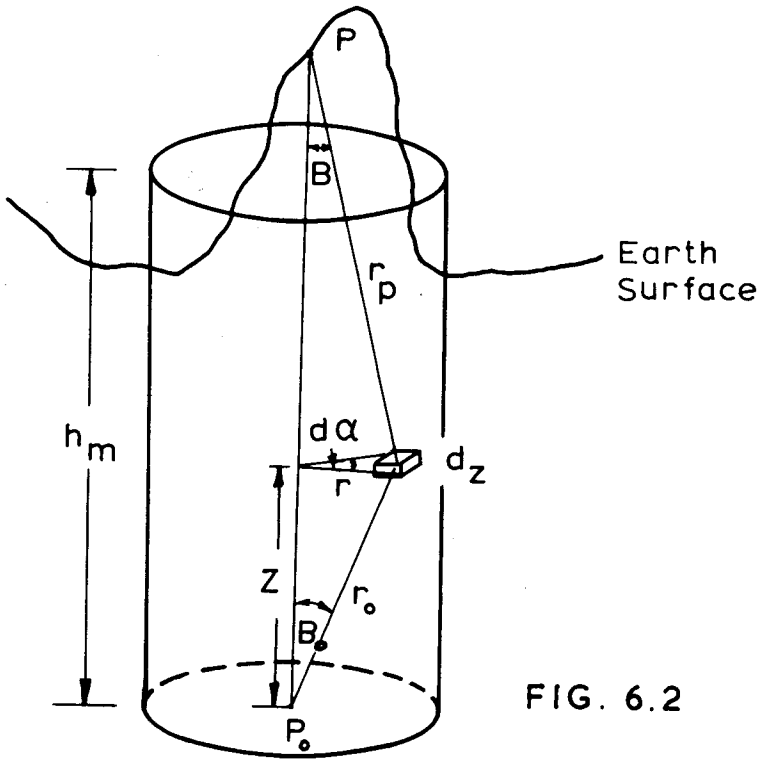
P
B
Earth
Surface
r_p
h_m
dα
d_z
r
Z
r_o
B_o
P_o

FIG. 6.2

where $\Delta g_c = \left(\frac{\partial \phi_e}{\partial h}\right)_S - \left(\frac{\partial \phi_e}{\partial h}\right)_G + 2\left(\frac{\partial \phi_{ei}}{\partial h}\right) + \frac{4\phi_{ei}}{R}$ .....(6.6)

The term ϕ_{ei}

The terms ϕ_e, ϕ_{ei} and their derivatives require careful evaluation in order to formulate the indirect effect for the free air geoid. To obtain a solution correct to the order of the flattening, the earth can be treated as a sphere of radius R and terms of order $\frac{h}{R}$ or less can be neglected.

Consider figure (6.1) and let P_o be the computation point on the geoid and P (elevation h_p) be the equivalent point on the earth's surface. Let dz be a height increment above an elevation z over a surface area element dS at Q, where the elevation of the topography at Q is h. ϕ_{e_p} is given by,

$$\phi_{e_p} = \iiint \frac{k\ dm}{r_o}$$

$$= \iiint \frac{k\ \rho\ dS\ dz}{r_o}$$

where k is the universal gravitational attraction constant,

dm the element of mass whose volume is $dS\ dz$,

ρ the density of matter,

and r_o is given by,

$$r_o^2 = R^2 + (R + z)^2 - 2\ R\ (R + z)\ \cos\psi$$

$$= 4\ R^2\ \sin^2\psi/2 + 4\ R\ z\ \sin^2\psi/2 + z^2$$

$$= r^2 + \frac{r^2\ z}{R} + z^2$$

Thus to the order of the flattening,

$$r_o^2 = r^2 + z^2 \qquad \text{.....(6.7)}$$

For larger values of r,

$$r_o^2 = r^2 \left(1 + \frac{z^2}{r^2}\right)$$

and $\left(\frac{z^2}{r^2}\right) < f$ when $r > 150\text{-}200$ km $\qquad$ .....(6.8)

Assuming 150 km as the limit for the necessity of inclusion of z into formula for r_o, the evaluation of ϕ_{ei} can be performed in three stages, where the innermost zone of radius r_o is treated as a cylinder *(Mather,1968a,pp.107-109)*, viz.,

$$\phi_{e_p} = \left(\iint \frac{k\rho dS}{r} \int_0^h dz \right)_{r>150} + \left(\iint \frac{k\rho dS}{r} \int_0^h dz \left(1-\frac{1}{2}\left(\frac{z}{r}\right)^2+\frac{3}{8}\left(\frac{z}{r}\right)^4\right) \right)_{r_o<r<150}$$

$$+ 2\pi k\rho h_p r_o \left(1 - \frac{h_p}{2r_o} + \frac{h_p^2}{6r_o^2} - \frac{h_p^4}{40r_o^4}\right) - \phi_c$$

where ϕ_c is the potential due to a surface layer of density ρh_p over the area covered by the cylindrical assumption, i.e.,

$$\phi_c = 2\pi k\rho h_p r_o$$

Upon integration with respect to z,

$$\phi_{e_p} = \iint \frac{k\rho h dS}{r} - \iint \frac{k\rho h^3 dS}{6r^3}\left(1-\frac{9}{20}\left(\frac{h}{r}\right)^2\right) - \pi k\rho h_p^2 \left(1-\frac{1}{3}\left(\frac{h_p}{r_o}\right)+\frac{1}{20}\left(\frac{h_p}{r_o}\right)^3\right)$$

.....(6.9)

A comparison of equations (6.3) and (6.9) gives,

$$\phi_{ei} = - \iint \frac{k\rho h^3 dS}{6r^3}\left(1-\frac{9}{20}\left(\frac{h}{r}\right)^2\right) - \pi k\rho h_p^2 \left(1-\frac{1}{3}\left(\frac{h_p}{r_o}\right)+\frac{1}{20}\left(\frac{h_p}{r_o}\right)^3\right) \text{.....(6.10)}$$

and $\tau = k\rho h$ .....(6.11)

From a consideration of equations (6.11) and (6.3), it is possible to define ϕ_{ei} as the difference between ϕ_e and a surface layer of density ρh. From the above derivation it is clear that ϕ_{ei} is dependent only on the near mass distribution and not on distant zones. The magnitude of ϕ_{ei} can be approximately evaluated by considering all values of h equal to h_p and using a series summation for the terms $\left(\frac{h}{r}\right)^3$ in the range $r_o < r < 150$ km where an inner cylinder of radius r_o is excluded. A convenient value for r_o was 0.1^o, as a height data set for Australia has been prepared on this basis.

An approximate calculation shows that the surface integral term contributes only - 0.1 kgal metres to ϕ_{ei} in mountainous regions (elevations up to 10 km). The cylindrical term is of order $- 6 \times h^2 \times 10^{-2}$ kgal metres where h is in kilometres. This term will also only be significant in elevated regions e.g. when h = 5 km, ϕ_{ei} is approximately - 1.5 kgal metres.

The attraction term $\frac{\phi_{ei}}{R}$ is of order $9 \times 10^{-3} \times h^2$ mgal where h is in kilometres, and can be neglected in all regions. The term $\frac{4\phi_{ei}}{R}$ does approach 2 or 3 mgals in the highest regions of the world, but other terms contribute so much more to Δg_c (equation (6.6)) that its inclusion in any solution at the present stage of gravimetric coverage is unwarranted. The effect of this term over a relatively low region like Australia is negligible, approaching only 0.05 mgal in the Snowy Mountains region.

The term $\left(\frac{\partial \phi_e}{\partial h}\right)_G$

It has been shown *(Mather, 1968a, pp.90-91)* that the attractive effects of regions further than 200 km are negligible in the evaluation of $\left(\frac{\partial \phi_e}{\partial h}\right)_G$. This term is the upward attraction at a point on the geoid of the topography exterior to the geoid.

If figure (6.2) is considered, the following expression for $\left(\frac{\partial \phi_e}{\partial h}\right)_G$ can be obtained,

$$\left(\frac{\partial \phi_e}{\partial h}\right)_G = - \iiint \frac{k \, dm}{r_o^2} \cos B_o$$

It is wise to evaluate the integral in two stages,

$$\left(\frac{\partial \phi_e}{\partial h}\right)_G = - \iint k\rho dA \int_o^z \frac{\cos B_o}{r_o^2} \, dz + \text{inner cylinder effect} \qquad .....(6.12)$$

The undulation of the near zone topography is the largest influence on the value of the differential terrain correction Δg_c. In fact regions further than 0.1^o from the computation point generally provide less than 10% of the value of Δg_c. For this reason the inner cylinder effect on Δg_c will be calculated separately later in a manner which allows for some topographical undulation within 0.1^o of the computation point.

If $\left(\frac{\partial \phi_e}{\partial h}\right)_{Go}$ represents the effect outside 0.1^o, then,

$$\left(\frac{\partial \phi_e}{\partial h}\right)_{Go} = - k \iint \frac{\rho dA}{2R} \int_o^h (r^2 - 2Rz) \, (r^2 + z^2)^{-3/2} \, dz \qquad .....(6.13)$$

where $\cos B_o$ in equation (6.12) has been evaluated from a

consideration of figure(6.1) and equation (6.7) as,

$$\cos B_o = \frac{R^2 + r_o^2 - (R + z)^2}{2 R r_o}$$

$$= \frac{r^2 - 2 R z}{2 R r_o} \qquad \ldots\ldots(6.14)$$

The right-hand side of equation (6.13) can be expressed as the difference of two integrals which can be integrated in the manner of *(Lamb, p.175)*, viz.,

$$\left(\frac{\partial \phi_e}{\partial h}\right)_{Go} = - k\rho \iint dA \left(\frac{r^2}{2R} \int_o^h (r^2+z^2)^{-3/2}\, dz - \int_o^h z\, (r^2+z^2)^{-3/2}\, dz \right)$$

$$= - k\rho \iint dA \left(\frac{r^2}{2R} \frac{1}{r^2} z\, (r^2+z^2)^{-\frac{1}{2}} \Big)_o^h + (r^2+z^2)^{-\frac{1}{2}} \Big)_o^h \right)$$

$$= - k\rho \iint dA \left(\frac{h}{2R} (r^2+h^2)^{-\frac{1}{2}} - \frac{1}{r} + (r^2+h^2)^{-\frac{1}{2}} \right) \qquad \ldots\ldots(6.15)$$

<u>The term</u> $\left(\frac{\partial \phi_{ei}}{\partial h}\right)$

Unlike $\left(\frac{\partial \phi_e}{\partial h}\right)_G$ the term $\left(\frac{\partial \phi_{ei}}{\partial h}\right)$ constitutes a major part of both the non-Stokesian term ϕ_{res} (equation (6.4)) and the Stokesian term Δg_{oc}. The inner zone effect of $\left(\frac{\partial \phi_{ei}}{\partial h}\right)$ must be calculated at this stage of the derivation so that it can be included in the formulation of ϕ_{res}. Later this inner zone effect will be revised for its inclusion into the derivation of Δg_c. It will be seen later that it is impractical to include a derivation based on undulating topography within the inner zone in "working" formulae for ϕ_{res}.

ϕ_{ei} may be interpreted as the difference between two scalars,

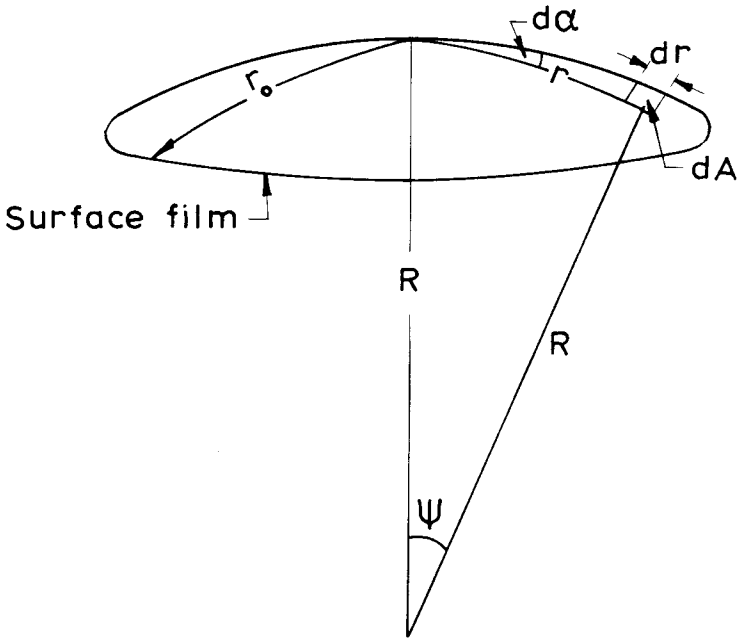

FIG. 6.3

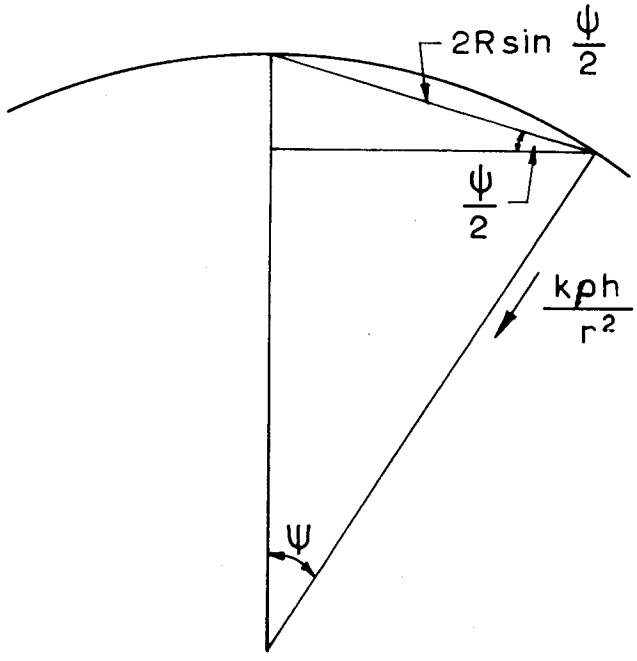

FIG. 6.4

$$\phi_{ei} = \phi_e - \iint \frac{k\rho h}{r}\, dA \qquad .....(6.16)$$

$$= \phi_e - \phi_s$$

where ϕ_s is the potential due to a surface film of density ρh. Upon differentiation we obtain,

$$\left(\frac{\partial \phi_{ei}}{\partial h}\right) = \left(\frac{\partial \phi_e}{\partial h}\right)_G - \frac{\partial}{\partial h}\left(\iint \frac{k\rho h}{r}\, dA\right)$$

$$= \left(\frac{\partial \phi_e}{\partial h}\right)_G + \iint \frac{k\rho h}{r^2} \sin\psi/2\, dA \qquad .....(6.17)$$

The second term in equation (6.17) was obtained from a consideration of the actual physical quantities involved. The problem resolved itself into converting the potential of the surface film over an area dA into an attractive force acting at a distance r from the computation point (consider figures (6.3) and (6.4)).

Distant zones have a negligible effect on $\left(\frac{\partial \phi_{ei}}{\partial h}\right)$, so since r will never be greater than 150 km, the following approximation to the order of the flattening is permissible,

$$\sin\psi/2 = \frac{r}{2R} \qquad .....(6.18)$$

Treating the inner zone effect of $\left(\frac{\partial \phi_e}{\partial h}\right)_G$ as a cylinder of radius r_o *(see Heiskanen and Moritz, 1967, p.128, equation (3.6) for general formula for the attraction of a cylinder)* and substituting equation (6.15) into (6.17),

$$\left(\frac{\partial \phi_{ei}}{\partial h}\right) = k\rho \iint dA \left(\frac{1}{r} - (r^2+h^2)^{-\frac{1}{2}} \right) \left(1 + \frac{h}{2R} \right) + \iint_{r \leqslant r_o} \frac{k\rho h}{2Rr} dA$$

$$+ 2\pi k\rho \left(h + r_o - (r_o^2+h^2)^{\frac{1}{2}}\right) \qquad .....(6.19)$$

The second term in equation (6.19) can be readily evaluated as below,

$$\iint_{r \leqslant r_o} \frac{k\rho h}{2Rr} dA = k\rho h \int_o^{r_o} \int_o^{2\pi} \frac{r \, d\alpha \, dr}{r^2} \frac{r}{2R}$$

$$= \frac{k\rho h \pi r_o}{R} \qquad .....(6.20)$$

Since this term (equation (6.20)), is always less than 1% of the magnitude of the inner zone cylinder term, it will be neglected from later evaluations. In fact it never exceeds 1 mgal even when the height is extended to 10 km.

The final form of $\left(\frac{\partial \phi_{ei}}{\partial h}\right)$ becomes,

$$\left(\frac{\partial \phi_{ei}}{\partial h}\right) = k\rho \iint dA \left(\frac{1}{r} - (r^2 + h^2)^{-\frac{1}{2}} \right) \left(1 + \frac{h}{2R} \right)$$

$$+ 2\pi k\rho \left(h + r_o - (r_o^2 + h^2)^{\frac{1}{2}}\right) \qquad .....(6.21)$$

From a comparison of equations (6.15) and (6.21) and noting that $\frac{h}{2R}$ is of the order of the flattening, it can be concluded that,

$$\left(\frac{\partial \phi_{ei}}{\partial h}\right) = \left(\frac{\partial \phi_e}{\partial h}\right)_G + O\{f \frac{\partial \phi_{ei}}{\partial h}\} \qquad .....(6.22)$$

The term $\left(\frac{\partial \phi_e}{\partial h}\right)_S$

This term represents the attraction effect of the topography

exterior to the geoid at a point on the physical surface of the earth.

In a manner similar to the derivation for $\left(\frac{\partial \phi_e}{\partial h}\right)_G$ and considering figure (6.2),

$$\left(\frac{\partial \phi_e}{\partial h}\right)_S = - \iint \frac{k \, dm}{r_p^2} \cos B \qquad \ldots\ldots (6.23)$$

where to the order of the flattening, and for r less than 300 km,

$$r_p^2 = (h_p - z)^2 + r^2 \qquad \ldots\ldots (6.24)$$

and
$$\cos B = \frac{r_p^2 + (R+h_p)^2 - (R+z)^2}{2 \, r_p \, (R+h_p)}$$

$$= \frac{r^2 + (h_p - z)^2 + 2 R (h_p - z) + h_p^2 - z^2}{2 \, r_p \, R \left(1 + \frac{h_p}{R}\right)}$$

$$= \frac{r^2 + 2 R (h_p - z) + 2 h_p (h_p - z)}{2 \, r_p \, R} \qquad \ldots\ldots (6.25)$$

If the technique of subdividing the integration into two zones based on an inner zone cylinder boundary of radius r_o is employed, then for the same reasons as with the derivation of $\left(\frac{\partial \phi_e}{\partial h}\right)_G$ leaving the inner zone evaluation until later, and using the subscript o to refer to evaluation outside a radius r_o of the computation point,

$$\left(\frac{\partial \phi_e}{\partial h}\right)_{So} = - \iint \frac{k \rho dA}{2R} \int_o^h \frac{r^2 + 2 R (h_p - z) + 2 h_p (h_p - z)}{(r^2 + (h_p - z)^2)^{3/2}} \qquad \ldots\ldots (6.26)$$

$$= - \iint k \rho dA \int_o^h \left(\frac{\frac{r^2}{2R} + (h_p - z)}{(r^2 + (h_p - z)^2)^{3/2}} \right) dz$$

$$\text{i.e. } \left(\frac{\partial \phi_e}{\partial h}\right)_{So} = \iint k\rho dA \int_o^h \left(\frac{r^2 \, d(-z)}{2 R \, (r^2 + (h_p - z)^2)^{3/2}} + \frac{(h_p - z) \, d(h_p - z)}{(r^2 + (h_p - z)^2)^{3/2}} \right) \quad \ldots\ldots (6.27)$$

The integration of equation (6.27) can be performed in the manner of *(Lamb, p.175)*, viz.,

$$\left(\frac{\partial \phi_e}{\partial h}\right)_{So} = \iint k\rho dA \left(\frac{r^2}{2R} \frac{1}{r^2} \left(\frac{h_p - h}{(r^2 + (h_p - h)^2)^{\frac{1}{2}}} - \frac{h_p}{(r^2 + h_p^2)^{\frac{1}{2}}} \right) - (r^2 + (h_p - h)^2)^{-\frac{1}{2}} + (r^2 + h_p^2)^{-\frac{1}{2}} \right) \quad \ldots\ldots (6.28)$$

As the first half of the terms on the right-hand side of the above equation are much smaller than those in the latter half, equation (6.28) may be rewritten, without making any significant errors as,

$$\left(\frac{\partial \phi_e}{\partial h}\right)_{So} = \iint k\rho dA \left((r^2 + h_p^2)^{-\frac{1}{2}} - (r^2 + (h_p - h)^2)^{-\frac{1}{2}} \right) \quad \ldots\ldots (6.29)$$

The Non-Stokesian Term in the Indirect Effect.

This term is given by,

$$\frac{2}{\gamma_m} \phi_{res} = \frac{2}{\gamma_m} \left(\phi_e - \frac{1}{4\pi} \iint \frac{1}{r} \left(2 \left(\frac{\partial \phi_{ei}}{\partial h} \right) + \frac{\phi_{ei}}{R} \right) dS \right) \quad \ldots\ldots (6.30)$$

From the discussion immediately following equations (6.10) and (6.11) it was decided that the inclusion of the term $\frac{\phi_{ei}}{R}$ is unwarranted at the present stage of world gravimetric coverage. Incorporating equation (6.21) into equation (6.30),

$$\frac{2}{\gamma_m} \phi_{res} = \frac{2}{\gamma_m} \left(\phi_e - \frac{1}{2\pi} \iint \frac{dS}{r} k\rho \left(\iint dA \left\{ \frac{1}{r} - (r^2 + h^2)^{-\frac{1}{2}} \right\} + 2\pi \left(h + r_o - (r_o^2 + h^2)^{\frac{1}{2}} \right) \right) \right)$$

$$\text{i.e. } \frac{2}{\gamma_m}\phi_{res} = \frac{2}{\gamma_m}\left(\phi_e - \iint \frac{k\rho h dS}{r} + \iint \frac{k\rho dS}{r}\left((r_o^2+h^2)^{\frac{1}{2}} - r_o - \frac{1}{2\pi}\iint dA\left\{\frac{1}{r} - (r^2+h^2)^{-\frac{1}{2}}\right\}\right)\right)$$

From equation (6.16),

$$\phi_{ei} = \phi_e - \iint \frac{k\rho h dS}{r}$$

A more suitable form of the non-Stokesian term in the indirect effect for the free air geoid is given by,

$$\frac{2}{\gamma_m}\phi_{res} = \frac{2}{\gamma_m}\left(\phi_{ei} + \iint \frac{k\rho dS}{r}\left((r_o^2+h^2)^{\frac{1}{2}} - r_o - \frac{1}{2\pi}\iint dA\left\{\frac{1}{r} - (r^2+h^2)^{-\frac{1}{2}}\right\}\right)\right) \quad \ldots\ldots(6.31)$$

where ϕ_{ei} is defined by equation (6.10).

The Stokesian Term in the Indirect Effect.

The differential terrain correction Δg_c was represented in equation (6.6) as,

$$\Delta g_c = \left(\frac{\partial \phi_e}{\partial h}\right)_S - \left(\frac{\partial \phi_e}{\partial h}\right)_G + 2\left(\frac{\partial \phi_{ei}}{\partial h}\right) + \frac{4\,\phi_{ei}}{R}$$

However, from the discussion concerning the term ϕ_{ei} and from equation (6.22), this may be rewritten as,

$$\Delta g_c = \left(\frac{\partial \phi_e}{\partial h}\right)_S + \left(\frac{\partial \phi_e}{\partial h}\right)_G \quad \ldots\ldots(6.32)$$

without the introduction of significant error. The outer zone contribution to Δg_c has been derived in equations (6.15) and (6.29) and neglecting the small order terms may be expressed as below,

$$\Delta g_{co} = \iint k\rho dA\left((r^2+h_p^2)^{-\frac{1}{2}} - (r^2+h^2)^{-\frac{1}{2}} + \frac{1}{r} - (r^2 + (h_p-h)^2)^{-\frac{1}{2}}\right) \quad \ldots\ldots(6.33)$$

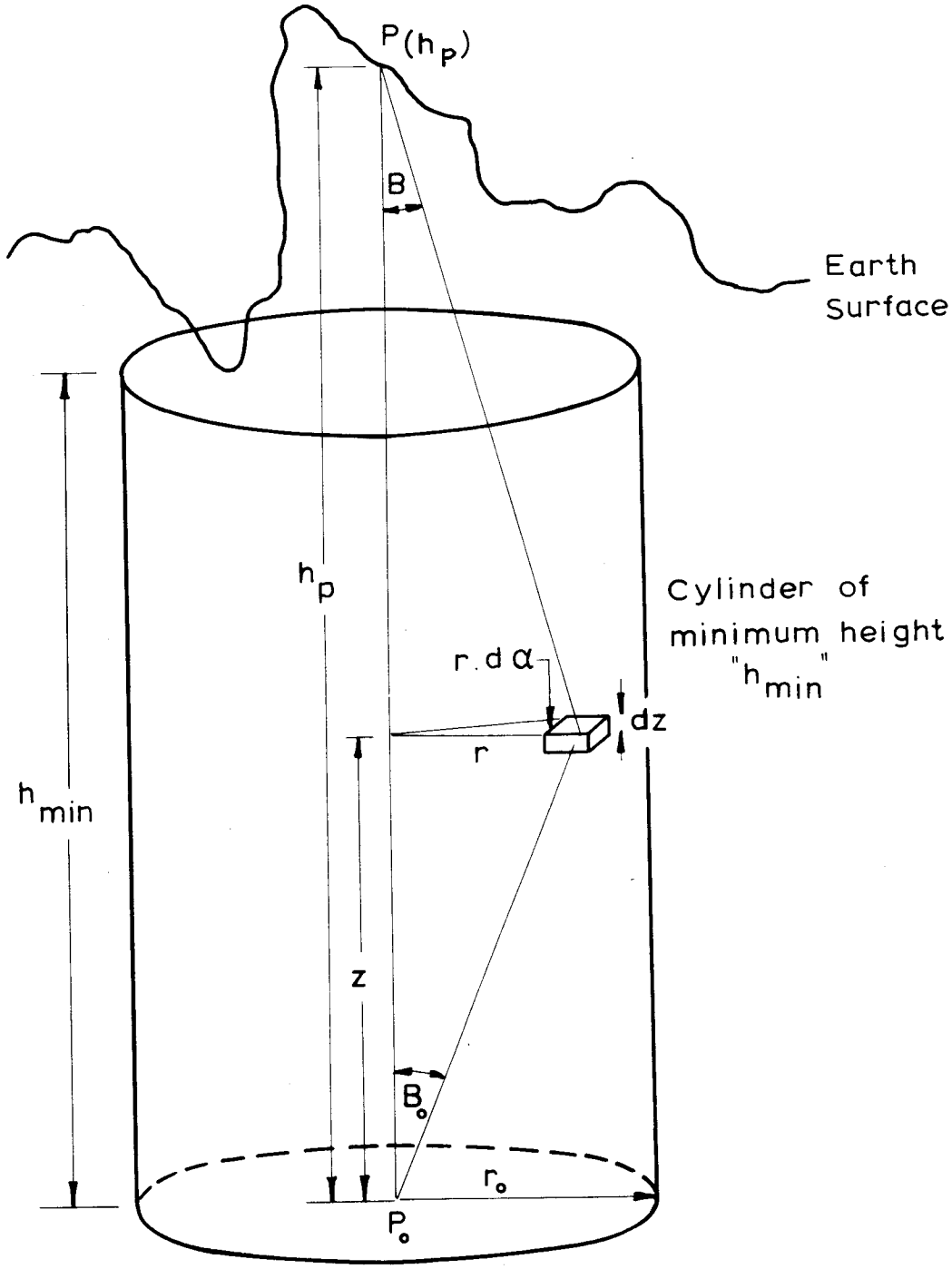
P(h_P)
B
Earth
Surface
h_p
Cylinder of
minimum height
"h_min"
r.dα
dz
r
h_min
z
B_o
r_o
P_o

FIG. 6.5

As mentioned earlier, the inner zone effect generally contributes approximately 90% of the value of Δg_c. The evaluation of the inner zone of radius r_o has therefore been performed in two stages. The effect of a cylinder of height equal to the minimum h_{min} in the inner zone is calculated separately from the effect of the undulating topography above that cylinder. Consider figure (6.5) and,

$$\left(\frac{\partial \phi_e}{\partial h}\right)_{Gi} = \int_o^{h_{min}} \int_o^{r_o} \int_o^{2\pi} \frac{k\rho r d\alpha dz dr \cos B_o}{(z^2 + r^2)} + k \iint \rho dA \int_{h_{min}}^{h} \frac{dz \cos B_o}{(z^2 + r^2)}$$

$$= \int_o^{h_{min}} \int_o^{r_o} \int_o^{2\pi} \frac{k\rho r d\alpha dz dr\, z}{(z^2 + r^2)^{3/2}} + k \iint \rho dA \int_{h_{min}}^{h} \frac{dz\, z}{(z^2 + r^2)^{3/2}}$$

$$= 2\pi k\rho \left(h_{min} + r_o - (h_{min}^2 + r_o^2)^{\frac{1}{2}}\right) + k\rho \iint dA \left((h_{min}^2 + r^2)^{-\frac{1}{2}} - (h^2 + r^2)^{-\frac{1}{2}}\right) \quad \ldots\ldots (6.34)$$

Also,

$$\left(\frac{\partial \phi_e}{\partial h}\right)_{Si} = - \int_o^{h_{min}} \int_o^{r_o} \int_o^{2\pi} \frac{k\rho r d\alpha dz dr \cos B}{((h_p - z)^2 + r^2)} - k \iint \rho dA \int_{h_{min}}^{h} \frac{dz \cos B}{((h_p - z)^2 + r^2)}$$

$$= - \int_o^{h_{min}} \int_o^{r_o} \int_o^{2\pi} \frac{k\rho r d\alpha dz dr (h_p - z)}{((h_p - z)^2 + r^2)^{3/2}} - k \iint \rho dA \int_{h_{min}}^{h} \frac{dz\, (h_p - z)}{((h_p - z)^2 + r^2)^{3/2}}$$

$$= - 2\pi k\rho \left(h_{min} + ((h_p - h_{min})^2 + r_o^2)^{\frac{1}{2}} - (h_p^2 + r_o^2)^{\frac{1}{2}}\right) + k\rho \iint dA \left((r^2 + (h_p - h_{min})^2)^{-\frac{1}{2}} - (r^2 + (h_p - h)^2)^{-\frac{1}{2}}\right) \quad \ldots\ldots (6.35)$$

From equation (6.32), without the introduction of significant error,

$$\Delta g_{ci} = 2\pi k\rho \left(r_o - (h_{min}^2+r_o^2)^{\frac{1}{2}} + (h_p^2+r_o^2)^{\frac{1}{2}} - ((h_p-h_{min})^2 + r_o^2)^{\frac{1}{2}}\right) + k\rho \iint dA \left\{(r^2+h_{min}^2)^{-\frac{1}{2}} - (r^2+h^2)^{-\frac{1}{2}} - ((h_p-h)^2 + r^2)^{-\frac{1}{2}} + ((h_p-h_{min})^2 + r^2)^{-\frac{1}{2}}\right\} \quad .....(6.36)$$

The differential terrain correction to be used in the Stokesian term in the indirect effect for the free air geoid is defined by equations (6.33) and (6.36).

6.3 Computational Procedures.

The Non-Stokesian Term.

The non-Stokesian (potential) term of equation (6.31) has one surface integral inside another. As the outer integral is a global effect, the computer time required would have been excessive if the inner integral had to be continually evaluated. The outer integral uses area mean values of the function D (in gm/cm^2), where,

$$D = \rho \left((r_o^2+h^2)^{\frac{1}{2}} - r_o - \frac{1}{2\pi} \iint dA \left\{\frac{1}{r} - (r^2+h^2)^{-\frac{1}{2}}\right\}\right) \quad .....(6.37)$$

The size of the area to be used in the outer integral depends on the distance of that area from the computation point. Upon examination of equation (6.31), it was concluded that for all regions further than r_o from the computation point the inner surface integral could be approximated to the following series expansion, noting that $h < r_o < r$,

$$\iint dA \left\{\frac{1}{r} - (r^2+h^2)^{-\frac{1}{2}}\right\} = \sum\sum \frac{dA}{2}\left(\frac{h^2}{r^3} - \frac{3}{4}\frac{h^4}{r^5} + \ldots.\right) \qquad .....(6.38)$$

Ideally the evaluation of the right-hand side of equation (6.38) would involve values for h at all small areas dA which are at a distance r from the centre of the area dS which is to be used in the outer integration. Point by point computations are impractical and so mean height values over small areas must be employed. If 0.1^o x 0.1^o mean height values are used to represent the areas dA for the inner summation out to a distance of 3^o from the centre of the area dS, then a complete world-wide coverage of tenth degree mean height values is required. This is the same problem that makes an accurate calculation of the Stokesian term impractical.

The problem is overcome in this case by assuming that all 0.1^o x 0.1^o mean height values within 3^o of the centre of the area being used in the evaluation are the same and are equal to the 1^o x 1^o mean height representing the centre of the area. The summation of $\frac{1}{r^3}$ and $\frac{1}{r^5}$ may now be separately undertaken on a tenth degree grid basis up to 3^o. The results of these calculations for each degree of latitude were obtained in the form of card output so that they could be fed directly into the computer programs dealing with the calculation of the non-Stokesian term. 3^o was decided upon as the practical limit for the summation of equation (6.38) after tests involving the convergence of $\frac{1}{r^3}$.

The non-Stokesian computations on a global scale were based on a $5^o \times 5^o$ area for dS. The value of each of these $5^o \times 5^o$ areas was derived from the mean of 25 values of the function D (equation (6.37)) where values of h used were the 25 $1^o \times 1^o$ mean heights enclosed by the particular $5^o \times 5^o$ area. Approximately 1200 $5^o \times 5^o$ areas had values different from zero, the remaining 1400 areas being in regions totally occupied by oceans, or possessing land masses of a size too small to produce an overall positive mean height in a $1^o \times 1^o$ world-wide grid system.

An estimate of the accuracy of the mean height assumption in equation (6.31) was obtained from the calculations below. This assumption should provide summation values of $\frac{h^2}{r^3}$ and $\frac{h^4}{r^5}$ to an accuracy of a few percent of the values obtained using detailed height control. If an area is considered with an average height of 5 km, composed of tenth degree squares whose mean heights are 4 km and 6 km, the value of h^2 using the mean height for the total area is 25 km^2, while h^2 has a value of,

$$\frac{(16 + 36)}{2} \text{ km}^2 = 26 \text{ km}^2$$

using the tenth degree squares. The error here is 4% and since the global mean value of the non-Stokesian term is approximately 3 metres, this corresponds to 12 cm. The sign of this error will be globally systematic but the magnitude will not be constant. The magnitude of this error will be approximately the same as that arising from errors

in the mean height values themselves.

The method of computation which should give the best results is numeric integration. Mean values of D were to be introduced into the calculation over areas which increased in size with distance from the computation point. Originally it was intended to use an input data technique similar to that employed in the free air geoid calculation (Table 4.1). Preliminary calculations showed that the technique referred to above was too time consuming and not essential for the indirect effect formulae. The system employed in the calculations is best explained with reference to figure (6.6). The $5^{o} \times 5^{o}$ square that the computation point lies in is established, and then the eight $5^{o} \times 5^{o}$ squares bordering this square are located. This total area of $15^{o} \times 15^{o}$ is evaluated using $1^{o} \times 1^{o}$ mean heights. The D values of the precalculated $5^{o} \times 5^{o}$ areas are employed for all regions outside the $15^{o} \times 15^{o}$ area.

The density used in the indirect effect formulae is one of the two variable density with respect to height formulae developed from a world-wide sampling *(Hunter 1966)*. The formula chosen for the purpose here is,

$$\rho = 2.77 - \frac{h}{21} \quad gm/cm^{3} \quad \text{for} \quad h<2.1 \text{ km} \ldots\ldots (6.39)$$

For values of h greater than 2100 metres the standard value of 2.67 is adopted for the density. This formula is that which has been adopted by Mather for his free air geoid studies in Australia.

METHOD OF NON-STOKESIAN TERM EVALUATION

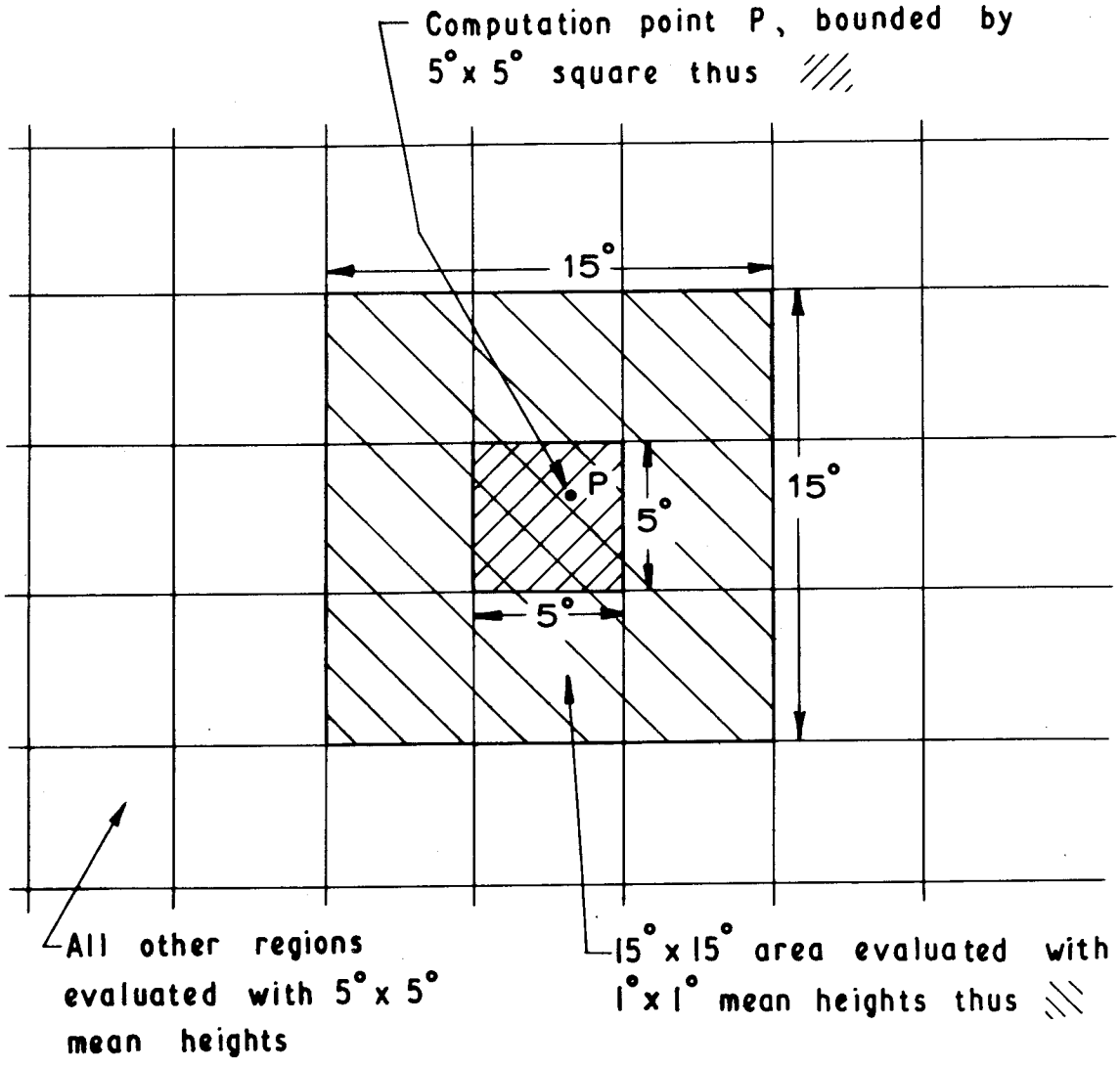

FIG. 6.6

The $1^{o} \times 1^{o}$ height data set was prepared by W.H.K. Lee of the University of California. The mean height values in this set refer to topographical features, and as the indirect effect formulae includes a rock density function which varies with height, (equation(6.39)) the Antarctic ice coverage *(Atlas Antarktiki)* had to be converted to an equivalent rock thickness. The base rock height values for Antarctica are not extremely reliable at the present time. Their values have been obtained from the limited amount of seismic study carried out in the region with large areas relying on interpolation. This situation cannot be expected to rapidly improve in the near future and any solution for the indirect effect of the free air geoid will be preliminary to this extent. The ice thickness in the Antarctic often exceeds 2000 metres and as height terms enter the non-Stokesian formulae raised to the second power, large errors would otherwise have been introduced at this stage of calculation.

During the data preparation it was observed that a $5^{o} \times 5^{o}$ mean height data set designed solely for geodetic purposes of a similar nature to this project did not exist. The result was the geodetic height data set displayed in figures (6.7) to (6.10). All ocean areas in the $1^{o} \times 1^{o}$ mean height data set were given a value of zero metres and then $5^{o} \times 5^{o}$ mean heights were obtained. In the Antarctic polar regions the ice coverage *(Atlas Antarktiki)* was converted to an equivalent rock thickness by multiplication with the ratio of ice to rock densities. Regions on these figures where no

GEODETIC 5°x5° MEAN HEIGHT DATA SET(metres): Northern Hemisphere, Western Longitudes

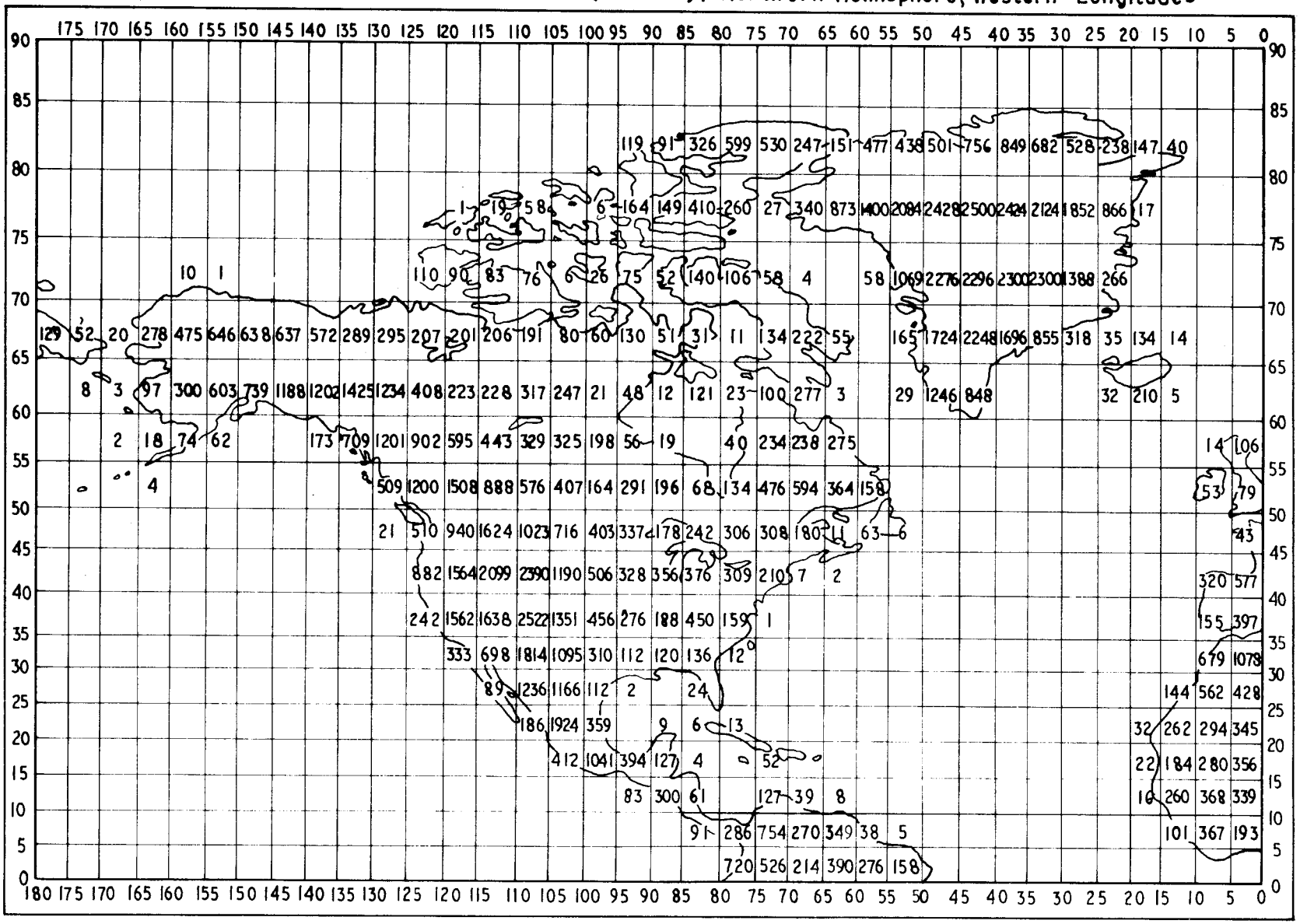

FIG. 6.7

GEODETIC 5° x 5° MEAN HEIGHT DATA SET (metres): Northern Hemisphere, Eastern Longitudes

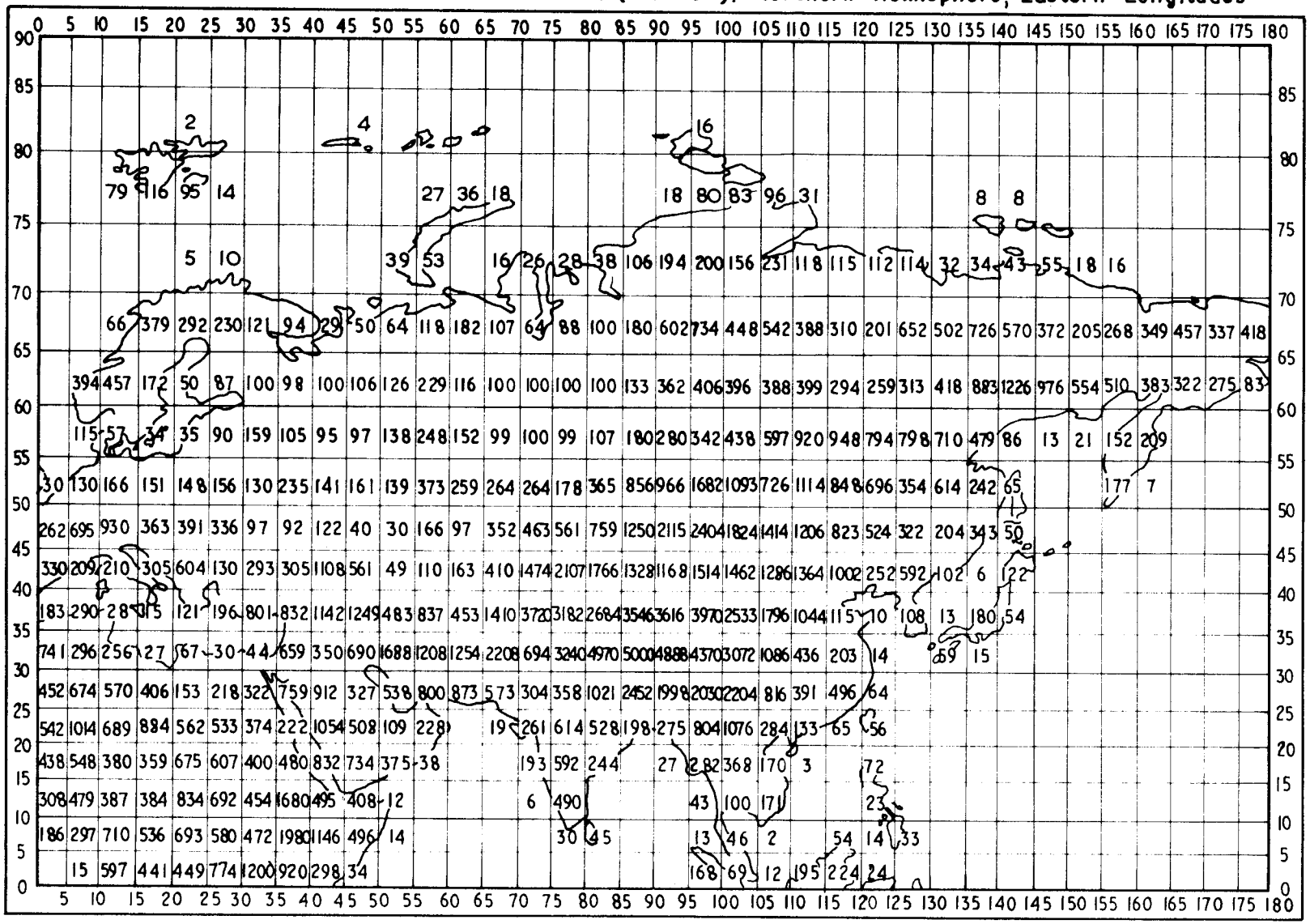

FIG. 6.8

GEODETIC 5°x 5° MEAN HEIGHT DATA SET (metres): Southern Hemisphere, Western Longitudes

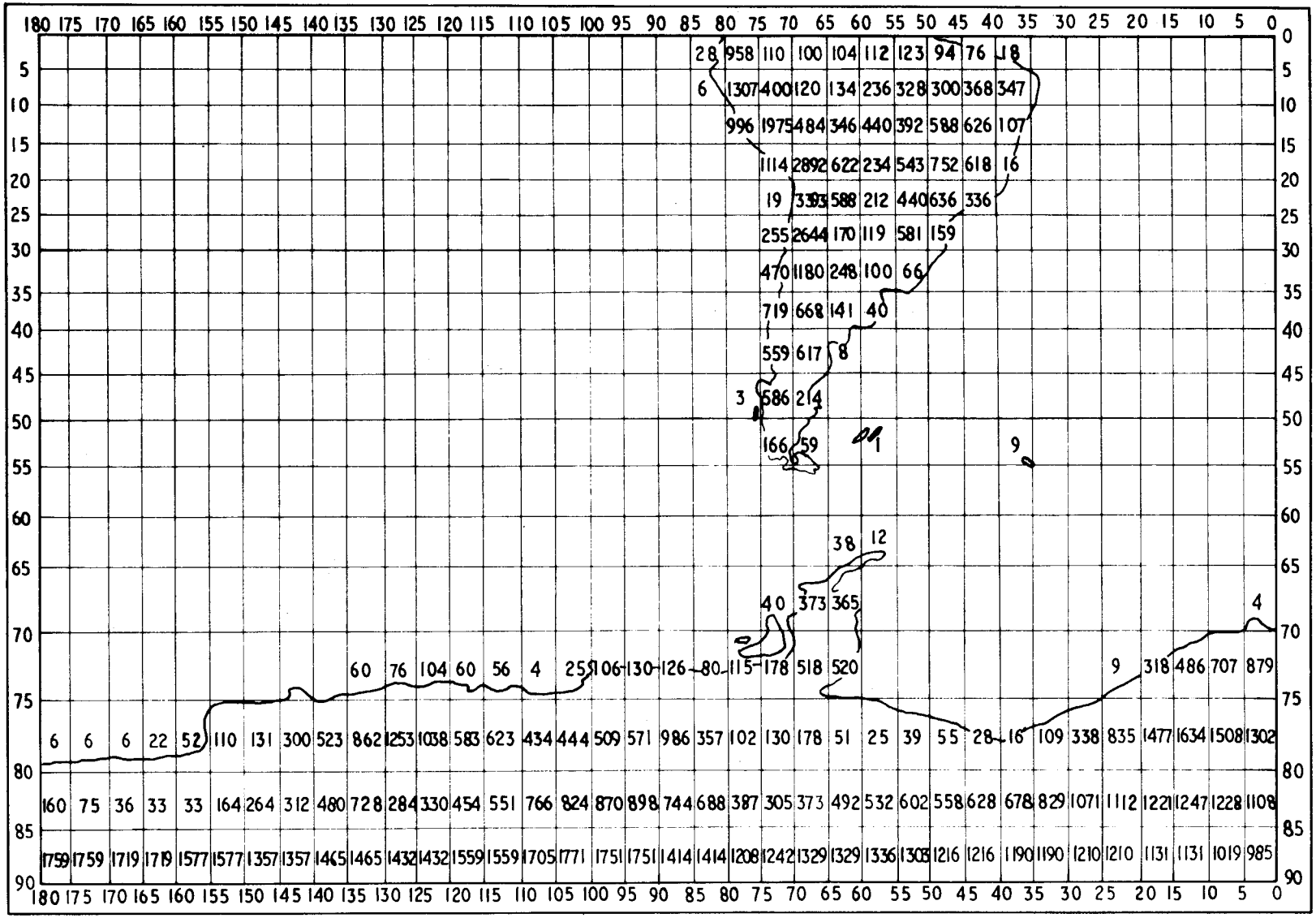

FIG. 6.9

GEODETIC 5°x 5° MEAN HEIGHT DATA SET(metres): Southern Hemisphere, Eastern Longitudes

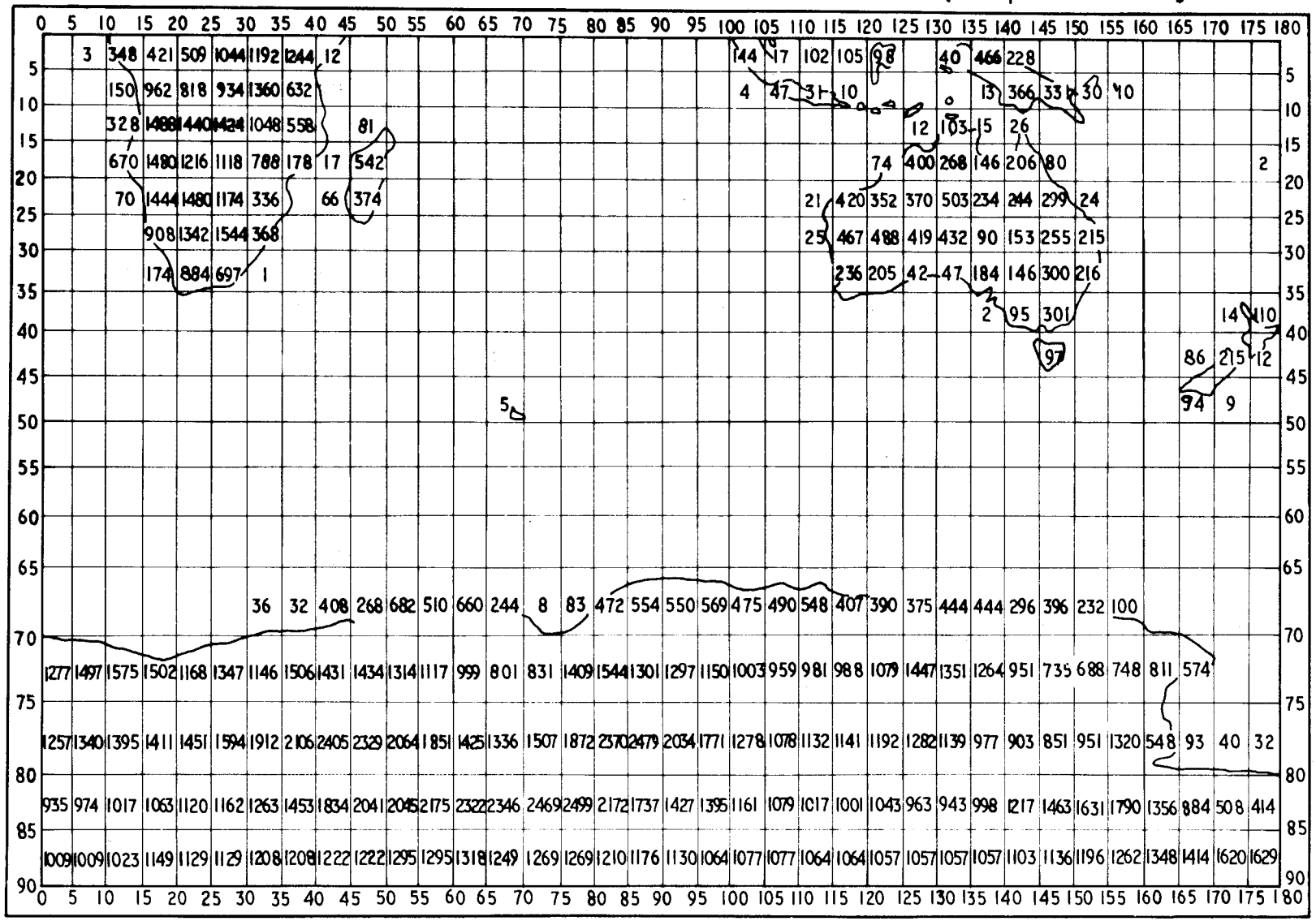

FIG. 6.10

height values are displayed are ocean areas where any islands are too small to record an overall positive mean height value in the 1^{o} x 1^{o} grid system. There are 1160 positive values in the geodetic height data set compared with approximately 860 in an ordinary 5^{o} x 5^{o} height data set.

The other method for calculating the non-Stokesian term employed spherical harmonic analyses of the 5^{o} x 5^{o} precalculated D set of data. These analyses were carried out to orders 4,4, 6,6 and 8,8. All these sets of coefficients appear in Table 6.1. The solution of equation (6.31), excluding the term ϕ_{ei} which was separately calculated, can be expressed in spherical harmonic notation in the following manner *(after Heiskanen and Moritz, 1967, p.30)*,

$$Y_n(\theta,\lambda) = \frac{c(2n+1)}{4\pi} \int_{\lambda'=o}^{2\pi} \int_{\theta'=o}^{\pi} f(\theta',\lambda') \, P_n(\cos\psi) \, \sin\theta' \, d\theta' \, d\lambda' \qquad .....(6.40)$$

where $Y_n(\theta,\lambda)$ is the spherical harmonic solution to degree n representing ϕ_{res} (excluding the term ϕ_{ei}),

c is a constant coefficient containing γ_m, R, k, etc.,

f (θ',λ') are the spherical harmonic coefficients of the data set D,

and P_n $(\cos\psi)$ is the spherical harmonic representation of $\frac{1}{r}$.

The solutions were only performed to order 8,8 because the trends of ϕ_{res} were clearly pronounced at this stage and any higher order solutions would have involved excessive computer time.

SPHERICAL HARMONIC CO-EFFICIENTS OF 5^ox 5^o DATA SET "D" (gm/cm^2)

$$D = \rho\left((r_o^2 + h^2)^{\frac{1}{2}} - r_o - \frac{1}{2\pi}\iint dA\left\{ \frac{1}{r} - (r^2 + h^2)^{-\frac{1}{2}} \right\} \right) \quad \ldots.(6.37)$$

		4,4		6,6		8,8	
n	m	A_{nm}	B_{nm}	A_{nm}	B_{nm}	A_{nm}	B_{nm}
0	0	254.6		246.4		244.4	
1	0	127.6		137.1		133.4	
1	1	86.6	131.2	87.1	136.5	87.1	136.0
2	0	-53.6		-78.1		-83.1	
2	1	-14.1	239.4	-13.3	240.2	-13.6	237.6
2	2	-181.0	44.6	-183.8	44.6	-183.8	44.6
3	0	-161.4		-122.8		-131.0	
3	1	-52.7	33.9	-47.6	86.8	-47.9	83.8
3	2	-227.3	73.8	-232.0	79.0	-235.9	79.1
3	3	-32.4	-20.4	-34.8	-3.5	-35.0	-4.4
4	0	-44.3		-139.8		-150.2	
4	1	9.1	-108.7	14.7	-102.8	13.7	-112.6
4	2	-138.3	19.5	-181.7	20.6	-181.8	20.7
4	3	51.5	-206.5	52.4	-208.0	52.1	-210.1
4	4	99.1	86.2	84.5	90.5	84.9	90.6
5	0			-70.4		-102.0	
5	1			-14.5	-152.5	-16.3	-170.4
5	2			22.8	-25.1	-17.1	-23.9
5	3			22.6	-163.8	18.8	-182.8
5	4			190.0	-115.4	181.5	-118.2
5	5			-0.9	116.3	-0.7	105.4
6	0			176.6		136.6	
6	1			-15.2	-15.6	-20.8	-70.4
6	2			173.2	-4.2	172.5	-2.9
6	3			-5.3	9.7	-8.9	-18.6
6	4			181.1	-52.7	191.4	-50.2
6	5			-69.5	102.5	-70.3	90.5
6	6			-78.7	-24.2	-73.5	-26.0
7	0					59.0	
7	1					4.6	45.7
7	2					141.5	-4.2
7	3					19.6	97.4
7	4					68.2	22.0
7	5					-3.5	166.1
7	6					-124.0	40.3
7	7					-48.6	-101.1
8	0					75.4	
8	1					14.0	135.0
8	2					2.4	-4.2
8	3					15.8	125.0
8	4					-64.0	-15.6
8	5					9.0	113.3
8	6					-93.7	32.4
8	7					89.5	-75.7
8	8					-22.0	-8.2

TABLE 6.1

The term ϕ_{ei} was evaluated in two sections, as equation (6.10) would suggest. The latter half of that equation was solved by direct substitution of the nearest 1^{o} x 1^{o} mean height for the value of h_p. The double integral section was evaluated for the Australian case in two parts; from 0.1^{o} to 1^{o} from the computation point with 0.1^{o} x 0.1^{o} mean height values and from 1^{o} to 10^{o} with 1^{o} x 1^{o} mean heights.

This method of solution was impractical on a global scale due to the enormous task of 0.1^{o} x 0.1^{o} height data preparation. The innermost four 1^{o} x 1^{o} mean height values were utilised for the first part of the computation after considerations similar to those in the discussion of the preparation of the data set D. A maximum magnitude of - 2.92 metres for the term ϕ_{ei} was reached in the Himalayas and a breakdown of this value is presented below;

Direct substitution term (within 0.1^{o})	= - 2.55 metres
Integral term: 0.1^{o} - 1^{o}	= - 0.34 "
" " : 1^{o} - 10^{o}	= - 0.03 "
Total ϕ_{ei}	= - 2.92 metres

In the Snowy Mountains region of Australia this term totalled - 0.018 metres, nearly 200 times smaller than its Himalayan counterpart. The relationship between the size of the indirect effect in Australia and in the Himalayan Mountains is discussed in greater detail in Section 6.4.

The Stokesian Term.

The differential terrain correction Δg_c to be used in the Stokesian term of the indirect effect has been defined by equations (6.33) and (6.36) for outer and inner zones respectively. After some experiments concerning truncation errors, it was decided that 0.1^o x 0.1^o mean heights should be used on the outer zone formula from 0.1^o to 1^o and 1^o x 1^o mean heights from 1^o to 5^o. Height values further away have no significant effect on the result. In fact, approximately 90% of the value of Δg_c comes from within 0.1^o.

A calculation of the Stokesian term of the indirect effect on a global (or continental) scale would require a global coverage of values of Δg_c. Until a method was devised for estimating values of Δg_c from mean height values, the only reasonable alternative was to perform test calculations of the Stokesian effect over mountain ranges that were relatively isolated from other large topographical features. It was assumed that the Stokesian effect of distant zones would be of a constant nature to the regions concerned and the results obtained would validate the relevant formulae. The experience gained in performing these calculations was expected to provide a basis for obtaining estimates of Δg_c on a global scale.

Point by point computation would be the ideal method for the inner zone computation, but to derive mean heights for areas smaller than 0.1^o x 0.1^o would greatly increase both computer and data preparation time. An efficient system of height data input was

required for the computation of equation (6.36) in a reasonably fast time. Speed was essential since the Stokesian term profile (see Section 6.4) computed across the Himalayas was 17^{o} in length and values of Δg_{ci} from equation (6.36) were required every 0.1^{o} along the centre line and up to 5^{o} either side of it.

The cylinder of minimum height part of equation (6.36) was evaluated by averaging the four 0.1^{o} x 0.1^{o} mean heights around the computation point to give a value of h_p. The minimum height value, h_{min}, was the smallest of these four height values. The radius r_o of this cylinder was obtained by making the area of the cylinder base equal to the area of the four tenth degree squares around the computation point.

The undulating topography term (second part of equation (6.36)) used the above values for h_p and h_{min}. Each of the four 0.1^{o} x 0.1^{o} mean height values around the computation point were considered, in turn, as the height, h, of a quarter of a cylinder of radius r_o situated on top of the cylinder of minimum height. When $h = h_{min}$ the undulating topography effect is zero, a simple test of its derivation. The distance r was from the computation point to the centroid of each quarter cylinder. Using these procedures, this term can be quickly evaluated in a computer program. The time taken to compute the differential terrain correction at a point was less than 1 second and while this appeared to be fast, it meant that the gravity anomalies for the Himalayan profile took nearly 2 hours to compute.

6.4 Indirect Effect in Mountainous Regions.

Two studies of profiles were undertaken to investigate the variation of the indirect effect over a mountainous region. One was along the meridian 90^{o} East from 18^{o} to 35^{o} North latitude and the other was along the parallel 36^{o} South from 145^{o} to 152^{o} East longtitude. The former corresponded to a section across the Himalayas whilst the latter was through the Snowy Mountains, the highest region of the Great Dividing Range in Australia. In both cases $0.1^{o} \times 0.1^{o}$ height values were obtained for 5^{o} either side of the centre line of the profile and $1^{o} \times 1^{o}$ mean heights were available for 10^{o} either side. $5^{o} \times 5^{o}$ mean heights were used to calculate the outer zone effects of the non-Stokesian term (equation (6.31)) for regions outside the above-mentioned areas.

The differential terrain correction was calculated in the manner described in the last Section. The outer zone effect (equation (6.33)) was divided into two calculations; from 0.1^{o} to 1^{o} using $0.1^{o} \times 0.1^{o}$ mean heights and from 1^{o} to 5^{o} using $1^{o} \times 1^{o}$ mean heights. The inner zone component (equation (6.36)) of Δg_c was also divided into two calculations. The first part consisted of the cylinder of minimum height and the second of the undulating topography above this cylinder. In rugged mountainous regions the undulating topography effect was as much as twice the magnitude of the minimum height cylinder term. These two terms, which were always positive, together constituted approximately 90% of the value of Δg_c.

Following these procedures, values of Δg_c were computed in a 10^o band and used as data for a Stokesian evaluation along the profile centre line. While 5^o is a suitable limit for the evaluation of Δg_c, a Stokesian evaluation should really be extended to a global coverage. As the profiles were situated in regions possessing the largest values of Δg_c on their respective continents, the distant zone Stokesian effects were assumed to be of a constant nature throughout the profile. The variation of the indirect effect N value along the profile was the major consideration in these calculations and on this basis, the outer zone Stokesian effects were neglected.

Profile along Meridian 90^oE.

The contribution of the non-Stokesian term for the indirect effect N value is shown in figure (6.11). Compared with the average topography it rises smoothly and not as sharply as the physical surface. Mean 1^o topography values have been plotted because the rapidly changing profile surface could not be accurately represented at the small abscissa scale. Deviations from the mean height values plotted of over 1 km in less than 0.1^o of latitude were not uncommon in this region. As figure (6.11) depicts, these rapid variations in height are not directly reflected in values of N obtained from equation (6.31). The outer zone contributions remained constant at approximately 6.3 metres throughout the profile.

The values of Δg_c computed from equations (6.33) and (6.36) are greatly influenced by rapidly changing surface gradients. It is

PROFILES ALONG MERIDIAN 90° E

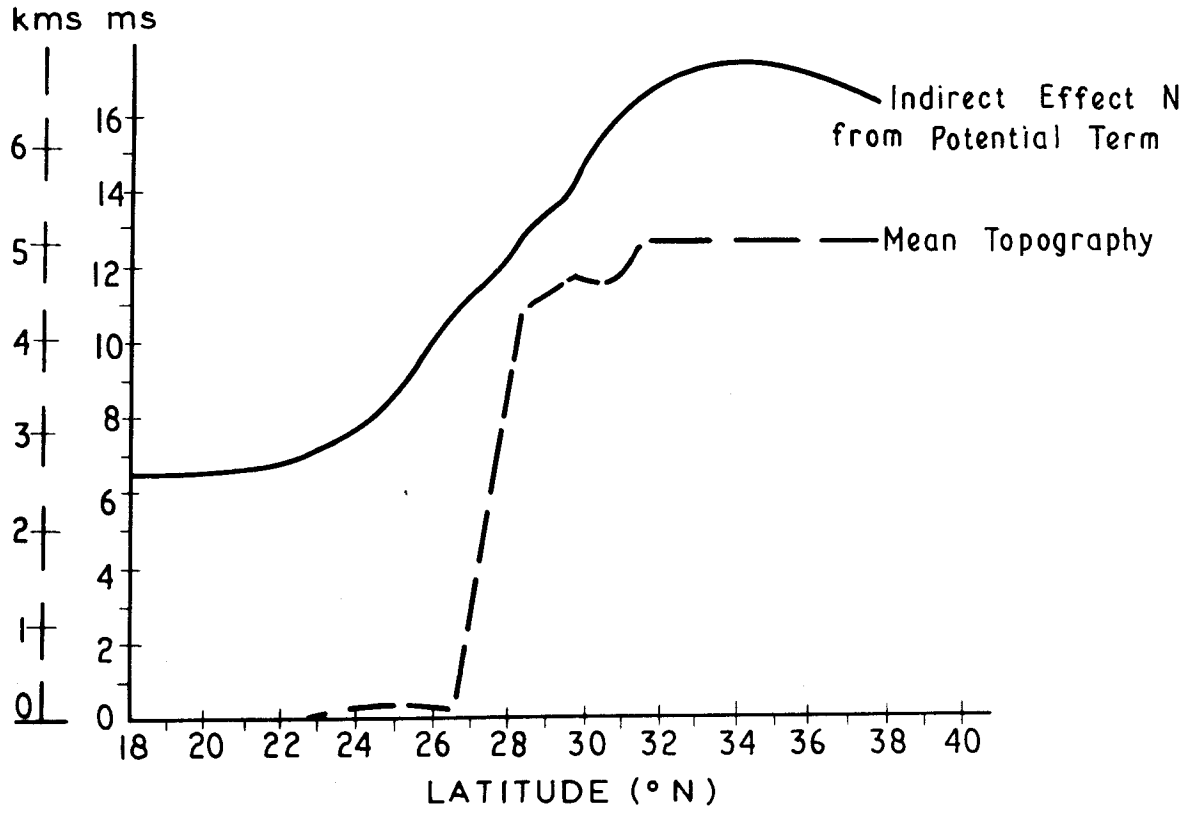

FIG. 6.11

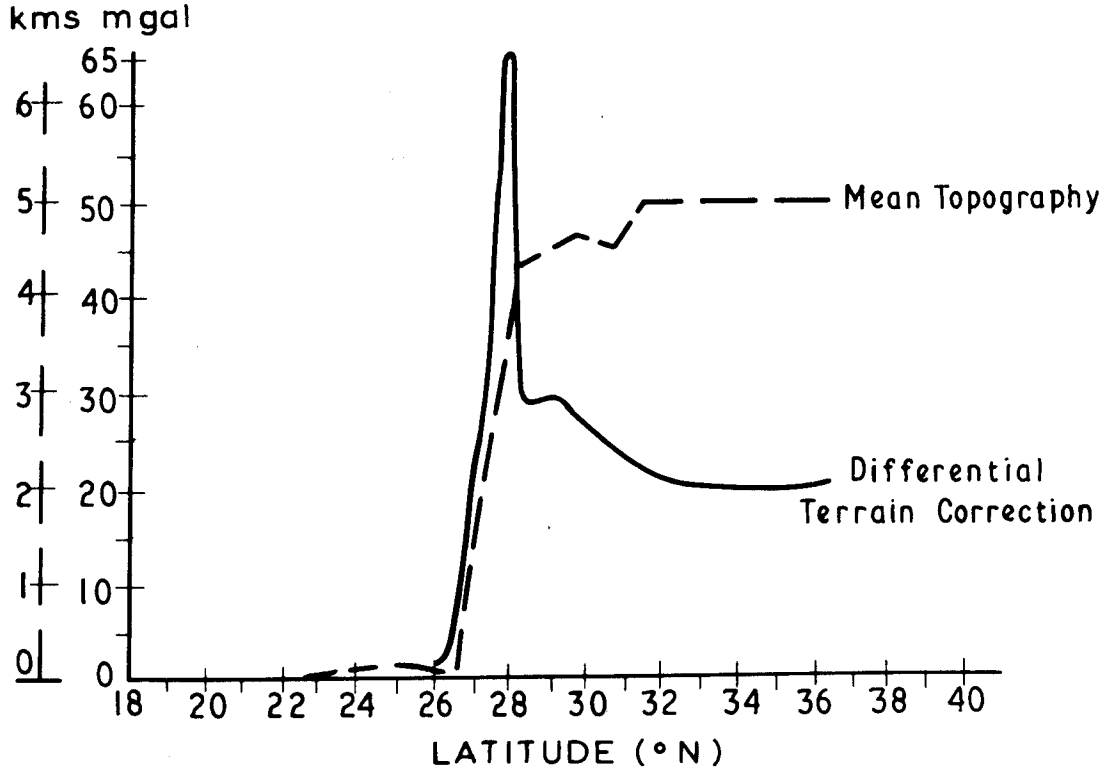

FIG. 6.12

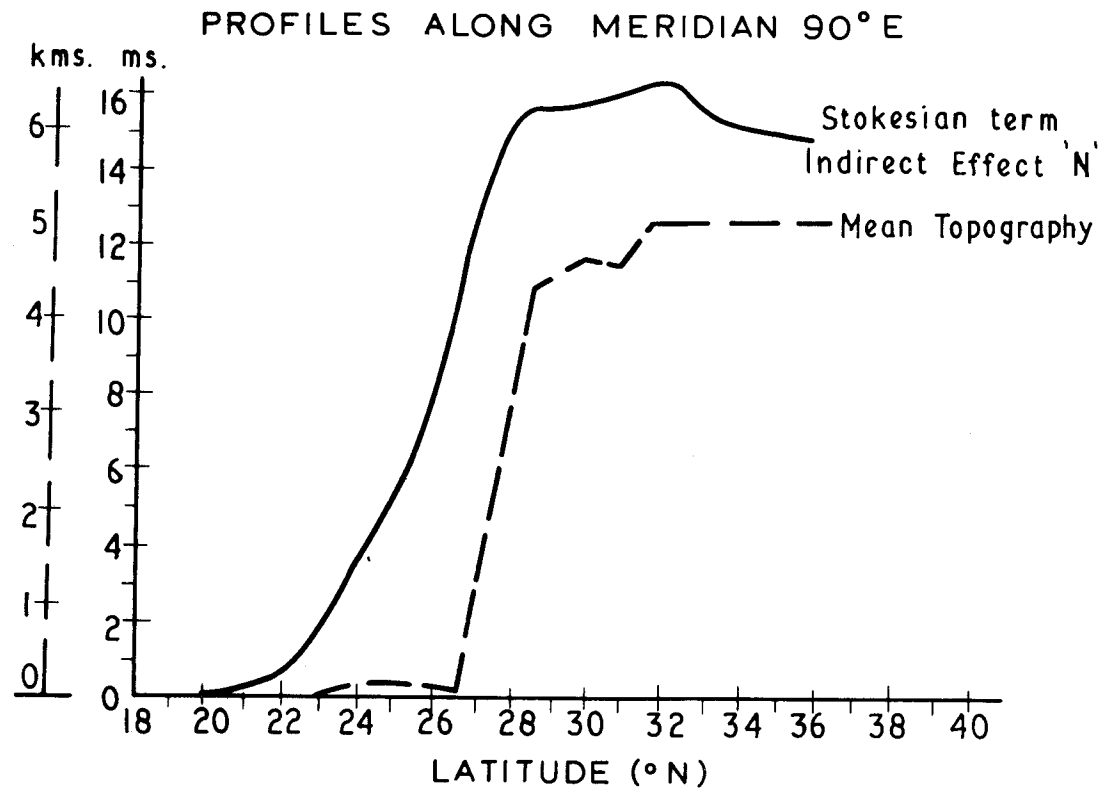

FIG. 6.13

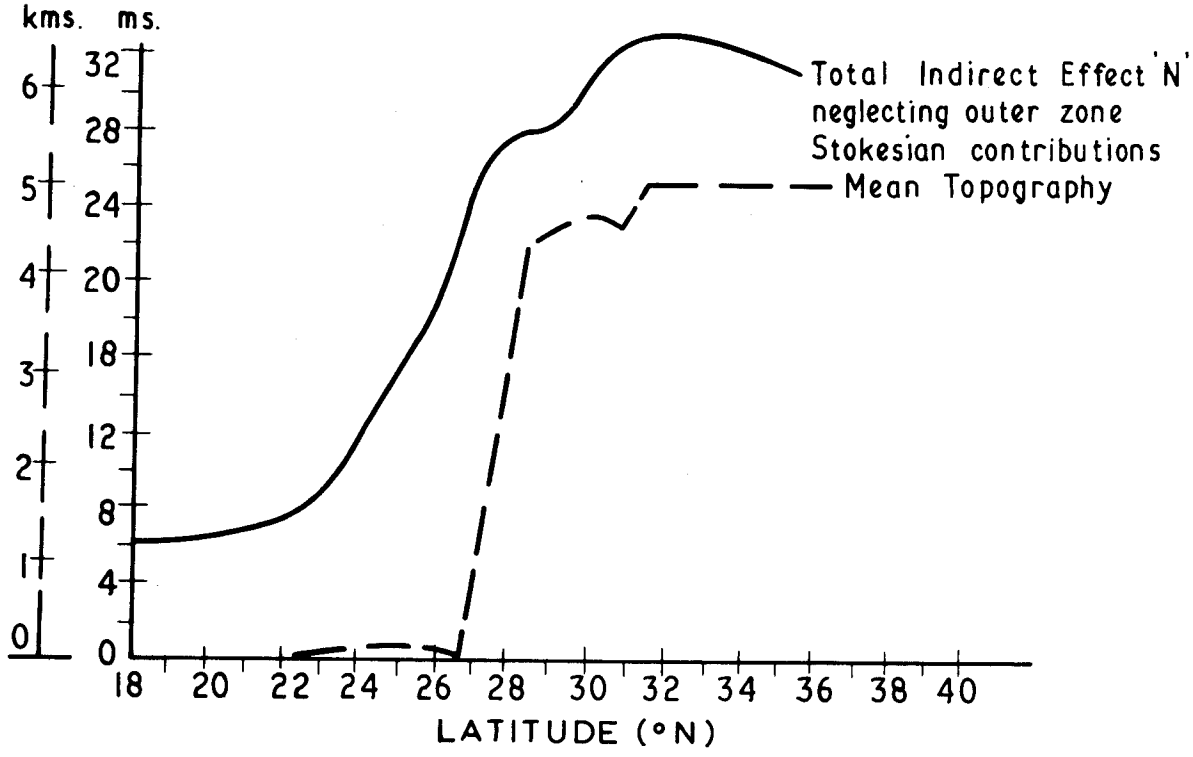

FIG. 6.14

interesting to note that at latitude 27.5°N, the value of Δg_c of + 65 mgal contained only + 11 mgals from outside a radius of 0.1°. The other + 54 mgals were composed of + 19 mgal from the cylinder of minimum height and + 35 mgal from undulating topography on top of that cylinder. The values of Δg_c reduced to a fairly constant average of approximately + 22 mgal per 1° x 1° square when the computations were performed in the plateau-like region from latitudes 31°N to 35°N. These values, shown in figure (6.12), are similar to those derived by Pellinen *(1962, p.64)*.

The Stokesian N value (figure (6.13)) computed from the differential terrain corrections described above shows a marked similarity to the mean surface topography. This similarity persists even when the Stokesian and non-Stokesian N values are added together (figure (6.14)). The correspondence shown in figure (6.14) displays the relationship existing between topographic masses above sea level and the indirect effect for the free air geoid.

Profile along Latitude - 36°N.

Although this profile is across the most mountainous region of Australia, the total non-Stokesian N value (figure (6.15)) is only 3 cms larger at the top of the range than it is 4° away where it has a value of 2.63 metres. The contribution of the near zone terms rises from 4 cms at 145°E to 10 cms at 149°E longtitude, but

this is masked by a fall of 3 cms in the outer zone contribution. This fall is caused by increasing distance from the Himalayas. At first appearances this increase in the non-Stokesian indirect effect N value may seem very small when compared with the near zone contribution of 10 metres across the Himalayas. However, the non-Stokesian term in the indirect effect does not respond quickly to relatively small mountain peaks, and will only reflect the presence of vast areas of high elevation. It would be difficult to accurately assess the comparative volumes of matter above sea level considered in the two profiles but an approximate estimate which includes the regions up to 5^{o} either side of the centre line would be,

Himalayan profile : Australian profile = 15:1

Since the height term enters all indirect effect formula raised to at least the second power, the ratio of the volumes squared is of the order of 200:1. On this basis, which is not strictly valid because of density variations with height above sea-level and terms in higher powers of h, a 6 cms rise in Australia would be equivalent to a 12 metre rise over the Himalayas. Allowing for the obvious approximations made in this qualitive approach, the above result does indicate that the method of computation in the rigorous solution does not include gross errors.

The magnitude of Δg_c in Australia (figure (6.16)) is much smaller than its Himalayan counterpart, and this can be easily explained by two facts. Firstly, the effect of the cylinder of minimum

height will be much smaller because mean heights along the profile are much smaller. The undulating topography term must also be less because sufficient topographic height does not exist to allow for large undulations. Variations in height the size of the whole Australian profile occur within a few tenths of a degree along the Himalayan profile.

A Stokesian summation will only attain a large value if the area around the computation point is represented by large values of the same sign. While this was the case with the Himalayas, in Australia only comparatively small values of Δg_c were detected in a limited region causing the Stokesian value of the indirect effect N to be accordingly low (see figure (6.17)).

The correlation of the total indirect effect with topography across the Himalayas is not repeated to the same extent in Australia. However, the correlation between Δg_c and the topography along the Australian profile is remarkable. Steep rises in topography produce corresponding increases in the values of Δg_c and even the small plateau between longtitudes 149^{o}E and 150^{o}E is reflected in a stabilising of the value of Δg_c in that region.

Unlike the Himalayan example where the centre line profile depicted in figures (6.11) to (6.15) is nearly identical with profiles up to 5^{o} either side, the Australian profile is on the southern end of a long mountain chain which runs parallel to the coastline and, as a consequence, just south of the profile the centre line changes

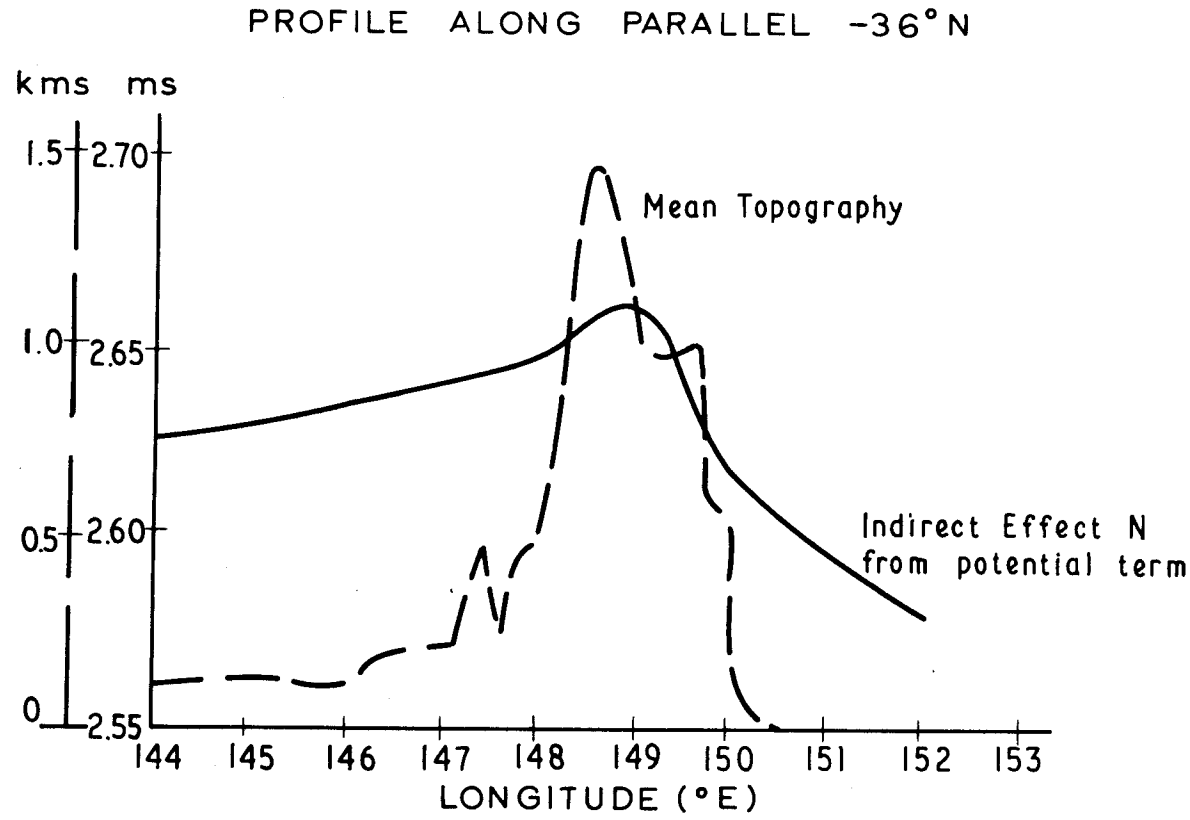

FIG. 6.15

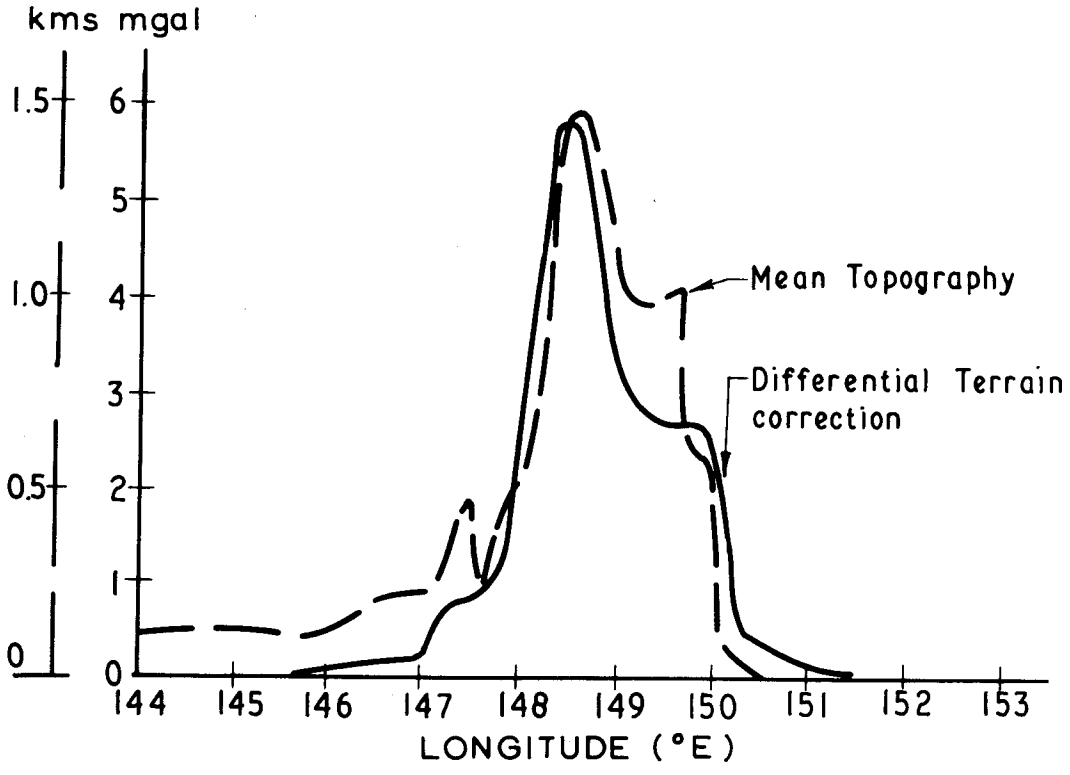

FIG. 6.16

PROFILE ALONG PARALLEL -36°N

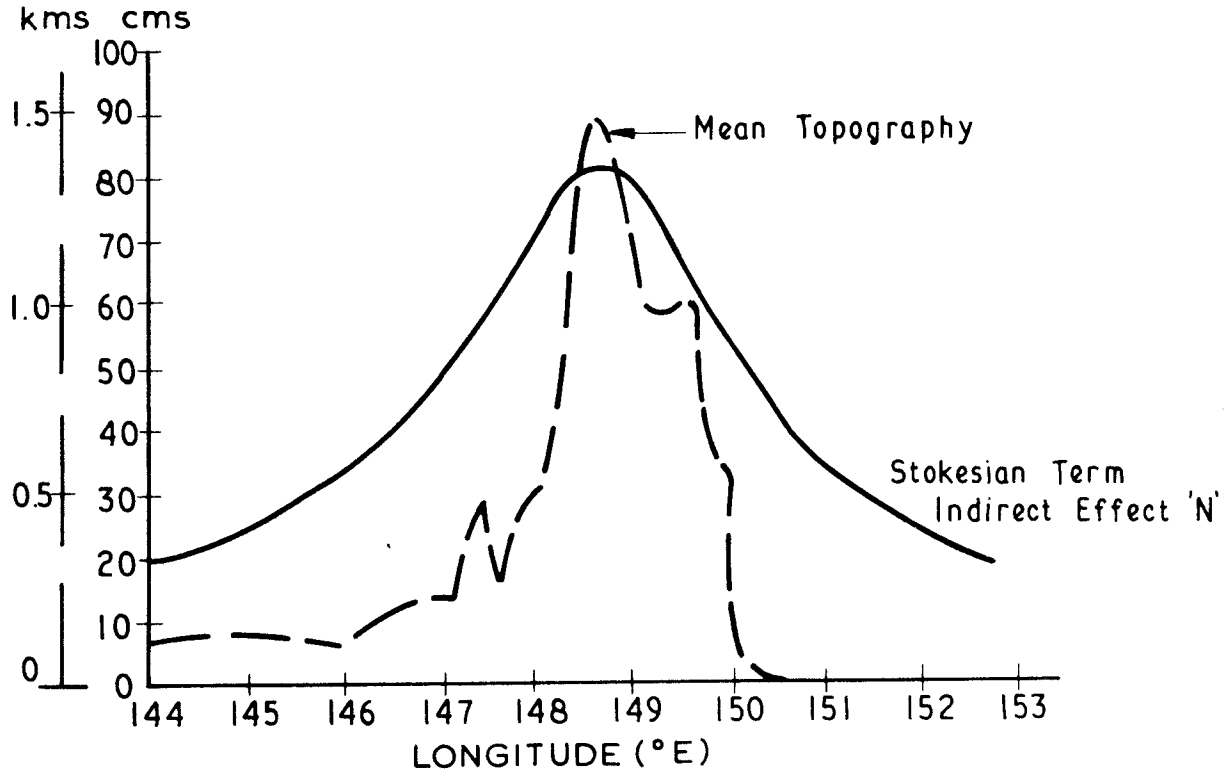

FIG. 6.17

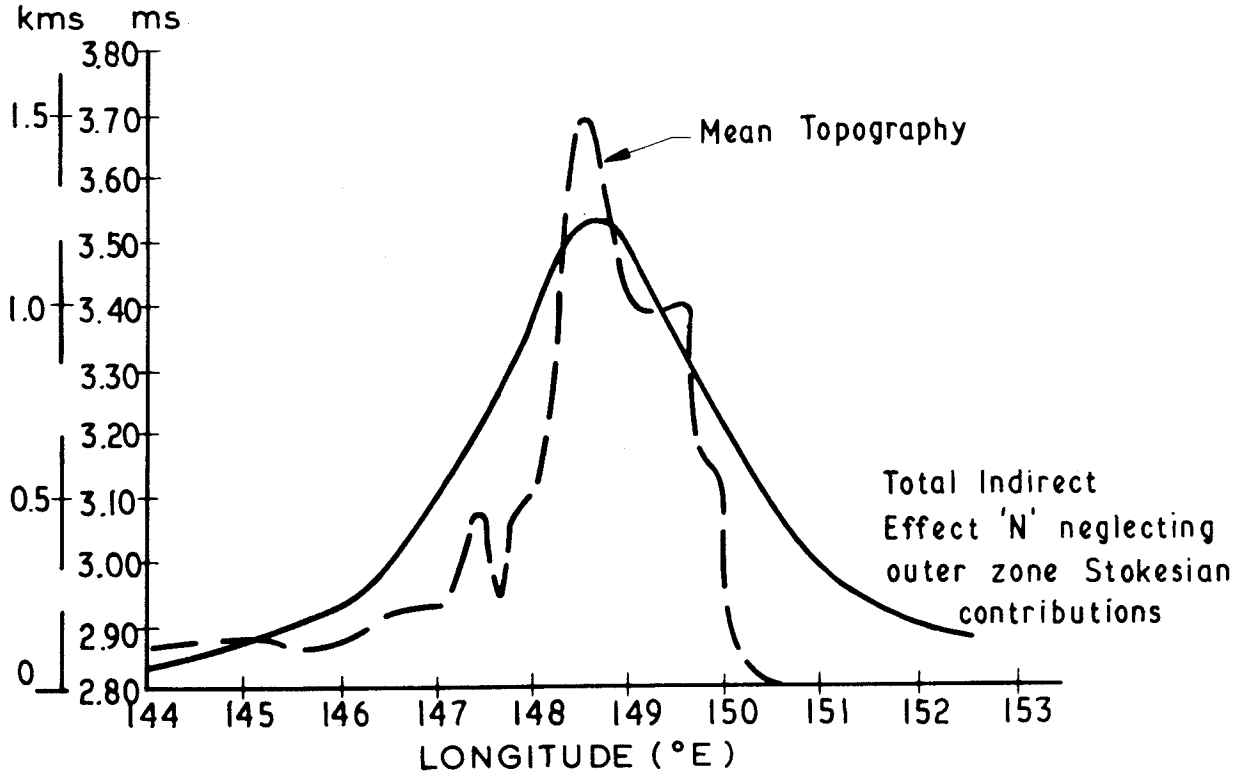

FIG. 6.18

its axis from a southerly to a westerly direction. This means that cross-sections either side of the profile centre line are not similar. The differential terrain correction profiles either side correspondingly differ. The Stokesian integration along the Australian example will therefore not reflect, to the same extent as in the previous case, the topography along the actual centre line. The resultant smoothened total indirect effect depicted in figure (6.18) is to be expected when the above facts are considered.

6.5 Estimation of the Differential Terrain Correction on a Global Scale.

Incorporating the approximations detailed in Section 6.3, a global estimation of the non-Stokesian term for the indirect effect for the free air geoid could be evaluated. A similar estimation of the Stokesian term was required so that the total indirect effect derived for Australia from the available $0.1^{o} \times 0.1^{o}$ height data could be examined in view of a total global estimation.

A technique for obtaining estimates of the differential terrain correction Δg_c without recourse to the preparation of enormous amounts of $0.1^{o} \times 0.1^{o}$ height data was required. A calculation of Δg_c for the land masses of the earth on the same basis as in the last Section would require in excess of two million $0.1^{o} \times 0.1^{o}$ mean height values. The only reasonable approach available to this problem was to utilise the $1^{o} \times 1^{o}$ height data set that was conveniently stored on computer disk.

Several methods for obtaining estimates were tried and only the most successful of these is presented. The test calculations were performed in the regions of the profiles discussed last Section where reasonable estimates of Δg_c derived from 0.1^o x 0.1^o mean heights were calculated. The first approximation made was to neglect the outer zone calculations from equation (6.33) as these usually contributed less than 10% of the total value of the gravity anomaly. The emphasis in the investigations was therefore centred on equation (6.36) which contained the cylinder of minimum height and undulating topography terms.

The basis of the estimation method was to develop a system for deriving values for the terms h, h_{min} and h_p in equation (6.36) which would produce values of Δg_c from that equation which were representative of the 100 0.1^o x 0.1^o areas in the 1^o x 1^o area under consideration. The following system was evolved for defining values for these terms;

(i) h_p was assumed to be the value of the 1^o x 1^o mean height nearest to the computation point,

(ii) the four values of h were derived from the *mean* of h_p and the values of the 1^o x 1^o mean heights to its immediate north, south, east and west and referred to as h_n, h_s, h_e and h_w respectively,

and (iii) the value adopted for h_{min} was the minimum value of h_n, h_s, h_e, h_w and $0.95\ h_p$. If, as is the case in sections of the

Himalayas, h_p, h_n, h_s, h_e and h_w are all equal then equation (6.36) will produce a value of zero mgals for Δg_c. Even though a Bouguer plate representation is obtained from some 1^o x 1^o mean heights in this region, there are, in reality, considerable undulations in topography within each 1^o x 1^o area. The average differential terrain correction for these regions is approximately 20 mgals (see figure (6.12) Section 6.4). The value of 0.95 h_p was included with h_n, h_s, h_e and h_w for the evaluation of h_{min} so that these significant anomalies would be detected in the global estimation.

An analysis of groups of 4 0.1^o x 0.1^o mean heights within 1^o x 1^o areas in mountainous regions showed that the average minimum height, relative to the mean height (h_p) of the 4 values considered was 0.95 h_p. The value of 0.95 was derived from several hundred tests and had a standard deviation of ± 0.03. The only regions considered for these tests were high mountainous areas where the assumptions (i) and (ii) above would lead to a zero value from equation (6.36). The tests were restricted to these regions as they provide the largest values of Δg_c and were therefore the most important for a global estimation of the Stokesian term.

In regions of low topography it was shown in the last Section that the magnitude of Δg_c was comparatively small, e.g. 6 mgal was the maximum value in the highest region of Australia (figure(6.16)). The general trends of the Stokesian effect on a global scale will be mainly derived from the regions of high elevations and on this

assumption the inclusion of the term 0.95 h_p with the values of h_n, h_s, h_e and h_w for the determination of a value of h_{min} was justified.

The values of Δg_c obtained from the estimation method and displayed in Table 6.2 for the Australian region are generally less than and within 1 mgal of the rigorously calculated values. The value of h_{min} used in each of these calculations was always considerably less than 0.95 h_p, as was expected in regions of comparatively low topography.

The values of Δg_c derived using the estimation technique in the Himalayan region are also close to the values derived for the profile, with the exception of the estimated value of 81 mgal. This anomaly occurs on the edge of the mountain range where the values of h_p, h_n, h_e, and h_w are 5000 metres and the value of h_s is 2400 metres. The assumptions of paragraphs (i) to (iii) above do not hold in these regions. If the values of h_p, h_n, h_e and h_w were only of the order of 3000 metres and h_s was 500 metres, then these assumptions would provide a good estimate of the gravity anomaly. It is only when the topography has a sharp gradient in one direction in regions of *very* high topography that the estimation technique described above loses precision.

A study of the major topographical features of the earth revealed that the lowering in precision of the estimation technique to this degree could occur in a maximum of 35 1^o x 1^o areas, with no more than 5 occurrences in any one 5^o x 5^o area. The 1^o x 1^o

COMPARISON OF 1^{o} x 1^{o} MEAN DIFFERENTIAL TERRAIN CORRECTIONS CALCULATED FROM RIGOROUS METHOD (SEC. 6.4) AND ESTIMATION TECHNIQUE

Test Calculation Region	Rigorous Method Mean of 100 values at 0.1^{o} Grid Spacing (mgal)	Estimation Technique (Sec. 6.5) (mgal)
Snowy Mountains Australia	4.1 4.5 4.9	3.5 3.0 5.4
Himalayan Mountains Asia	9.0 25 58 27	9.0 26 54 81

TABLE 6.2

differential terrain correction estimates were meaned into 5^o x 5^o areas, so the error in any 5^o x 5^o area could not exceed 10 mgal due to this cause.

On this premise, values of Δg_c were calculated globally and 5^o x 5^o area means obtained. These were analysed in the manner of spherical harmonics to orders 3,3, 4,4 and 6,6 so that global estimates of the Stokesian term could be obtained. A calculation using the direct substitution of the 5^o x 5^o mean values of Δg_c into Stokes' integral was performed to check the spherical harmonic solutions.

A summary of the theory which justifies the use of spherical harmonic analyses of gravity anomalies is presented below. If Δg is a gravity anomaly it may be conveniently represented as, *(for example see Heiskanen and Moritz, 1967, p.100 et.seq.)*.

$$\Delta g = - \left(\frac{2N\gamma}{R} + \frac{\partial V_d}{\partial h} \right) \qquad .....(6.41)$$

where N is the geoid spheroid separation,

γ is the value of normal gravity,

R is the mean radius of the earth,

$\frac{\partial V_d}{\partial h}$ is the rate of change of disturbing potential with respect to height, and

$$V_d = N\gamma \qquad .....(6.42)$$

If the disturbing potential can be represented by a set of spherical harmonics A_n then,

$$V_d = \sum_{n=o}^{\infty} \frac{A_n}{R^{n+1}} \qquad \ldots\ldots(6.43)$$

$$\text{hence} \quad N = \frac{1}{\gamma} \sum_{n=o}^{\infty} \frac{A_n}{R^{n+1}} \qquad \ldots\ldots(6.44)$$

Upon differentiation of V_d with respect to height,

$$\frac{\partial V_d}{\partial h} = - \sum_{n=o}^{\infty} (n+1) \frac{A_n}{R^{n+2}} \qquad \ldots\ldots(6.45)$$

Incorporating equations (6.42), (6.43) and (6.45) into (6.41),

$$\Delta g = - \left(2 \sum_{n=o}^{\infty} \frac{A_n}{R^{n+2}} - \sum_{n=o}^{\infty} (n+1) \frac{A_n}{R^{n+2}} \right)$$

$$= \sum_{n=o}^{\infty} (n-1) \frac{A_n}{R^{n+2}} \qquad \ldots\ldots(6.46)$$

Let g_n be a surface harmonic of degree n representing values of Δg, such that in equation (6.46),

$$g_n = (n-1) \frac{A_n}{R^{n+2}}$$

$$\text{or} \quad \frac{A_n}{R^{n+1}} = \frac{g_n R}{(n-1)} \quad , \quad n \neq 1 \qquad \ldots\ldots(6.47)$$

Substituting equation (6.44) into (6.47),

$$N = \frac{R}{\gamma} \sum_{n=o}^{\infty} \frac{g_n}{(n-1)} \quad , \quad n \neq 1 \qquad \ldots\ldots(6.48)$$

Equation (6.48) shows that a spherical harmonic representation of gravity anomalies should not include terms of degree one *if* the harmonic representation is to be used for an evaluation of values

of N *(ibid, p.89)*. The term (n-1) in the denominator of equation (6.48) precludes the inclusion of first degree harmonics for this purpose. In general, if the first degree terms are included in a spherical harmonic analysis, the spheroid of reference is no longer centred at the earth's centre of mass *(Mather, 1970a, p.57)*. The spherical harmonic method of Stokesian solution was chosen for three reasons,

(a) The results of the global analysis of the values of Δg_c could be compared with the results of Pellinen *(1962)*.

(b) The computer time taken is much less than the conventional method of direct substitution into Stokes' integral,

and (c) The zero order term of the Stokesian solution is immediately available.

Pellinen *(1962)* obtained values for the conventional terrain correction of the order of 20 mgals in the regions of the Caucasus, the Alps and the Himalayas. Using these values as a basis, he "forecast the Δg_{pm} values in similar areas elsewhere". For these forecasted values, spherical harmonic coefficients to order 3,3 were obtained.

The magnitude of the terrain corrections obtained by Pellinen are less than those obtained from equations (6.33) and (6.36). Pellinen's method was to express the mountainous topography as an infinite series of "sinusoidal ridges". This is a smoothened

topographical approach which in view of the calculations in the previous Section, where the *undulations* of topography within 0.1^{o} of the computation point contributed approximately 60% of the value of Δg_c, would indicate a considerable underestimation of the magnitude of the differential terrain correction.

Pellinen included the first degree terms in his spherical harmonic analysis which precludes the use of his 3,3 coefficients in the formula given in equation (6.48). So that his work could be directly compared with the results of this thesis, Pellinen's spherical harmonic coefficients were used to regenerate his data set on a $5^{o} \times 5^{o}$ area basis. This set of data was analysed to produce 3,3 spherical harmonic coefficients with the first degree terms held fixed at zero. Table 6.3 shows Pellinen's original 3,3 spherical harmonic coefficients, his recomputed coefficients described above and a set of 3,3 coefficients of the $5^{o} \times 5^{o}$ differential terrain corrections which used the estimation technique proposed earlier in this Section.

A study of Table 6.3 indicates that the *trends* of a global Stokesian solution using Pellinen's coefficients would be similar to those obtained from analyses of the values of Δg_c derived from the estimation technique. Global Stokesian solutions (Section 6.6) enforce this statement, and show that only the magnitudes of the global mean values and the fluctuations differ.

In Table 6.4 spherical harmonic coefficients to orders 4,4 and 6,6 of the differential terrain correction are presented. The A_{oo}

COMPARISON OF 3,3 SPHERICAL HARMONIC ANALYSES OF GLOBAL ESTIMATES OF DIFFERENTIAL TERRAIN CORRECTIONS

		Pellinen *(1962)* $A_{1m}, B_{1m} \neq 0$		Pellinen Recomputed $A_{1m}, B_{1m} = 0$		Results of Sec.6.5 $A_{1m}, B_{1m} = 0$	
n	m	A_{nm}	B_{nm}	A_{nm}	B_{nm}	A_{nm}	B_{nm}
0	0	0.39		0.390		0.828	
1	0	0.24		0.0		0.0	
1	1	0.08	0.18	0.0	0.0	0.0	0.0
2	0	-0.07		-0.070		0.002	
2	1	0.00	0.32	0.000	0.320	-0.038	0.413
2	2	-0.28	0.08	-0.280	0.080	-0.603	0.120
3	0	-0.21		-0.099		-0.332	
3	1	-0.05	0.06	-0.045	0.072	-0.021	0.311
3	2	-0.28	0.19	-0.280	0.190	-0.558	0.255
3	3	-0.07	-0.04	-0.070	-0.040	-0.159	0.012

TABLE 6.3

SPHERICAL HARMONIC CO-EFFICIENTS OF GLOBAL ESTIMATES OF THE DIFFERENTIAL TERRAIN CORRECTION

		4,4		6,6	
n	m	A_{nm}	B_{nm}	A_{nm}	B_{nm}
0	0	0.841		0.828	
1	0	0.0		0.0	
1	1	0.0	0.0	0.0	0.0
2	0	0.065		0.028	
2	1	-0.036	0.580	-0.033	0.595
2	2	-0.545	0.113	-0.551	0.114
3	0	-0.333		-0.228	
3	1	-0.021	0.311	-0.045	0.399
3	2	-0.558	0.255	-0.562	0.284
3	3	-0.159	0.012	-0.170	0.060
4	0	-0.113		-0.259	
4	1	-0.007	-0.546	0.015	-0.442
4	2	-0.406	0.050	-0.501	0.077
4	3	0.169	-0.518	0.174	-0.509
4	4	0.219	0.255	0.186	0.270
5	0			-0.171	
5	1			0.070	-0.249
5	2			0.017	-0.144
5	3			0.105	-0.461
5	4			0.405	-0.375
5	5			0.043	0.237
6	0			0.270	
6	1			-0.059	-0.281
6	2			0.379	-0.106
6	3			-0.036	-0.059
6	4			0.414	-0.189
6	5			-0.259	0.204
6	6			-0.149	-0.169

TABLE 6.4

term alters by less than 2% when the analysis is extended from order 4,4 to 6,6.

6.6 Results.

The result of the computation for the non-Stokesian term of the indirect effect for the free air geoid in Australia is shown in figure (6.19). The significant feature of this figure is the dependence on the non-Stokesian term in Australia on the high mountainous regions of Asia. The local effect due to the Snowy Mountains region was calculated in Section 6.4 (figure (6.11)) and amounted to a rise of approximately 6 cms. This amount was reduced to 3 cms by a fall across the profile of 3 cms from the outer zone contributions. The bulge on the 2.6 metre contour line shows this local effect.

The Stokesian term computation for Australia derived from the global 6,6 spherical harmonic analysis of the differential terrain correction estimates is shown in figure (6.20). The local effect due to the Snowy Mountains region depicted in figure (6.13) was not included in figure (6.20). In Section 6.4 the Stokesian effect was computed over a limited region. It would have been uneconomical to continue the rigorous method of Stokesian term computation over the entire continent and therefore figure (6.20) only shows the general trend of the Stokesian term across Australia. The values of Δg_c derived for the region of the Snowy Mountains were, however, included in the global $5^o \times 5^o$ data set of differential terrain correction estimates.

The Stokesian term for Australia when viewed with respect to its global estimation (see figure (6.23)) is in a region possessing a very small rate of change. The influence of the mountainous regions of Asia is dissipated by 10^{o} South latitude, 120^{o} East longitude while the effects from Antarctica and South and North America tend to cancel one another in the Australian region.

The total indirect effect for Australia is depicted in figure (6.21) where the variation of the effect across the continent is shown to be less than one metre. The rigorous Stokesian term calculations in the Snowy Mountains region do not appear on this figure as it was not possible to extend their evaluation across the entire continent. It could be estimated that a rigorous Stokesian calculation would increase the value of this term along the eastern coastal regions by approximately one metre. The total indirect effect would be increased by this amount along the eastern coastline and by lesser amounts over the rest of the continent but it is unlikely that this would alter the statement that the variation across Australia of the indirect effect for the free air geoid is less than one metre.

The global estimation of the indirect effect for the free air geoid is shown in figure (6.24). It is a combination of figures (6.22) and (6.23) which represent global estimates of the non-Stokesian and Stokesian terms respectively. The numerical integration method for the computation of the non-Stokesian term provided

NON-STOKESIAN TERM - INDIRECT EFFECT
AUSTRALIA
Contour Interval 0.1 m

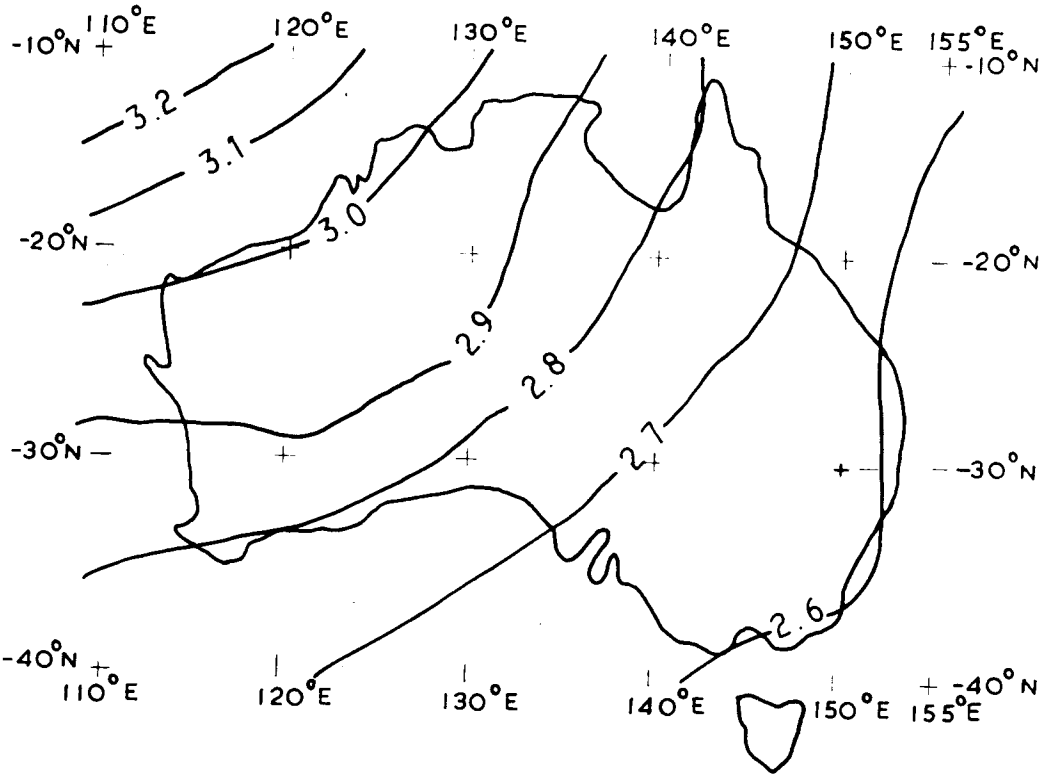

FIG. 6.19

STOKESIAN TERM – INDIRECT EFFECT

AUSTRALIA

Derived from Global 6.6 Spherical Harmonic Analysis

Contour Interval 0.1 m

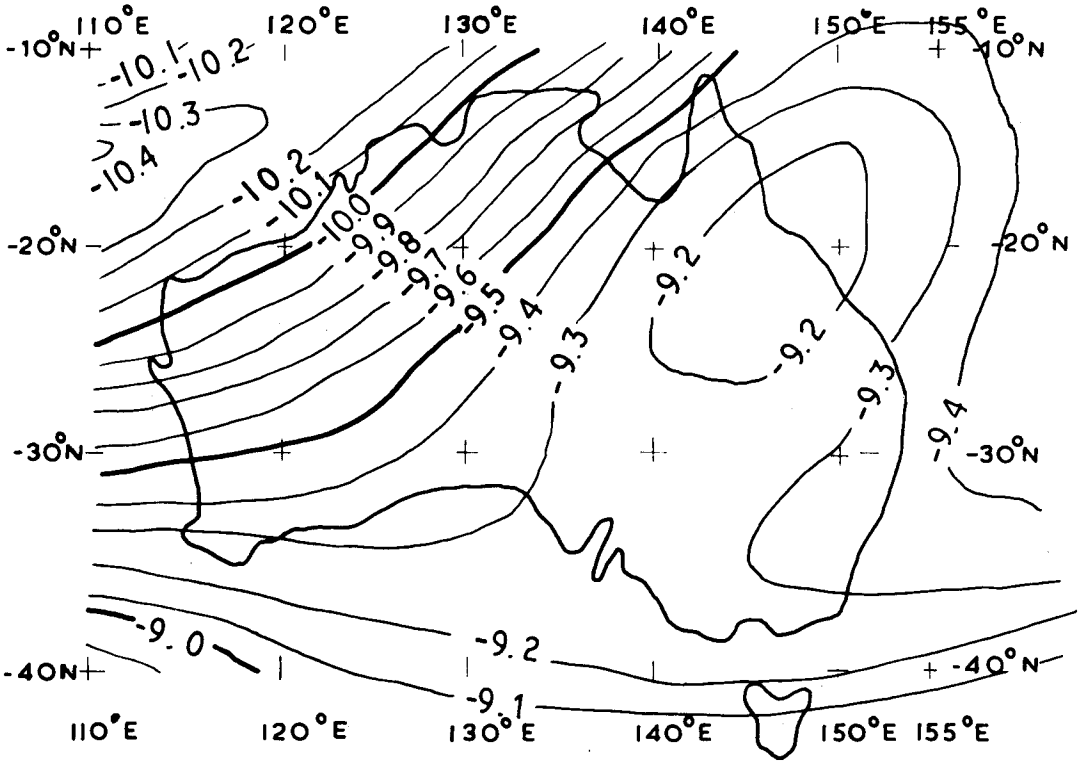

FIG. 6.20

TOTAL INDIRECT EFFECT FOR AUSTRALIA
Contour Interval 0.1m

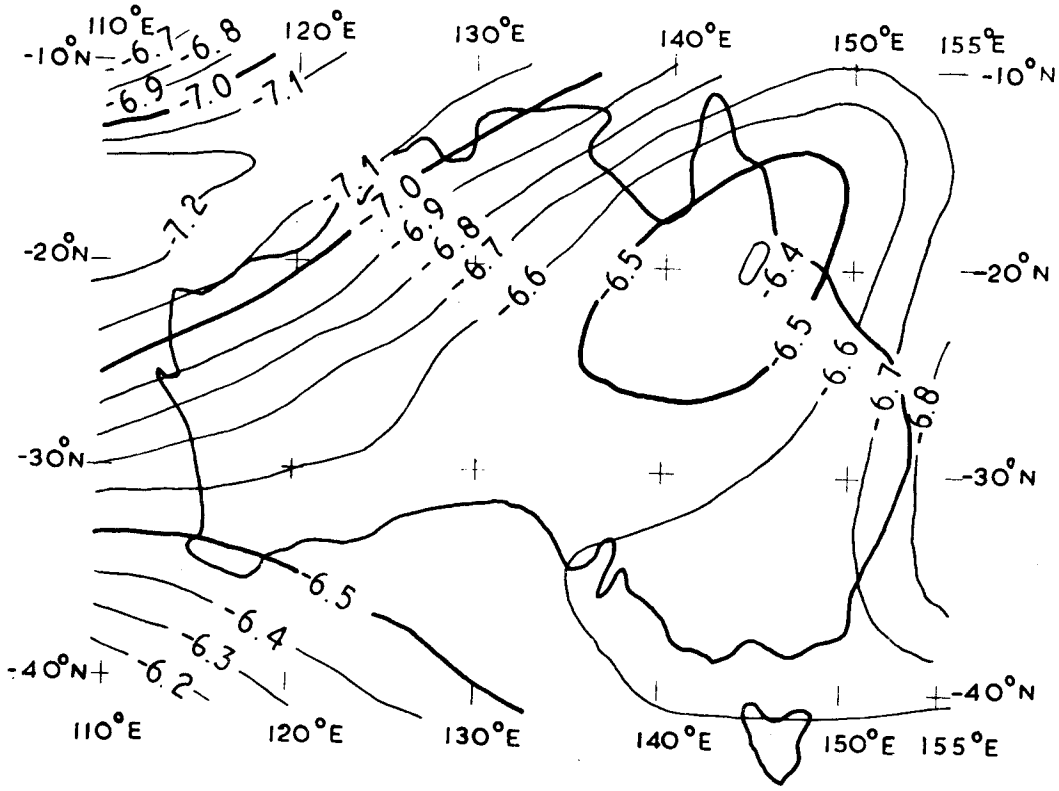

FIG. 6.21

a solution which was more detailed than the corresponding 8,8 spherical harmonic solution. The global mean value can be directly obtained from the latter and was found to be + 2.6 metres. The Stokesian term was computed from both a direct solution using Stokes' integral and from a 6,6 spherical harmonic analysis of the estimates of the differential terrain corrections derived in the previous Section. The global mean value was found from the latter solution to be - 5.4 metres.

A consideration of figure (6.24) shows that in the region of the Australian continent, the rate of change of the total indirect effect is the global minimum. To a limited extent, the non-Stokesian and Stokesian terms tend to cancel one another across Australia. This means that the free air geoid solution for Australia, apart from a zero order correction, is a very good representation of the geoid itself.

A representation of a global geoid solution is presented in figure (6.25). The global free air geoid solution *(Rapp, 1969, p.59)* has been used in combination with the estimate of the indirect effect displayed in figure (6.24). When figure (6.25) is compared with the free air geoid solution it can be seen that several of the extreme values of that solution are decreased in magnitude by the addition of the indirect effect. The global geoid solution displays essentially the same trends as the free air geoid with the rate of change of N values slightly reduced in most regions.

A check on the global estimates of the differential terrain correction was provided by the work of Pellinen *(1962)*. Table 6.3 displays these comparisons and the text pertaining to that Table discusses the different techniques used to obtain the respective sets of spherical harmonic coefficients.

The non-Stokesian term in comparison to the Stokesian term is less variable globally, but the value of + 17 metres for the Himalayan region of Asia was investigated further. The assumption of isostatic compensation, using the Airy-Heiskanen model *(Heiskanen and Moritz, 1967, p.136)*, was made and the net increase in potential at the centre of a 1000 km square topographic block of density 2.67 gm/cm^3 was calculated. The crustal thickness T was varied in steps of 5 km from 20 km to 50 km and the height of the topographic block in steps of 1 km from 1 km to 6 km. The formulae used in the calculations were applications of the general formulae relating to the gravimetric potential and attraction of a simple cylinder *(ibid, pp.127-130)*.

The results of these calculations are displayed in Table 6.5 where it can be seen that for T = 30 km and a mean topographic height of 4500 metres, the net increase in potential is approximately 18 kgalm. This indicates that the approximations made for the evaluation of the non-Stokesian term did not introduce gross errors. The area chosen for the topographic model is approximately the size of the Himalayas where the mean height of the topography is of the

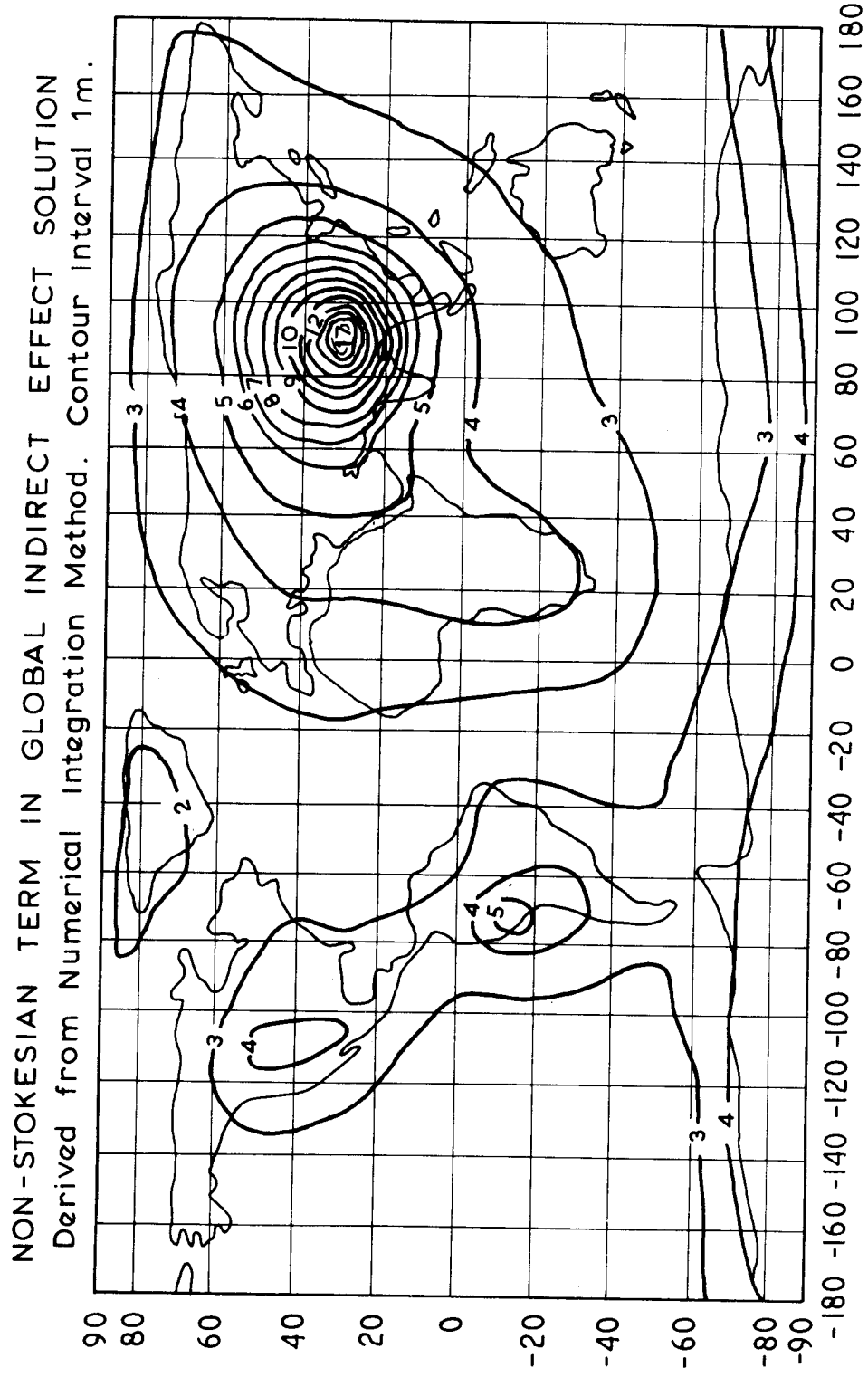
NON-STOKESIAN TERM IN GLOBAL INDIRECT EFFECT SOLUTION
Derived from Numerical Integration Method. Contour Interval 1m.
90
80
60
40
20
0
-20
-40
-60
-80
-90
-180 -160 -140 -120 -100 -80 -60 -40 -20 0 20 40 60 80 100 120 140 160 180

FIG. 6.22

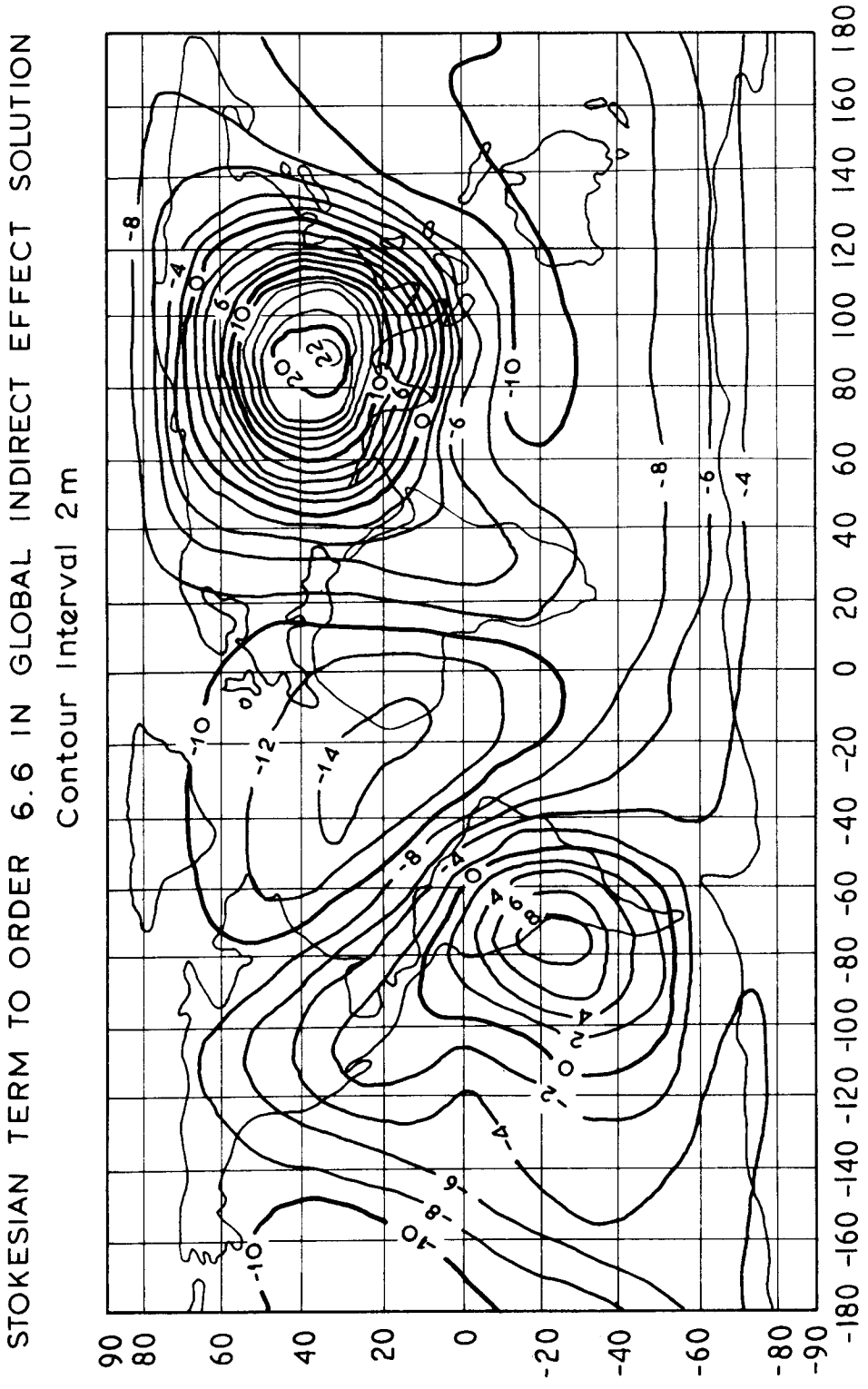
STOKESIAN TERM TO ORDER 6.6 IN GLOBAL INDIRECT EFFECT SOLUTION
Contour Interval 2m
90 80 60 40 20 0 -20 -40 -60 -80 -90
-180 -160 -140 -120 -100 -80 -60 -40 -20 0 20 40 60 80 100 120 140 160 180

FIG. 6.23

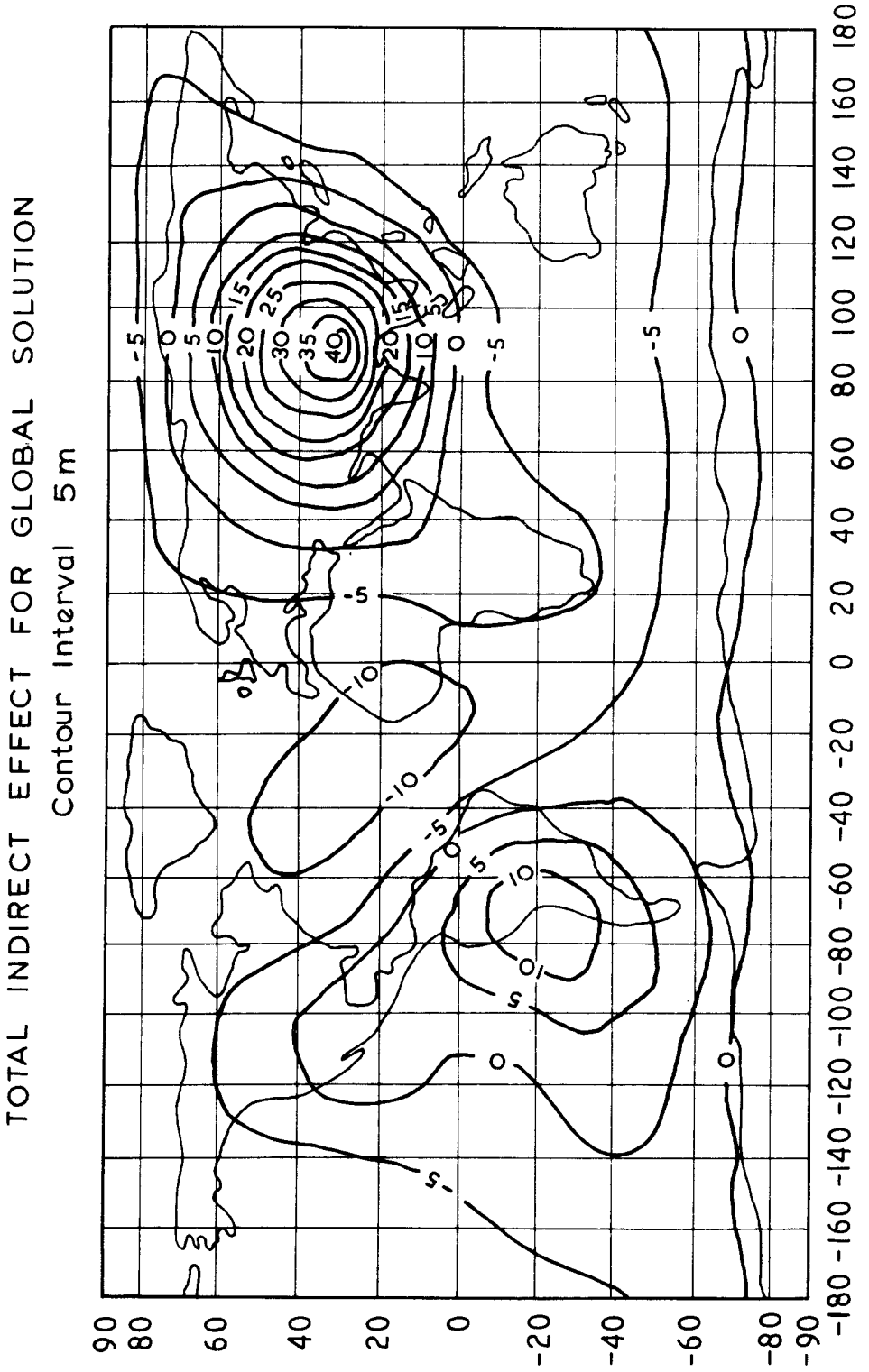
TOTAL INDIRECT EFFECT FOR GLOBAL SOLUTION
Contour Interval 5m
90 80 60 40 20 0 -20 -40 -60 -80 -90
-180 -160 -140 -120 -100 -80 -60 -40 -20 0 20 40 60 80 100 120 140 160 180

FIG. 6.24

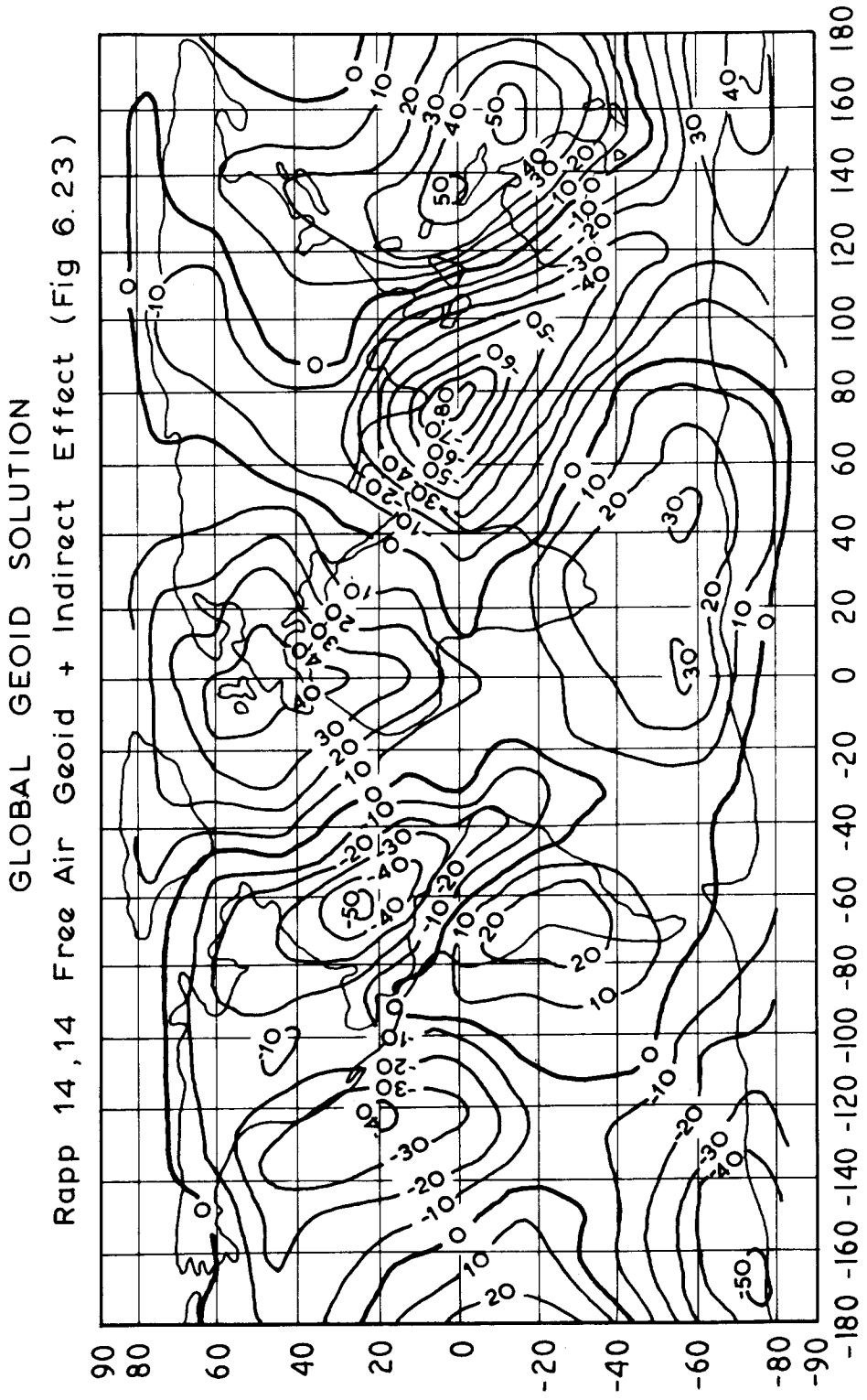
GLOBAL GEOID SOLUTION
Rapp 14,14 Free Air Geoid + Indirect Effect (Fig 6.23)
90
80
60
40
20
0
-20
-40
-60
-80
-90
-180 -160 -140 -120 -100 -80 -60 -40 -20 0 20 40 60 80 100 120 140 160 180

FIG. 6.25

INCREASES IN POTENTIAL (KGALM) AT THE CENTRE OF A 1000 KM SQUARE AREA FOR COMBINATIONS OF CRUSTAL THICKNESS AND TOPOGRAPHY ASSUMING THE AIRY-HEISKANEN SYSTEM OF ISOSTATIC COMPENSATION

Crustal Thickness "T"	Mean Height of Topographic Feature					
	1 km	2 km	3 km	4 km	5 km	6 km
20 km	2.4	5.1	8.2	11.7	15.5	19.6
25 km	2.9	6.2	9.8	13.8	18.0	22.7
30 km	3.4	7.2	11.4	15.8	20.6	25.8
35 km	3.9	8.3	12.9	17.9	23.2	28.9
40 km	4.5	9.3	14.4	19.9	25.7	31.9
45 km	5.0	10.3	15.9	21.9	28.2	34.9
50 km	5.5	11.3	17.4	23.9	30.7	37.8

TABLE 6.5

order of 4500 metres. The value of 30 km for T was chosen in the above example as it appears to be the generally accepted value in most texts which deal with isostasy *(ibid, p.136)*.

A test of the indirect effect computation was its addition to the free air geoid so that comparisons with the astro-geodetic geoid in the Australian region could be undertaken. It was expected that the standard deviation of the residuals after back substitution of the geocentric orientation parameters would reduce in magnitude if the indirect effect calculation was correct. The 1968 free air geoid for Australia has a variation across an earth centred spheroid in the Australian region of approximately 90 metres. The line of maximum slope lies in a north-easterly direction. The indirect effect for Australia has a variation across the continent of less than one metre and the line of maximum slope is in a south-easterly direction. The geocentric orientation parameters obtained from the comparisons of the geoid solutions were essentially the same as those derived in Chapter 5, apart from a zero order term in ΔN_o. The standard deviations of the residuals did not alter. It may be concluded that the 1968 free air and astro-geodetic geoid solutions were too insensitive to detect any improvements arising from the indirect effect in Australia.

6.7 Conclusions.

The complete definition of the geoid requires solutions for both a co-geoid and an indirect effect. Computations of the free

air geoid from combinations of satellite and terrestrial gravimetric data over continental and global extents have been performed in recent years. To the author's knowledge, very few serious attempts of the computation of the indirect effect for the free air geoid have been made, probably because at the present stage of global terrestrial gravimetric coverage such calculations were deemed unwarranted. The free air geoid has been shown to be a good first approximation of the geoid itself *(e.g. Mather, 1968b)*. The low standard deviations of the residuals upon back substitution of the geocentric orientation parameters for the Australian Geodetic Datum derived in Chapter 5 provide ample evidence to support this statement.

The calculation of the indirect effect over Australia shows a variation of less than one metre compared with approximately ninety metres for the free air geoid solution. When the total geoid was obtained for Australia no significant differences in either the geocentric orientation parameters or the standard deviations of the residuals were obtained. This implies that the 1968 free air and the Fischer/Slutsky astro-geodetic geoid solutions for Australia are not sensitive enough to detect any improvements arising from the addition of the small indirect effect. The free air geoid is weakest near the coastline because of extrapolation of the gravity fields into ocean areas. The astro-geodetic solution is at its weakest in the mountainous regions, the largest of which runs along the eastern Australian coastline. It is in this coastal mountainous region that the local indirect effects are a maximum

and therefore remain undetected. Similarly in the flat interior of the continent the astro-geodetic and free air geoid solutions are more accurate but the local indirect effects are minimal.

The indirect effect formulae as derived in Section 6.2 differs only in emphasis from similar formulae derived by several geodesists, notably Molodenskii et.al., *(1962)*, Moritz *(1968a)* and Pellinen *(1962)*, all of whom used the terrain (or topographic) correction approach. The changes in emphasis were outlined in the introduction to this Chapter, the main aim being the derivation of formulae suitable for computation on a large scale using the available data. This aim was impossible to achieve in a strictly rigorous sense and several approximations were made so that a global estimation of the indirect effect could be obtained. These approximations have been discussed in Section 6.3, and in nearly every case involved the unavailability of $0.1^{o} \times 0.1^{o}$ mean heights. Assumptions which assign the height of a computation point equal to the $1^{o} \times 1^{o}$ mean height in that region were made in the computation of both the Stokesian and non-Stokesian terms. This assumption allowed the separate computation of the summations of $\frac{1}{r^3}$ and $\frac{1}{r^5}$ so that a considerable saving in computer time could be made.

The accuracy of the indirect effect both in the Australian and global solutions was affected by the assumptions made and the exact extent of this lowering in precision is difficult to estimate. A general aim of the calculations was to keep the errors due to the

assumptions made down to a minimum and, if possible, as small as the expected errors in the mean heights themselves. The relative errors in the values of the height means were expected to be approximately 5%. The assumption involving the height of a computation point being equal to the mean height in the region was shown in Section 6.3 to be of this magnitude for the non-Stokesian term.

The errors arising from the global Stokesian solution could exceed the above figure, as the technique for estimating values of Δg_c did have limitations along the escarpments of regions of high topography. The purpose of the estimation technique was to obtain the *general trends* of an evaluation of the global Stokesian term so that the indirect effect in Australia could be viewed in the light of a global indirect effect estimation. This aim has been achieved, the spherical harmonic coefficients derived in Section 6.5 showing the same trends as those of Pellinen. A study of the terrain corrections of Pellinen has led the author to believe that a smoothened topographical approach underestimates the magnitude of Δg_c. The necessity to preclude the first degree spherical harmonic terms from analyses dealing with terrain type corrections was illustrated in that Section where Pellinen's harmonic coefficients were recomputed. Doubts must still exist, however, about the extreme values of the Stokesian term displayed in figure (6.23) as they are larger than were expected.

If the magnitudes of the differential terrain corrections

derived in Section 6.4 for the mountainous profiles are accepted however, the magnitude of the global Stokesian term is justified. The regions of large differential terrain corrections, viz., the Rocky Mountains in North America, the Andes in South America and the Himalayan regions of Asia, are so situated on the earth that they complement one another in a Stokesian evaluation to produce relatively large positive and negative values.

Australia is situated in relation to these large mountainous regions such that the Stokesian term is comparatively constant across the continent, the Himalayan contribution being negative and the North and South American influences being positive. The non-Stokesian term is also comparatively constant in Australia , with its slight gradient across the continent tending to nullify the Stokesian term effect.

The use of low order spherical harmonic analyses to check the general trends in the numerical integration solution for the non-Stokesian term proved successful. The main areas of disparity between the two methods are the regions of high mountain ranges described above. These differences in solutions are attributable to the orders of the harmonic analyses employed being too low to detect sharp gradients and the method of near zone calculation for the numerical integration solution being more sensitive than the spherical harmonic solution. The spherical harmonic analyses provided the best estimates of the global mean values for both the

non-Stokesian and Stokesian solutions.

A zero order term must be added to the geocentric orientation parameter ΔN_o derived from free air geoid studies in Australia although the exact value of the zero order term is a matter which requires further investigation. In Chapter 4, Section 4.3, it was shown that a difference of approximately 17 metres occurred in ΔN_o values for the Johnston Origin when the global free air anomaly data sets of Kaula and Rapp were alternatively used. The value of 17 metres was composed of approximately 5.0 metres from differences in Stokesian solution and 11.6 metres from the difference in the zero order terms of the global mean free air anomalies. The 1970 free air geoid solution for Australia *(Mather, 1970a)*, however, has included the zero order term of the global free air anomaly data set used.

The global mean value of the differential terrain correction estimates was approximately + 0.8 mgal which corresponded to a zero order term of - 5.4 metres. The global mean value of the non-Stokesian term was + 2.6 metres. The zero order term arising from the global estimation of the indirect effect can be interpreted in either one of two ways;

(i) If W_o is assumed to be equal to U_o then the zero order term of the indirect effect can be interpreted as a global linear displacement between the geoid and Reference Ellipsoid 1967. This would imply that different volumes are enclosed by these surfaces,

a condition which does not affect the definition of the geoid given in equation (6.1) *(see Mather, 1968b, p.42)*.

(ii) If the geoid and Reference Ellipsoid 1967 are held to possess equal volumes, the zero order term of the indirect effect can be used as a basis for deriving the difference in potential between W_o and U_o. Any differences in potential would be indicative of the existence of errors in one or both of the adopted values for a and kM in Reference System 1967, assuming the value adopted for f from satellite methods is reliable. External evidence from scale determinations would be necessary before any changes in the currently adopted value for a would be warranted. The adoption of this line of reasoning could only lead to altering the presently adopted value for kM.

It was not the intention of this work to derive new values for the parameters of Reference System 1967 as the implications arising from the adoption of new values for a, f or kM require careful examination. The global estimate of the indirect effect was obtained to illustrate the indirect effect computation in Australia with respect to its global trends.

The variation of the indirect effect across the Australian continent has been approximated in this Chapter and it is unlikely, even with refinements in global estimations of the differential terrain correction, that it will exceed one metre. The global indirect effect displayed in figure (6.24) shows that the Australian

continent is in the region of minimum indirect effect gradient. The free air geoid in Australia can be used directly for extensive geoidal investigations as it approximates this surface closely.

CHAPTER 7.

THE EFFECT OF THE GEOID ON A GEODETIC CONTROL NETWORK.

7.1 Introduction.

The free air geoid in Australia has been defined (Chapter 4) and has been shown to be an excellent first approximation of the geoid itself in this region (Chapters 5 and 6). This Chapter is designed to investigate any effects, perhaps systematic, the geoid may have on a geodetic control network that has been calculated without making any allowance for its presence. The investigations take place in Sections 7.3 and 7.4 under the broad headings of the Effects on Loop Closure and on Scale. It is meaningless to quote the size of the effects between any two stations on the network in metres or express them in parts per million (p.p.m.) unless the magnitude of the error that can reasonably be expected to be present between the two stations is also quoted. Thus Section 7.2 of this Chapter attempts to evaluate the random, systematic and total errors that can be expected between any two control stations depending on the average length of line between adjacent stations and the method of traversing (instruments) used. The total length between control stations is varied from 15 km (triangulation baselines) to 3000 km (baselines for geodetic satellite purposes) so that the results obtained will be as general as possible.

7.2 Error Propagation.

The use of standardised invar tapes is virtually only of historical interest in geodetic surveying. Baselines for triangulation control and trilateration networks are observed with electronic distance measuring devices which use differing sections of the spectrum of electro-magnetic radiation. The tellurometer uses a section consisting of micro waves and the geodimeter uses part of the visible section, i.e. light waves. The laser geodimeter uses a very small bandwidth of the visible light section in a highly concentrated energy form and on present indications is the most accurate of these instruments.

Although these instruments can measure distances up to 60 km in the time space of minutes, there are errors involved which require closer examination. These errors are summarised generally as being partly systematic (of an instrumental nature) and partly random (due to varying atmospheric conditions affecting the velocity of the wave propagation). Unlike some other error systems, the systematic errors in this context have a tendency to vary in sign over a period of time, e.g. a calibration crystal may "wander" slowly about its assumed frequency *(Hodges, 1969, p.21)*.

The instrumental errors for electronic distance measuring devices can be expressed as $\pm$ a 10^{-2} metres per measurement, where a is in centimetres *(ibid, p.20)*. The magnitude of a remains unaltered irrespective of the line length as it is representative of the uncertainties in the instrument make-up. Typical values of a are

presented in Table 7.1. The atmospheric-type random errors are conveniently expressed in terms of parts per million. They arise due to the observers not being able to sample the prevailing metrological conditions with sufficient accuracy to obtain a precise value for the refractive index of the atmosphere along the wave path. The refractive index controls the velocity of the wave propagation and is, of course, directly related to the accuracy of the distance measured. Let this random error be designated by ± b (p.p.m.) and thus if the distance between two adjacent stations is ℓ (kms), then the magnitude of the random error in metres is $\pm\ b\ \ell\ 10^{-3}$. To obtain a complete expression for an estimate of the total error e in a measured line between two adjacent stations these two types of errors can be combined as follows,

$$e = \pm\ a\ 10^{-2} \pm\ b\ \ell\ 10^{-3} \qquad .....(7.1)$$

In the above form, this total error estimate (virtually a standard deviation estimate) is quite awkward to manipulate due to the presence of the two sets of ± signs. A much more convenient form of this error estimate would be as below,

$$e = \pm\ (a\ 10^{-2} + b\ \ell\ 10^{-3}) \text{ metres} \qquad .....(7.2)$$

In equation (7.2), the error estimate takes the largest values of equation (7.1) and so any error estimate thus derived will indicate the extreme upper and lower limits of the range in which the real standard deviation should lie.

The general law of the propagation of variances can be applied to the quantity e as it is analogous to a standard deviation *(Clark, 1964, p.8)*. Basically this law allows the variances e^2 for each section of the line between adjacent stations to be summed to produce a variance for the entire length between the terminal stations. For the following calculations, it will be assumed that all n sections ℓ of the entire length L are equal in length.

Thus $L = n\,\ell$ .....(7.3)

If E is the error estimate for the entire length L, then from the law of the propagation of variances,

$$E = \pm (a\,10^{-2} + b\,\ell\,10^{-3})\,n^{\frac{1}{2}} \text{ metres} \qquad .....(7.4)$$

If A is the relative accuracy for the entire length,

$$A = \frac{E}{L}$$

$$= \pm \left(\frac{a\,10^{-5}}{\ell\,n^{\frac{1}{2}}} + \frac{b\,10^{-6}}{n^{\frac{1}{2}}} \right) 10^6 \text{ p.p.m.}$$

i.e. $$A = \pm \left(\frac{a\,10}{\ell\,n^{\frac{1}{2}}} + \frac{b}{n^{\frac{1}{2}}} \right) \text{p.p.m.} \qquad .....(7.5)$$

where a is in centimetres, b in parts per million and ℓ in kilometres.

Estimates of values for a and b were obtained for various types of tellurometer and geodimeter instruments from the results of investigations of Robinson *(1968)* and are displayed in Table 7.1. The value of 5 p.p.m. for b for tellurometers in Australia in

Table 7.1 requires clarification. Generally a figure of 6 p.p.m. would be an acceptable estimate considering the diversified conditions encountered on most survey operations. However, such diversified conditions are the exception rather than the rule over the majority of the Australian continent where the topography, except for some isolated areas, shows very little relief. The metrological conditions thus tend to become somewhat more stable than would generally be the case.

ESTIMATES OF SYSTEMATIC AND RANDOM ERRORS IN ELECTRONIC DISTANCE MEASURING DEVICES FOR USE IN AUSTRALIA.

INSTRUMENT	a (± cms)	b (± p.p.m.)
Tellurometer		
MRA 1	6.5	5
MRA 2	5	5
MRA 101	2.5	5
MRA 3 (101)	2.5	5
Laser Geodimeter		
A.G.A. Model 8	0.5	1 to 2

TABLE 7.1

The figures in Table 7.1 for the tellurometer are for a measurement of a line in one direction only. The procedure adopted for the Australian Geodetic Datum was to measure the line from both ends and use the mean value. This has the effect of reducing the size of the error estimate for a line by a factor of the square root of two. Although the MRA 1 was used in the early stages of the Australian Geodetic Datum (mainly composed of large tellurometer loop traverses with some triangulation and trilateration), the MRA 2 was used most extensively throughout the entire network and therefore it is with the estimates of it's errors that the following discussion is concerned *(Bomford, 1969)*. The estimate of error e in the mean measured distance of a line length ℓ in Australia, when the instrument used was a MRA 2 tellurometer is given by,

$$e = \pm (3.5\ 10^{-2} + 3.5\ \ell\ 10^{-3}) \text{ metres} \qquad .....(7.6)$$

Similarly the error estimate for a line measured both ways with the laser geodimeter is given by,

$$e = \pm (0.35\ 10^{-2} + 1.4\ \ell\ 10^{-3}) \text{ metres} \qquad .....(7.7)$$

To test if these error estimates, especially the tellurometer one, were representative of those actually encountered under field conditions, the results of the adjustment of the Australian Geodetic Datum were examined *(Bomford, 1967a, p.66)*. Briefly, the adjustment was performed by obtaining bearings and distances for 161 section lengths between terminal stations (average section length was 313 kms) and by using a variation of co-ordinates program *(Bomford, 1967b)* to

give adjustments in length and direction to each of these sections simultaneously. A comprehensive system for weighting each section was devised and generally this system appeared suitable for the task *(Bomford, 1967a, pp.62 et.seq.)*. The average section adjustments were 0.45 metres lengthwise and 0.56 seconds in azimuth. The average number of stations per section was eleven with a station spacing of 28.5 kms. If the values of a and b in equation (7.6) are applied to equation (7.4) with ℓ and n equal to 28.5 km and 11 respectively, then the error estimate E for an average section of the Australian Geodetic Datum is obtained as 0.44 metres. This is so remarkably close to the actual value of 0.45 metres that one must presume that the values of 3.5 for both a and b are extremely good estimates of the actual errors present. On this premise, these values have been adopted for use in later work in this Chapter where error estimates for various lengths are required.

With regard to the adjustment in azimuth, if the laws of propagation of variances are applied to the section adjustments, the average azimuth error per section may be expressed as $0.17\ n^{\frac{1}{2}}$ seconds where n is the number of control stations spaced approximately 30 km apart. The errors to be expected in azimuth can only be considered as approximations as the spacing of Laplace stations over the control network was not regular. The azimuth between two stations widely spaced on the continent could be determined more precisely from the results of latitude and longitude observations at those stations (see

Table 4.1) than from "carrying" the azimuth through the control network. This Chapter is concerned more with distance measurements than with azimuth control methods.

For a certain electronic distance measuring device, given estimated values of a and b and a definite length L to be measured, is there a particular value of the lengths ℓ that will make the total error estimate E a minimum? A formula can be found to satisfy this question and it is derived by differentiating either equation (7.4) or (7.5) with respect to ℓ. In the following, equation (7.4) has been used.

From equation (7.3),

$$n^{\frac{1}{2}} = \frac{L^{\frac{1}{2}}}{\ell^{\frac{1}{2}}} \qquad \ldots\ldots(7.8)$$

Thus equation (7.4) becomes,

$$E = \pm \left(\frac{a\ 10^{-2}}{\ell^{\frac{1}{2}}} + b\ \ell^{\frac{1}{2}} 10^{-3}\right) L^{\frac{1}{2}} \qquad \ldots\ldots(7.9)$$

where L is the total length to be measured. Differentiating equation (7.9) with respect to ℓ and putting it equal to zero for a minimum,

$$\frac{dE}{d\ell} = 0$$

$$\text{i.e. } \frac{b\ 10^{-3}}{2} = \frac{a\ 10^{-2}}{2\ \ell} \qquad \ldots\ldots(7.10)$$

$$\text{Solving, } \ell = 10\ \frac{a}{b} \qquad \ldots\ldots(7.11)$$

To test if this value of ℓ is a minimum, equation (7.11) was substituted into the second derivative of E with respect to ℓ and a positive result was obtained. Hence equation (7.11) gives the value of ℓ (in kms) that for a given instrument with estimated values of a (in cms) and b (in p.p.m.) will produce an error accumulation of minimum size. This value of ℓ also produces the lowest possible figure for the relative accuracy (p.p.m.) for the total length L for the given instrument system. Note that the total length is not a contributing factor here, except of course, from an economic point of view. It may be impractical to use this method of minimum error accumulation if the optimum length ℓ is so small that the cost involved with a large number of set-ups becomes prohibitive.

At this stage, it would therefore be prudent to re-examine the values for a and b in equations (7.6) and (7.7), derived from Table 7.1. Using equation (7.11) with the a and b values for the typical tellurometer traverse on the Australian Geodetic Datum, it can be seen that line lengths of 10 km would produce minimum error accumulation. Although some areas of Australia have series of lines of this length, the national average station spacing is approximately 30 km. A consideration of figures (7.1) and (7.2) shows the differences in error accumulation and relative accuracy that occur by using ℓ = 30 km and ℓ = 10 km.

An interesting application of equation (7.11) is to use the a and b values for the laser geodimeter, in view of the fact that

Error Estimates Vs Total Lengths between Terminal Station for Laser Geodimeter and Tellurometer for various values of intermediate lengths 'ℓ'.

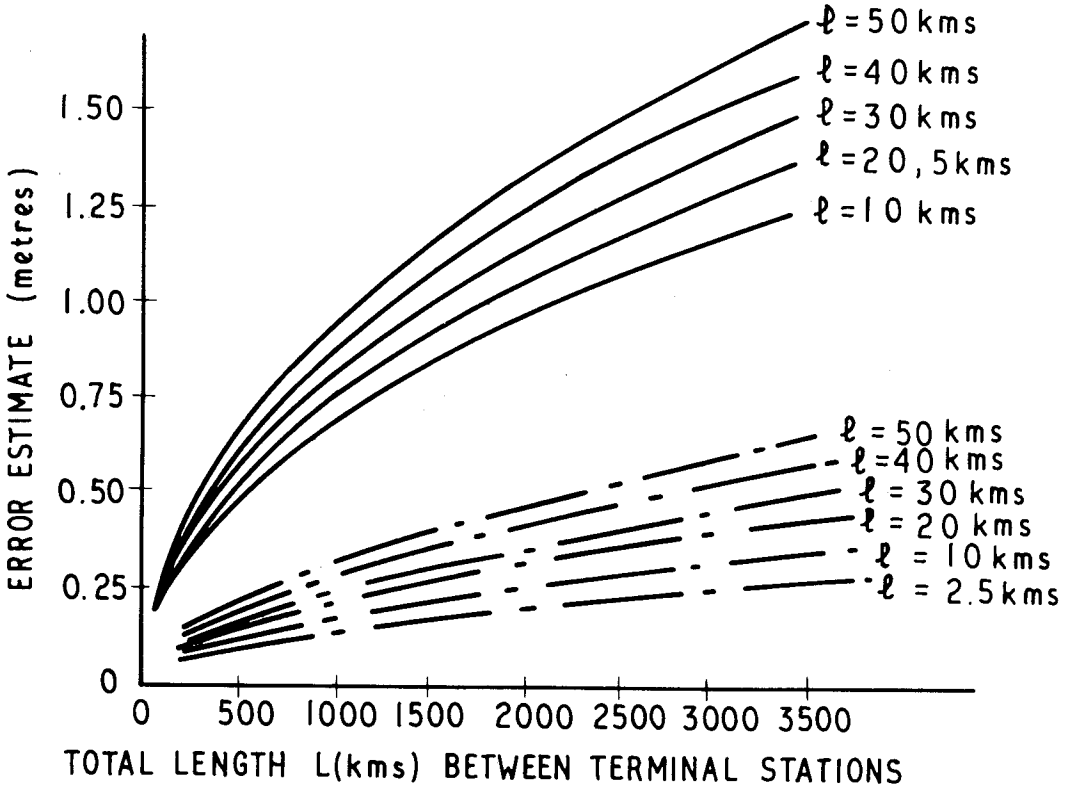

FIG. 7.1

LEGEND:

——— refers to Tellurometer traverse, expected error propagation given by equation (7.6) as ± (0.035 m + 3.5 p.p.m) per line.

——— - ——— refers to Laser Geodimeter traverse, expected error propagation given by equation (7.7) as ± (0.0035 m + 1.4 p.p.m) per line.

Relative Accuracies Vs Total Lengths between Terminal Stations for Laser Geodimeter and Tellurometer traverse for various values of intermediate lengths 'ℓ'.

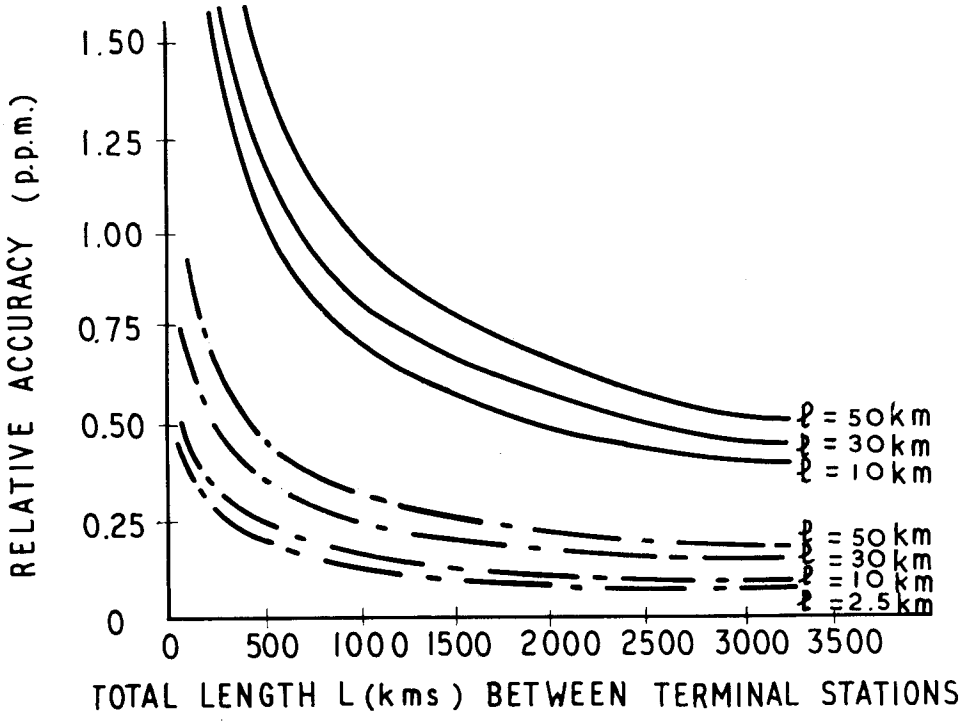

FIG. 7.2

Legend as per Fig. 7.1

this instrument is being used to check the measurements of the high precision sections of the Australian Geodetic Datum that constitute baselines for satellite tracking stations. The main advantage of the laser geodimeter has been described as its ability to measure lines up to 60 km with a relative accuracy considerably lower than the tellurometer due to less dependence on varying metrological conditions. However, the use of equation (7.11) shows that 2.5 km is the ideal line length for using the laser geodimeter. The laser geodimeter is generally used over lines much longer than 2.5 km and as figures (7.1) and (7.2) illustrate, a distance measured with a laser geodimeter traverse composed of intermediate line lengths of 50 km should be twice as accurate as a tellurometer traverse with average line lengths of 10 km.

No mention has been made of other important considerations in the above analyses. There is always a centring error at the master and remote stations, and this error will accumulate more rapidly if the length of line is comparatively small since the number of set-ups will be larger. The improved accuracy arising from short lines from the error propagation of the factors a and b will be offset by an increased accumulation of centring errors. Large survey organisations, in general, do not have the staff or the time to observe lines of length smaller than approximately 30 km and so this economic consideration will most probably design the configuration of the geodetic network.

It should be stressed that the figures for relative accuracies are really internal consistencies. There may be overall scale errors in the network of the order of a few parts per million, but these will remain undetected until inter-continental connections to other geodetic datums are made. Once a high order of internal consistency has been obtained, it is a simple matter to apply an overall scale correction to the entire network. Although Section 7.4 of this Chapter refers to a scale effect, the word scale is applied in a slightly different sense to that mentioned immediately above. In Section 7.4, the scale effect examined is really an effect of varying scale throughout the network caused by the use of elevations above the geoid in the reduction of measured lengths. A varying scale throughout a geodetic control network constitutes an attack on internal consistency, i.e. relative accuracy. Thus although the word scale appears in Sections of this Chapter, it does not necessarily preclude the use of relative accuracy estimates.

Whilst figures (7.1) and (7.2) give examples of the magnitude of the errors and relative accuracies that can reasonably be expected from length measurements over long lines, no mention of the accuracy attainable over triangulation baselines has yet been made. Figures (7.3) and (7.4) are intended to show this, for distances from 5 to 60 km. These figures contain two studies. The first one assumes that measurements from both the laser geodimeter and the tellurometer are made from the terminal stations of the baseline and the mean value

adopted. The error estimates and relative accuracy values for the curves denoted by (i) will therefore be indicative of the maximum standard deviations and accuracies arising from the a and b factors that one could reasonably expect upon measuring the baseline with only set-ups at the terminal stations.

The other study (ii) uses the optimum lengths for both the tellurometer and laser geodimeter so that comparisons of the two types of baseline measurement can be made. This second method has a number of intermediate set-ups and so takes longer to perform. A greater accumulation of centring errors will be present in this method, although the use of modern centring devices should keep these errors to a minimum *(Hodges, 1969, p.24)*. The distance between the master and remote instruments is comparatively small in this case and the b factor will probably be reduced as the observers should be able to obtain metrological data which is representative of the actual conditions along the line.

From figures (7.3) and especially (7.4) it can be seen that to obtain a baseline measured with an internal consistency approaching one part per million that several measurements using method (i) would have to be taken from both terminal stations. For a baseline 20 km long, at least 25 readings from both ends would have to be taken using a tellurometer and approximately 4 from both ends using the laser geodimeter. The figures clearly illustrate that the use of the optimum length ℓ for each instrument allows the minimum error

Error Estimates for various Baseline Lengths for both the Tellurometer and the Laser Geodimeter

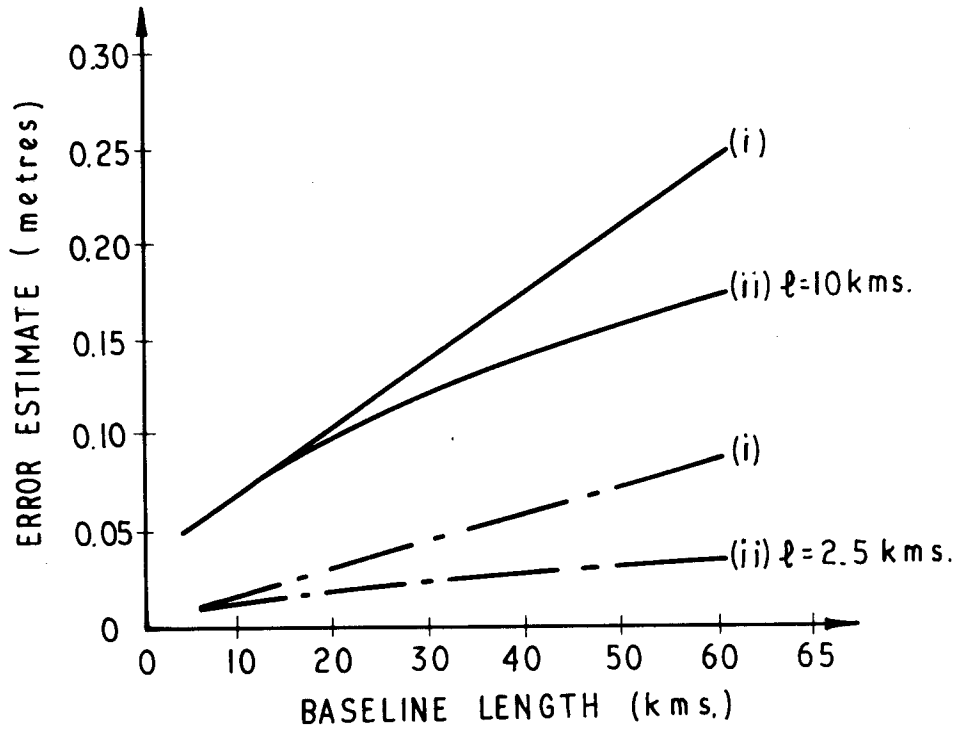

FIG. 7.3

LEGEND AND NOTE:

———— refers to Tellurometer: expected error propagation (two way measurement) of the form ±(0.035 met.+ 3.5 p.p.m.) per line.

—— - —— refers to Laser Geodimeter: expected error propagation (two way measurement) of the form ±(0.0035 met. + 1.4 p.p.m.) per line.

Baseline measurement with both instruments observed in two ways:-

(i) Measurements only taken at either end of baseline

(ii) Optimum lengths 'ℓ' used to give minimum error accumulation (i.e. intermediate set ups.)

Relative Accuracies for various Baseline Lengths for both the Tellurometer and the Laser Geodimeter

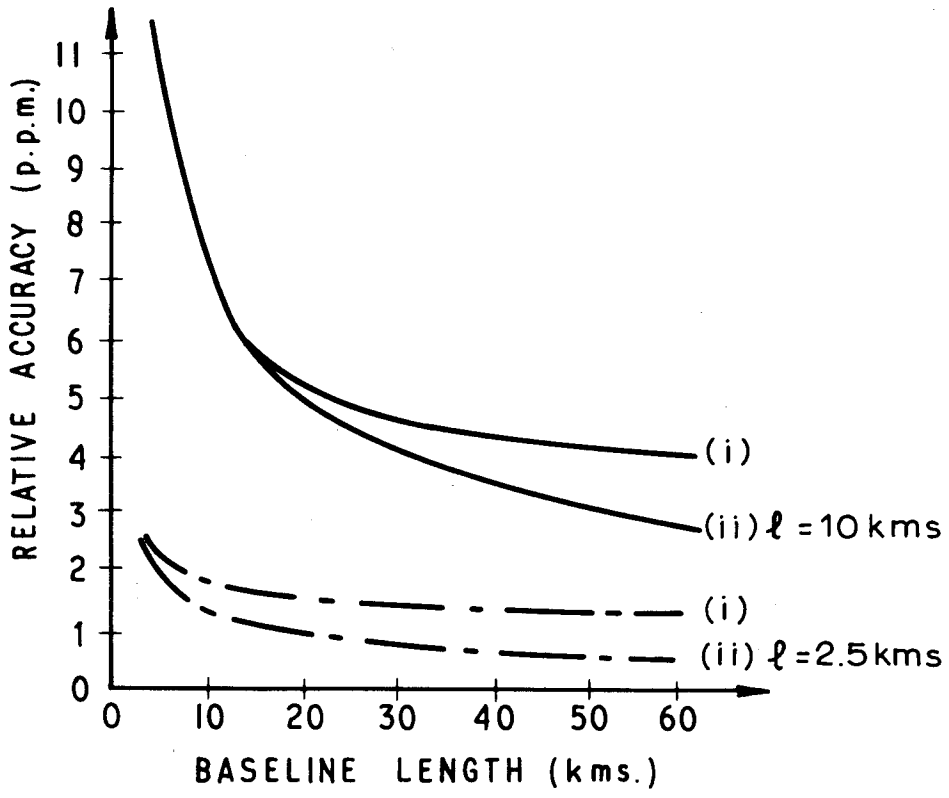

FIG. 7.4

(Legend and Notes as per Fig 7.3)

accumulation of the a and b factors. The size of the relative accuracy that could be expected in the pre-electronic distance measuring devices era was estimated to be one to two parts per million *(Bomford, 1962, p.61)*. The time taken for the determination was much longer however.

The results that emerge from this Section presume that electronic distance measuring devices have error estimates for single measurements that can be represented in the form of equation (7.2). If reasonable estimates for a and b can be obtained, predictions concerning the internal consistency between control stations in a geodetic network can be made. Figure (7.4) indicates that the relative accuracy between adjacent stations in a control network may be of the order of 4 or 5 parts per million. Over longer distances the relative accuracy decreases and at a distance of 3000 km it may be lower than one part per million (figure (7.2)). When the electronic measuring devices are used for short baselines several repetitious measurements are necessary for a high internal consistency.

7.3 Loop Closures.

In the previous Section the adjustment of the Australian Geodetic Datum was mentioned. Briefly, the adjustment was performed by obtaining bearings and distances for 161 sections of geodetic control between terminal stations, and, using a variation of co-ordinates program, adjustments were given in length and direction to each of these sections simultaneously. A comprehensive weighting system was used

in the simultaneous adjustment.

During the calculations to give the bearings and distances between the terminal stations for the 161 sections, whenever a number of sections forming a loop had been calculated, the loop closure in latitude and longitude was computed. Each loop was numbered and the perimeter length, number of stations and the misclosures in both metres and parts per million tabulated *(Bomford, 1967, p.61, Table 2)*. The average loop had a perimeter of 1438 kms and a misclosure vector of 2.19 parts per million (equivalent to a length misclosure vector of 3.15 metres). The loop misclosures were compiled so that a check was provided for the section calculations. This ensured that gross errors were not present in any distances or bearings to be used in the overall national adjustment. A loop misclosure of approximately 4 parts per million was the maximum allowable before the section calculations were re-investigated. This could even result in a field re-investigation of a certain section if the mistake was not found.

The procedure adopted for the adjustment of the Australian Geodetic Datum appears to have been suitable for the task involved, viz., to provide control for topographic mapping and to establish preliminary distances for satellite tracking stations. It was unavoidable that orthometric, instead of spheroidal, heights were used in the reduction of measured distances. An astro-geodetic geoid solution for Australia (see Chapters 3, 4 and 5) was not available until after the adjustment.

This Section investigates the effect on loop closure arising from the direct use of orthometric heights for the reduction of measured distances. If the geoid and spheroid were parallel to one another in the region of a loop, then obviously no effect on loop closure will occur. If the geoid spheroid separation is not constant around a loop, the individual lengths around that loop will possess different scale errors, with the result that the loop closure will be adversely affected. A derivation of formulae to calculate this effect follows below.

Consider figures (7.5) and (7.6) and let c be the curve (traverse loop) around which the misclosure effect caused by the use of orthometric heights instead of spheroidal heights in the reduction of measured distances is to be found. This misclosure effect could have been avoided if values of N_a, the astro-geodetic geoid spheroid separation, had been added to the orthometric heights. Let the axes system be as illustrated, the y axis being oriented along the line of maximum gradient of the geoid spheroid separation slope. It shall be assumed, for the purpose of expediency of solution, that the geoid slope is constant with respect to the spheroid in the regions of the traverse loop. This assumption is not unreasonable when the average size of a traverse loop and the generally uniform geoid slope over the majority of Australia is considered.

From figure (7.6),

$$\underline{t} = \underline{i}\,\frac{dx}{ds} + \underline{j}\,\frac{dy}{ds} \qquad \ldots\ldots(7.12)$$

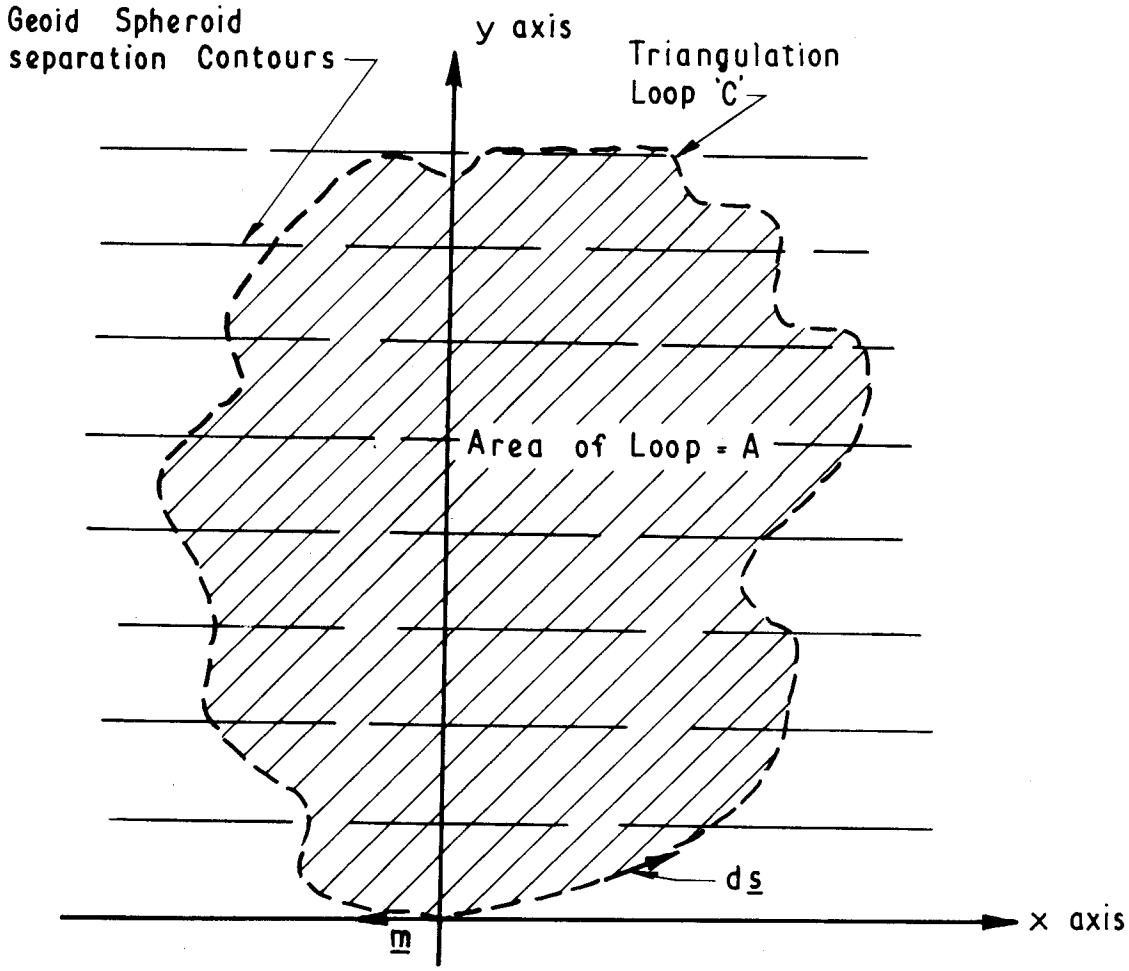

y axis orientated along line of maximum geoid-spheroid separation slope.

FIG. 7.5

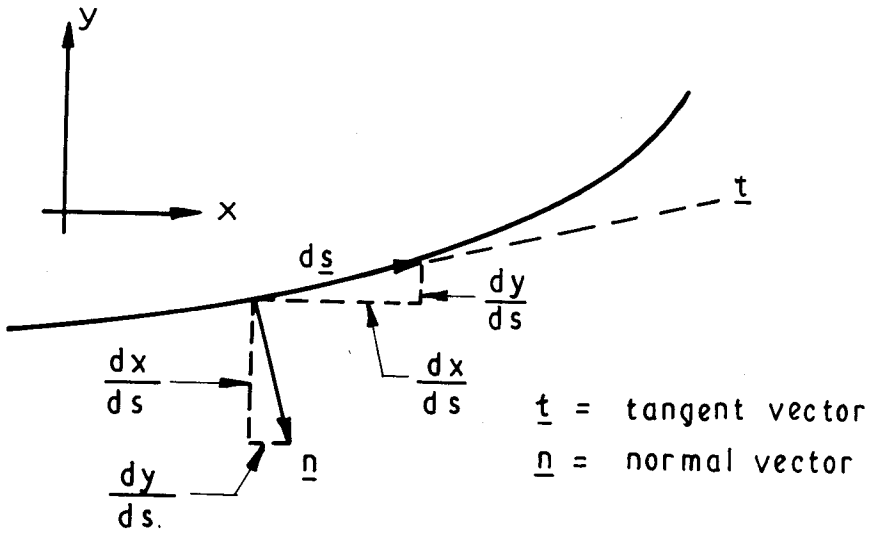
y
x
t
ds
dy/ds
dx/ds
dx/ds
n
dy/ds
t = tangent vector
n = normal vector

FIG. 7.6

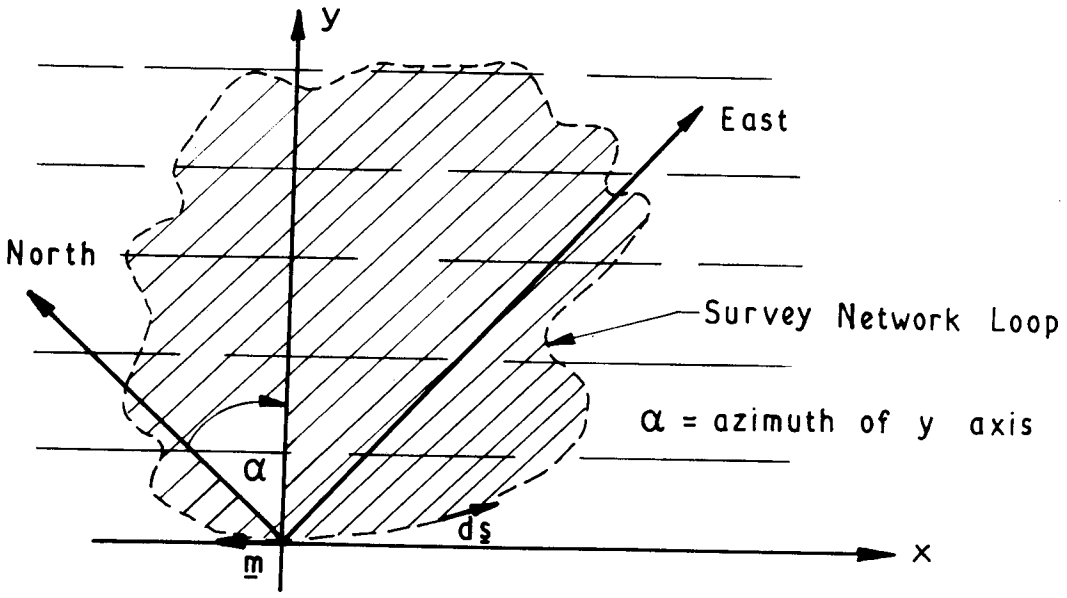
y
East
North
Survey Network Loop
α = azimuth of y axis
α
ds
m
x

FIG. 7.7

and since $\underline{t}.\underline{n} = 0$ .....(7.13)

then $$\underline{n} = \underline{i}\,\frac{dy}{ds} - \underline{j}\,\frac{dx}{ds} \qquad .....(7.14)$$

A form of Gauss' Theorem (divergence theorem) states,

$$\oint_c \underline{v}.\underline{n}\ ds = \int_A \underline{\nabla}.\underline{v}\ dA \qquad .....(7.15)$$

where subscripts c and A refer to the curve and the area inside the traverse loop respectively.

To manipulate equation (7.15) into a more suitable form, put,

$$\underline{v} = \underline{i}\,P + \underline{j}\,Q \qquad .....(7.16)$$

where P, Q are scalar functions of position and $\underline{i}$, $\underline{j}$ are unit vectors.

Note that $$\underline{\nabla}.\underline{v} = \frac{\partial P}{\partial x} + \frac{\partial Q}{\partial y} \qquad .....(7.17)$$

Also $$\underline{v}.\underline{n} = \left(\underline{i}\,P + \underline{j}\,Q\right)\left(\underline{i}\,\frac{dy}{ds} - \underline{j}\,\frac{dx}{ds}\right)$$

$$= P\,\frac{dy}{ds} - Q\,\frac{dx}{ds} \qquad .....(7.18)$$

and $$\oint_c \underline{v}.\underline{n}\ ds = \oint_c \left(P\,\frac{dy}{ds} - Q\,\frac{dx}{ds}\right) ds$$

$$= \oint_c (P\,dy - Q\,dx) \qquad .....(7.19)$$

From equation (7.17),

$$\int_A \underline{\nabla}.\underline{v}\ dA = \int_A \left(\frac{\partial P}{\partial x} + \frac{\partial Q}{\partial y}\right) dA \qquad .....(7.20)$$

Thus the divergence theorem in the desired form is,

$$\oint_C (P\,dy - Q\,dx) = \int_A \left(\frac{\partial P}{\partial x} + \frac{\partial Q}{\partial y}\right) dA \qquad .....(7.21)$$

If figure (7.5) is again considered, an equation for the geoid spheroid separation N, could be expressed as,

$$N = C + D\,y \qquad .....(7.22)$$

This implies that in the region of the traverse loop under consideration, the geoid is considered planar with respect to the spheroid. This is not an unreasonable assumption (discussed earlier). If the misclosure vector is designated by $\underline{m}$ (see figure (7.5)), then a component of this misclosure $d\underline{m}$ caused by a short distance $d\underline{s}$ which has not been reduced to spheroid level with a spheroidal height, can be represented by,

$$d\underline{m} = \frac{N}{R}\, d\underline{s} \qquad .....(7.23)$$

Equation (7.23) is analogous to the reduction of a measured distance to the spheroid (viz., $\frac{h}{R}\,s$), where R is the mean radius of earth curvature over the line of length s.

Resolving $d\underline{m}$ into its x and y components,

$$dm_x = \frac{N}{R}\, dx \qquad .....(7.24)$$

$$dm_y = \frac{N}{R}\, dy \qquad .....(7.25)$$

If R is set equal to the mean earth radius in the area of the

traverse loop, the total misclosures in the x and y directions will be given by,

$$m_x = \frac{1}{R} \oint_c N \, dx \qquad \text{.....(7.26)}$$

and

$$m_y = \frac{1}{R} \oint_c N \, dy \qquad \text{.....(7.27)}$$

If we put $-Q = N$

$$= C + D\,y$$

and $P = 0$ into equation (7.21)

then

$$\oint_c N \, dx = -\int_A D \, dA$$

$$= -D\,A \qquad \text{.....(7.28)}$$

Hence

$$m_x = -\frac{D}{R} A \qquad \text{.....(7.29)}$$

Also if we put $P = N$

$$= C + D\,y$$

and $Q = 0$ into equation (7.21)

then

$$\oint_c N \, dy = \int_A (0 + 0) \, dA$$

$$= 0 \qquad \text{.....(7.30)}$$

Hence

$$m_y = 0 \qquad \text{.....(7.31)}$$

These misclosures have been obtained for the case of one of the reference axes (the y axis here) being oriented along the line of maximum gradient of the geoid spheroid separation slope. In general,

if we consider the North and East directions as reference axes, then equation (7.29) can be expressed as,

$$m \text{ (north)} = - \frac{D\,A}{R} \sin\alpha \qquad .....(7.32)$$

and $$m \text{ (east)} = \frac{D\,A}{R} \cos\alpha \qquad .....(7.33)$$

where the angle α lies between the north direction and the line of maximum geoid spheroid separation slope (see figure(7.7)), the angle being measured clockwise from the north direction.

An examination of equation (7.22) reveals that the term D is the tangent of the maximum value of the deflection of the vertical ζ. This maximum deflection angle is assumed to remain constant over the region of the traverse loop and can be expressed in terms of ξ and η, the deflections of the vertical in the meridian and prime vertical directions respectively by,

$$\xi = \zeta \cos\alpha$$

and $$\eta = \zeta \sin\alpha \qquad .....(7.34)$$

where the azimuth α is defined as previous.

Since ζ for Australia is never greater than 25 seconds of arc, the tangent of ζ can be considered equivalent to its radian value, i.e.

$$D = \zeta \text{ (radians)} \qquad .....(7.35)$$

Hence the formulae for obtaining the loop misclosure due to geoid spheroid separation neglection are,

$$m \text{ (north)} = - \frac{\eta A}{R.206265} \text{ metres} \qquad .....(7.36)$$

$$\text{and } m \text{ (east)} = + \frac{\xi A}{R.206265} \text{ metres} \qquad .....(7.37)$$

where the area A is expressed in metres^2, the mean radius of curvature R is in metres and ξ and η are in seconds of arc.

A feature of the formulae above is the sign of the misclosure which arises because the mathematical procedure of mapping involved the transferring of the curve c from one surface to another (from geoid to spheroid), with directional vectors. A starting point was assumed and by proceeding anti-clockwise, the entire loop was transferred to the new surface. Although the loop was a closed figure on the geoid, it will not form a closed loop on the spheroid with the difference being designated by the misclosure vector $\underline{m}$. The direction of $\underline{m}$ and the direction of calculation was illustrated in figures (7.5) and (7.7) and it was upon resolution of the misclosure into the north and east directions that the algebraic signs of equations (7.36) and (7.37) occurred. The sign convention will be as shown in equations (7.36) and (7.37) only if the loop calculation proceeds in an anti-clockwise direction. If the loop calculation is performed in a clockwise direction then the signs of equations (7.36) and (7.37) must be reversed.

Another significant feature of these formulae is that although two constants (C and D) are relevant to the equation of the geoid (equation (7.22)), only the constant D is of importance in the final

formulae for the loop misclosure. The constant C refers to the magnitude of N at the origin of the axes and is the factor which relates to the general scale of the loop. If C is equal to 6.28 metres, a scale factor of approximately one part per million will exist in the initial section of this loop. The scale factor C is of no significance to the size of the loop misclosure, but it is an important quantity to consider when the inter-connection of two loops takes place. If these loops have C values of different magnitude then the whole network loses homogeneity and the calculation of a line from one loop to another will possess an irregular scale error. This type of error is dealt with in Section 7.4 of the Chapter.

It was believed that during the process of the above derivation a system may have been evolved which would indicate an optimum configuration for geodetic control traverse loops so that misclosure errors could be minimised. Such a system did not eventuate, simply because no particular arrangement of loops will have any inherent minimum error producing qualities with respect to any other system of shapes of loops. Equations (7.36) and (7.37) show that the only factors of relevance are the *area* of the loop and the values of the deflections of the vertical in this area. When a large area such as Australia is to be covered by control traverse loops, no special configuration of the loops can be devised which will inherently account for neglect of the geoid spheroid separation. The considerations that will decide the configuration to be used will consist of access, the

type of surveying to be used (triangulation, trilateration or tellurometer traverse), the topographical features, the desired spacing of azimuth control (Laplace stations) and check baselines and most importantly, the density (total number) of first order control stations desired in the total area to be surveyed.

The direct application of equations (7.36) and (7.37) to the Australian Geodetic Datum would not be strictly correct. The co-ordinates of control stations on that datum were *not* intended to apply to an earth centred reference figure directly. For the purpose of illustrating the above-mentioned equations however, let it be *assumed* that the co-ordinates of control stations on the Australian Geodetic Datum were intended to apply to an earth centred reference figure.

The misclosure effect for the traverse loops on the Australian Geodetic Datum as calculated from equations (7.36) and (7.37) never exceeded 0.40 parts per million (average value was 0.25 p.p.m.). A planimeter was used to obtain the loop areas from a large scale map of Australia which showed their location. Since the average loop misclosure was 2.19 parts per million, it can be seen that this effect was generally one order smaller than all other error accumulation. As the directions of the original loop computations were unknown, no attempts could be made to correct for this effect.

A computer program which calculated the amount $\frac{N\,s}{R}$ along each line of length s around a loop was devised to test if equations (7.36) and (7.37) had been correctly derived. This represented the

extra amount of reduction that would have occurred if spheroidal and not orthometric heights had been used to reduce measured lengths to spheroid level. The azimuth of each line s was calculated and then the effect $\frac{N\,s}{R}$ was resolved into north and east components. All these components were summed for the misclosures in the north and east directions. Loops numbered 7, 14, 52, 75 and 76 on the Australian Geodetic Datum *(Bomford, 1967a, figure 1)* were used as data for this program and the results were compared with those obtained from the use of equations (7.36) and (7.37). In every case the results were close enough to be considered identical, especially after considering the accuracy attainable with a planimeter and the fact that the geoid slope is not exactly uniform.

7.4 Scale Effect.

The previous Section of this Chapter showed that if a control traverse loop possessed a variable scale around its perimeter, it will also possess a misclosure. This misclosure is directly attributable to the use of orthometric instead of spheroidal heights for the reduction of measured distances to assumed spheroid level. The extra amount of reduction is $\frac{N\,s}{R}$ (metres) where N is the average geoid spheroid separation value for the line length s and R is the mean radius of earth curvature. This Section attempts to find the error due to the above-mentioned cause which would be present in distances calculated from geographical co-ordinates on the Australian Geodetic Datum and intended to represent lengths on a geocentred

reference spheroid. For the purposes of this Chapter, the geocentric orientation parameters as per equation (5.1) have been adopted. Zero order terms in ΔN_o have been neglected (see discussion Section 6.7).

The value of N does not vary very much over short baseline distances, hence the value of N at the mid-point would suffice to obtain an estimate of the error of the assumption in the previous paragraph. For distances of continental extent, the geoid slope across an earth centred spheroid in the Australian region is not completely uniform, and it would not be acceptable to merely use the mid-point value of N to obtain what shall be termed the scale effect T. To obtain T to an acceptable degree of accuracy the terms $\frac{N\,s}{R}$ should be calculated approximately every 30 km along the line using the mean values of N for each of these sections. The total scale effect T will be the sum of the scale effects for each section. This method would be tedious over a length of 3000 km. This Section derives a formula to calculate T from an integration approach and checks that the derived formula is correct. Some examples of the size of the scale effect on both hypothetical triangulation baselines and proposed satellite baselines on the Australian Geodetic Datum have been given in Tables 7.2, 7.3 and 7.4.

The general aims of the derivation were to keep the formula for T as general as possible, the geographical co-ordinates of the terminal stations and the geocentric orientation parameters being the only data input requirements. The value of T should be obtained from the use of

one formula. No form of repetitious calculation such as discussed earlier (every 30 km) was desired, although the formula was to be incorporated in a computer program so that T could be rapidly calculated over several lengths in a minimum of time.

The scale effect t in the immediate vicinity of any point P (ϕ,λ) on the line between P_1 (ϕ_1,λ_1) and P_2 (ϕ_2,λ_2) can be represented by,

$$t = \frac{N\ ds}{R} \qquad .....(7.38)$$

where N is the geoid spheroid separation, ds is a length increment at P and R is the mean radius of earth curvature at P. In Chapter 2, equation (2.29), it was shown that N at any point P (ϕ,λ) can be represented by,

$$\begin{aligned} N = {} & \Delta\xi_o\ (\rho_o+h_o)\ (-\sin\phi\cos\phi_o + \sin\phi_o\cos\phi\cos(\lambda-\lambda_o)) \\ & - \Delta\eta_o\ (\nu_o+h_o)\cos\phi\sin(\lambda-\lambda_o) \\ & + \Delta N_o\ (\sin\phi\sin\phi_o + \cos\phi\cos\phi_o\cos(\lambda-\lambda_o)) \end{aligned} \qquad .....(7.39)$$

where $\Delta\xi_o$, $\Delta\eta_o$ and ΔN_o are the geocentric orientation parameters for the origin P_o (ϕ_o,λ_o) of the geodetic control network. From a consideration of spheroidal geometry, the distance ds may be expressed as,

$$ds = \rho\ d\phi\ \cos A + \nu\ d\lambda\ \cos\phi\ \sin A \qquad .....(7.40)$$

where A is the azimuth of the line P_1 P_2 and ρ, ν are the radii of curvature in the meridian and prime vertical sections respectively. The total scale effect T will be the sum of all the

individual scale effects along the line $P_1 P_2$ and can be expressed as,

$$T = \int_{P_1}^{P_2} \frac{N\, ds}{R} \qquad \ldots\ldots (7.41)$$

Equation (7.41) cannot be integrated in this form directly. To make an evaluation both possible and convenient, the following approximations will be made,

(i) $R = \rho = \nu = R_m$ = mean earth radius

(ii) Azimuth A is constant along the line i.e. $\frac{d\lambda}{d\phi}$ = constant

(iii) Mean values, subscript $_m$, will be used for ϕ terms when the integration is with respect to λ and vice versa.

On these premises, equation (7.41) may be expressed as,

$$T = \cos A \int_{\phi_1}^{\phi_2} N\, d\phi + \sin A \cos\phi_m \int_{\lambda_1}^{\lambda_2} N\, d\lambda \qquad \ldots\ldots (7.42)$$

Upon integration, after substituting equation (7.39) for N,

$$\begin{aligned} T = {} & \Delta\xi_o R \{\cos A \cos\phi_o (B + C F \sin\phi_o) \\ & + \sin A \cos\phi_m (E \sin\phi_o \cos\phi_m - H \sin\phi_m \cos\phi_o)\} \\ & + \Delta\eta_o R \{-C G \cos A + D \sin A \cos^2\phi_m\} \\ & + \Delta N_o \{\cos A (C F \cos\phi_o - B \sin\phi_o) \\ & + \sin A \cos\phi_m (H \sin\phi_o \sin\phi_m + E \cos\phi_o \cos\phi_m)\} \end{aligned} \qquad \ldots\ldots (7.43)$$

where $B = \cos\phi_2 - \cos\phi_1$

$C = \sin\phi_2 - \sin\phi_1$

$D = \cos(\lambda_2 - \lambda_o) - \cos(\lambda_1 - \lambda_o)$

$E = \sin(\lambda_2 - \lambda_o) - \sin(\lambda_1 - \lambda_o)$

$F = \cos(\lambda_m - \lambda_o)$

$G = \sin(\lambda_m - \lambda_o)$

$H = (\lambda_m - \lambda_o)$ radians .....(7.44)

To check if equation (7.43) had been correctly derived, it was incorporated into a computer program which calculated T by the summation of the individual scale errors every 30 km along the line. The difference between the two methods was never greater than 0.1 parts per million. The standard deviations of the residuals for N found by back substituting the geocentric orientation parameters derived from the 1968 free air geoid solution was approximately ± 5 metres, so the value for T stemming from the integration of equation (7.39) should not be incorrect by more than 0.8 parts per million.

Error estimates were also calculated for each line considered. The error propagation estimate for a two-way tellurometer traverse of ± (0.035 metres + 3.5 p.p.m.) per line was adopted as it had been shown in Section 7.2 to be an error estimate with a high degree of reliability for Australian conditions. The average station spacing was assumed to be 30 km. Note that this error estimate will under-

estimate by up to 20% the error that would be actually propagated because it is calculated on the assumption of measuring the shortest possible distance between the terminal stations. In practice, the path of the traverse will wander due to topography, access, etc., and will be longer than the shortest distance. A lateral error estimate was also calculated and was expressed in both seconds of arc (azimuth error) and metres. The lateral error estimate was based on an expected error of ± 0.17 seconds of arc per 30 km section of the total line. Although this error will also underestimate by approximately 20%, it was shown in Section 7.2 that little emphasis can be placed on its results as astronomical determinations of position at the terminal stations will provide the best methods of azimuth control.

The data for Table 7.3 was an adaptation of that used by *(Lambeck, 1968b, p.283)* for a feasibility study of the application of the geometric method of satellite geodesy to the Australian Geodetic Datum. Lambeck gives the names and approximate geographical co-ordinates of nine stations where satellite tracking equipment is either installed or could be in the near future. Twenty lines would be observed between these nine stations, and equation (7.43) has been computed for them. The nine stations and their approximate co-ordinate values are shown in Table 7.2 and figure (7.8). Table 7.3 gives the estimates of scale error if Australian Geodetic Datum co-ordinates were used to calculate the distances between the stations in Table 7.2 and these distances were intended to represent lengths on a geocentred

Station Name	Approximate Co-ordinates	
	Latitude (degrees)	Longitude (degrees)
Woomera	-31.1	136.5
Muchea	-31.4	115.6
Port Hedland	-20.2	118.4
Darwin	-12.2	130.4
Thursday Island	-10.4	142.1
Townsville	-19.1	146.5
Culgoora	-30.3	149.6
Hobart	-42.5	147.2
Alice Springs	-23.4	133.5

TABLE 7.2

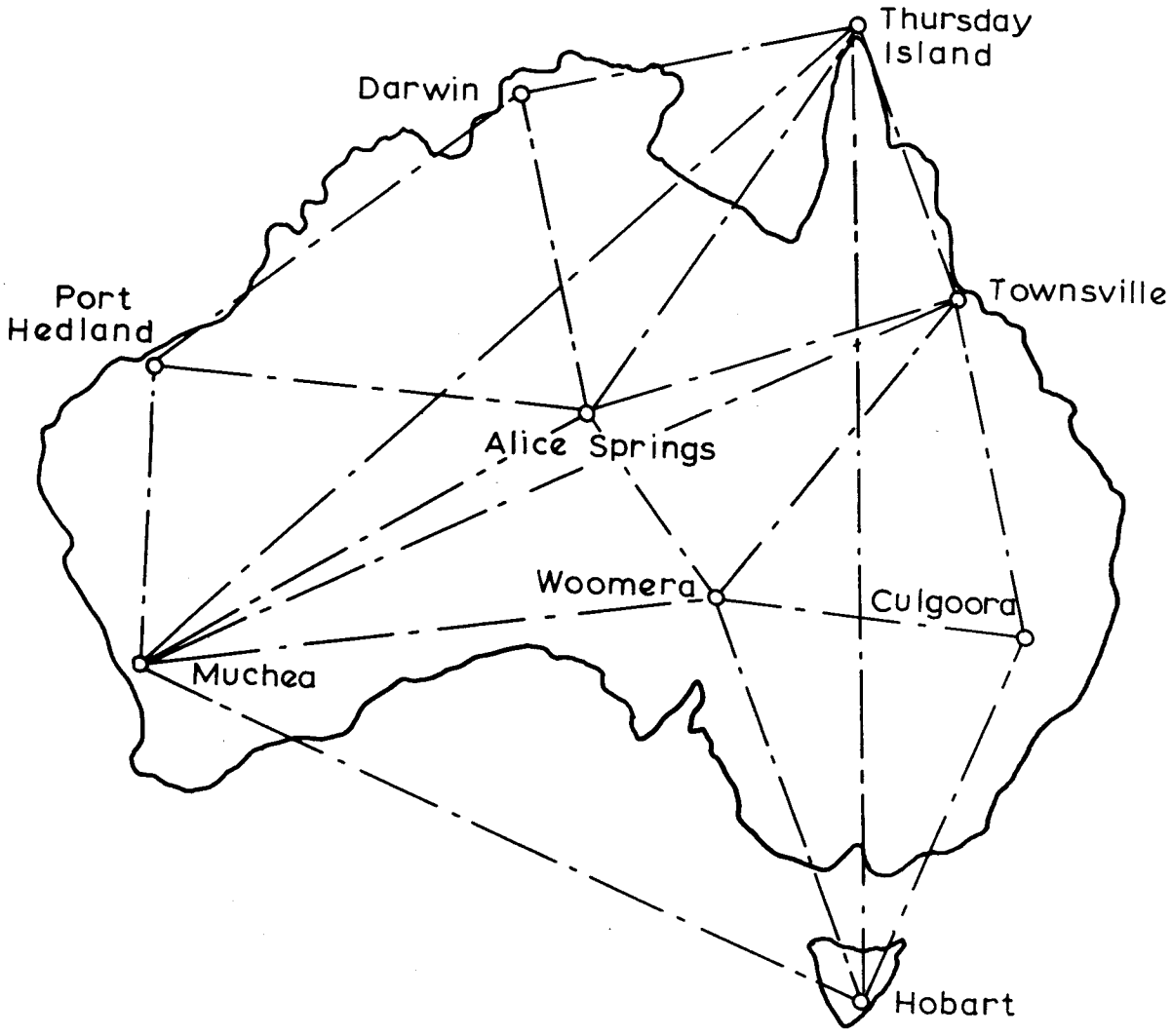
Thursday
Island
Darwin
Port
Hedland
Townsville
Alice Springs
Woomera
Culgoora
Muchea
Hobart

FIGURE 7.8

Line Under Consideration		Distance between Stations	Scale Effect T		Length Error Estimate		Lateral Error Estimate	
		km	m	p.p.m.	m	p.p.m.	sec	p.p.m.
Woomera	- Muchea	1990	-4.5	-2.3	1.2	0.52	1.4	13.4
	- Townsville	1670	8.7	5.2	1.1	0.63	1.3	10.3
	- Culgoora	1260	4.1	3.3	0.9	0.73	1.1	6.7
	- Hobart	1590	0.6	0.4	1.0	0.65	1.2	9.5
	-Alice Springs	920	2.1	2.3	0.8	0.85	0.9	4.2
Muchea	-Port Hedland	1280	-4.6	-3.6	0.9	0.73	1.1	6.9
	- Thursday Is	3630	9.2	2.6	1.5	0.43	1.9	33.0
	- Townsville	3430	5.4	1.6	1.5	0.44	1.8	30.3
	- Hobart	3100	-8.9	-2.9	1.4	0.46	1.7	26.0
	-Alice Springs	2000	-2.8	-1.4	1.2	0.58	1.4	13.5
Port Hedland	-Alice Springs	1600	1.9	1.2	1.0	0.65	1.2	9.7
	- Darwin	1560	4.8	2.7	1.0	0.66	1.2	9.2
Darwin	- Thursday Is	1300	11.5	8.9	0.9	0.72	1.1	7.2
	-Alice Springs	1280	6.3	4.9	0.9	0.73	1.1	6.9
Thursday Is	-Alice Springs	1700	12.5	7.3	1.0	0.63	1.3	10.6
	- Hobart	3600	19.8	5.5	1.5	0.43	1.9	32.4
	- Townsville	1080	11.1	10.1	0.8	0.80	1.0	5.3
Townsville	- Culgoora	1280	9.4	7.3	0.9	0.73	1.1	6.9
	-Alice Springs	1430	9.0	6.3	1.0	0.69	1.2	8.2
Culgoora	- Hobart	1370	3.1	2.3	1.0	0.70	1.2	7.7

TABLE 7.3

Geocentric orientation parameters used in equation (7.43) for the above calculations were $\Delta\xi_o$ = -4.65 sec, $\Delta\eta_o$ = -4.40 sec, ΔN_o =14.0 m.

spheroid in the Australian region. The free air geoid solution for Australia does not extend to Hobart or Thursday Island, but it has been assumed that its sloping trends will continue unaltered to these points. While this assumption will not be exactly correct, it is unlikely that the scale error estimates in Table 7.3 would be incorrect by more than one part per million due to this cause.

A consideration of Table 7.3 reveals some interesting features. For the network as outlined, scale errors ranging from - 3 to + 10 parts per million would exist if the control station co-ordinates were not corrected by the application of the geocentred orientation parameters for Johnston Origin. In every case, the scale error exceeds the size of the expected error propagated from two-way tellurometer traversing at a station spacing of 30 km.

Table 7.3 shows that the azimuth between two control stations separated by more than 1000 km can be obtained more precisely from a calculation involving astronomical co-ordinates than by being "carried" by the traverse. In practice, the azimuth would be computed from the nationally adjusted co-ordinate values of the control stations involved, but for the purpose of this Chapter, the above discussion is valid.

The scale effect over long lines only has been investigated in Table 7.3 and the use of equation (7.43) to do this has been justified. For short distances, the only consideration necessary is the magnitude of $\frac{N}{R}$. Over a triangulation baseline of length 8 to 20 km, the mid-point value of N may be used to calculate the scale effect without

THE SCALE EFFECT FOR HYPOTHETICAL TRIANGULATION BASELINES IN AUSTRALIA

State	Baseline Co-ordinates		Scale Effect
	Latitude	Longitude	(p.p.m.)
New South Wales	-32°N	146°E	3.8
Queensland	-23°N	144°E	7.9
South Australia	-29°N	135°E	1.9
Western Australia	-26°N	122°E	-0.7
Victoria	-37°N	145°E	2.3
Northern Territory	-21°N	134°E	5.0

TABLE 7.4

the introduction of significant error. This procedure has been adopted for Table 7.4 where the scale effects for hypothetical baselines in each state of Australia are shown. Baselines such as these do not actually exist, Table 7.4 was intended to illustrate the magnitudes of the scale effect that would be introduced into a geodetic control network based on triangulation in the Australian region if the existence of the geoid geocentred spheroid slope was ignored. The Australian Geodetic Datum has been scaled from the vast lengths of tellurometer traverse which run through every chain of the old triangulation scheme *(Bomford, 1969)*. The Australian network is based on a reference spheroid which has been oriented approximately parallel to the geoid slope in the Australian region and therefore the comments in this Chapter are not directly applicable.

If a geodetic control network was established using the baselines shown in Table 7.4, the scale errors, which in this case are relative to a geocentred reference system, would not be detected when the control was carried from baseline to baseline. The use of orthometric heights for the reduction of all distances will preclude the detection of the scale errors. No indications of a sloping geoid will be found as all measurements and calculations will have been made relative to the geoid. Only connections to other geocentred continental datums where spheroidal lengths have been used will show the existence of the geoid slope.

This Chapter has presented, in effect, a case for the establish-

ment of gravimetric geoid determinations over the regions covered by the major geodetic control networks of the earth, using as illustration, the situation in Australia *if* the geoid geocentred spheroid separation had been neglected.

CHAPTER 8

CONCLUSIONS.

8.1 The Free Air and Astro-geodetic Geoids in Australia.

The free air geoid was defined in Chapter 1. In Chapter 4 a description of its calculation in Australia from the gravimetric data available in 1968 was presented. In 1970 a recalculation of the free air geoid in Australia *(Mather, 1970a)* showed that the regions delineated as being of lower precision in the former solution have had their gravity anomaly fields strengthened to a considerable degree. The new geocentric orientation parameters for the Johnston Origin differ slightly from those obtained from the 1968 solution (equation (5.1)). A zero order term for ΔN_o has been included based on the value of the global mean free air anomaly obtained from a composite set of gravity anomaly data consisting of an amended version of the Rapp *(1968)* data set and the terrestrial gravity anomaly data held at the University of N.S.W. *(ibid, p.85)*. The Australian region is a very favourable one to perform calculations of the free air geoid as a dense terrestrial gravimetric coverage on a 0.1^o grid basis is available.

Comparisons with astro-geodetic deflections of the vertical and an astro-geodetic geoid solution have shown that the free air geoid for Australia is an excellent approximation of the geoid itself in this region. The number of Laplace stations on the Australian Geodetic Datum has been increased from approximately 600 in

1966 to 1200 in early 1970 with this figure expected to rise by another 300 by early 1971. A revision of the preliminary astro-geodetic geoid for Australia *(Fischer and Slutsky, 1967)* will be undertaken by the Australian Commonwealth's Division of National Mapping in 1970. This revised astro-geodetic geoid determination should be able to discriminate small geoid fluctuations to a finer extent than was possible with the 1967 solution.

The reliability of the 1970 free air geoid solution has improved to the extent that the standard deviations of the residuals of the original observation equations, upon back substitution of the geocentric orientation parameters, reduced in magnitude when the inner zone effects of the free air geoid solution were omitted from comparisons with the Fischer/Slutsky astro-geodetic geoid. This indicates that the latter is over-smoothened, which is not surprising when the station density of one per 12,000 km^2 is considered. The 1968 free air geoid solution was insufficiently precise to detect this effect, with the result that an estimated standard deviation of ± 1 metre for the 1967 astro-geodetic geoid solution in Chapters 4 and 5 was considered to be valid in most regions.

The lack of observed values of gravity anomalies in the ocean areas surrounding the Australian continent is the major factor preventing improved free air geoid determinations in Australia. The exact nature of the deflections of the vertical in limited regions, especially mountainous regions, is incompletely understood at present.

The Snowy Mountains regions of the Great Dividing Range on the eastern coastline of Australia would be an interesting location for an exacting study of this type, but the weak gravity fields in the nearby Pacific Ocean and Tasman Sea would significantly limit the investigations. It is believed that the Australian Bureau of Mineral Resources will strengthen the paucity of observed gravity data in this region in the near future but until such time any investigations of the nature described above must be considered preliminary. A dense coverage of astro-geodetic stations in the high mountainous regions of Australia would also be a prerequisite to allied studies.

8.2 The Indirect Effect.

The indirect effect for the free air geoid has been formulated and estimations calculated on global and continental bases in Chapter 6. All co-geoids will have an indirect effect which will consist of a potential dependent term (non-Stokesian in character), a Stokesian term and a zero order effect. The free air geoid is generally held to be the best approximation to the geoid itself and the only co-geoid of fundamental geodetic significance *(e.g. Mather, 1968b, p.45)*. The magnitude of its indirect effect is therefore generally held to be comparatively small.

For the case of Australia the above statement appears to be valid, the calculations in Chapter 6 showing that the indirect effect does not possess a variation of more than 1 metre across the continent.

The geocentric orientation parameters for the Johnston Origin of the Australian Geodetic Datum did not significantly alter when the indirect effect was added to the 1968 free air geoid. It has been preliminarily concluded that the 1968 free air and the Fischer/Slutsky astro-geodetic geoid solutions in Australia are not accurate enough to detect any small improvements arising from the addition of the indirect effect.

The estimate of the global indirect effect (figure (6.24)) displays variations which are much larger in magnitude than those that were originally expected. The close agreement of the free air and astro-geodetic geoids in Australia and the small indirect effect in this region do not, in themselves, provide sufficient evidence to conclude that the global estimation of the indirect effect is correct. Australia only represents 1½% of the total surface area of the earth and to extrapolate from studies in this area is unwise. The global solution does indicate that Australia lies in the region of minimum indirect effect gradient, a fact which also neither proves nor disproves the existence of the magnitudes of the global indirect effect variations.

Very few serious attempts at global estimation of the indirect effect have been undertaken, probably because geodesists have considered its evaluation unwarranted in view of the limited free air geoid studies of continental extents which have been performed. Pellinen *(1962)* obtained values of a terrain correction in the mountainous regions of the Alps, the Caucasus and the Himalayas and used

these values to forecast values for other regions. He obtained a 3,3 spherical harmonic analysis of these terrain corrections which, while showing the same general trends, is considerably smaller in magnitude than the spherical harmonic analysis of the global estimates of Δg_c derived in Chapter 6. The smoothened topographical approach used by Pellinen was shown in Chapter 6 to lead to an underestimation of the differential terrain correction whose magnitude is considerably influenced by the near zone undulating topography.

The exact calculation of both the Stokesian and non-Stokesian terms in the indirect effect requires a very precise global height data set. A significant improvement to the estimate of the indirect effect computed in this thesis would involve the preparation of a $0.1^{\circ} \times 0.1^{\circ}$ height data set on a global basis. Modern automatic photogrammetric plotters have a facility for digital readout of topographic height, so the preparation of such a data set would not be an overwhelming task for a large mapping organisation.

The technique developed in Chapter 6 for the global differential terrain correction estimates was shown to have a serious defect along the escarpments of high mountainous regions. This defect is not, however, the major cause of the large magnitude of the global Stokesian term shown in figure (6.23). The large mountainous regions of the world are so situated with respect to one another that the Stokesian contributions from these regions globally complement one another to produce the variation pattern in figure (6.23). The non-Stokesian

term complements the Stokesian variations to a considerable degree in the Asian and American regions. Across Australia it has the effect of reducing the magnitude of the Stokesian term variation.

The only check on the non-Stokesian term was provided from the consideration of the isostatically compensated (Airy-Heiskanen model) topographic block of dimensions similar to those of the Himalayas. This check had several limitations but the results indicate that the approximations made for the calculation of the non-Stokesian term did not introduce gross errors into its evaluation.

The implications of the adoption of the zero order term of the indirect effect with respect to the adopted values of a, f and kM for Reference System 1967 were reviewed in Section 6.7. The purpose of the global indirect effect estimation was not to revise these values although the calculations presented could form a basis for such a revision.

An estimation of the global geoid solution (figure (6.25)) was obtained from the addition of figure (6.24) and the free air geoid solution of Rapp *(1969)*. The inclusion of the indirect effect has smoothened most of the regions of extreme high and low values shown on the global free air geoid solution by approximately 10 metres. The magnitude of the geoid surface gradient has generally been reduced, although the basic trends remain unaltered. The geodetic and geophysical significance of this is a matter of conjecture, and

as the prime objective for obtaining the global indirect effect estimate in this thesis was to assist an evaluation of the indirect effect in Australia, the matter will not be further discussed.

8.3 The Application of the Geoid to Geodetic Control Networks.

The Australian Geodetic Datum has been discussed in several sections of this thesis, notably in Chapter 3 where a critical study of the National Mapping Council Resolution 293 which aligned the Australian National Spheroid parallel to an approximation of the mean geoid position in Australia was presented. In Chapter 7 an analysis of the tellurometer traverse loop misclosures resulted in the formulation of error estimates for electro-magnetic distance measuring devices which it is felt can be used in other contexts with a reasonable degree of reliability.

The free air and astro-geodetic geoids in the region of the Australian Geodetic Datum have been discussed in Section 8.1. The indirect effect for the free air geoid in Australia (Section 8.2) has been shown to possess a variation of less than 1 metre. The addition of the indirect effect to the 1968 free air geoid in Australia did not change the values of the geocentric orientation parameters $\Delta\xi_o$ and $\Delta\eta_o$ displayed in equation (5.1). A zero order term in ΔN_o will result from the adoption of the Australian and global indirect effect solutions.

The effect of neglect of the geoid in the reduction of measured

distances to assumed spheroid level was illustrated in Chapter 7. If control station co-ordinate values on the Australian Geodetic Datum are considered as referring to a geocentred reference spheroid, errors several times the magnitude of the relative positional error between these control stations may be introduced into distances for geodetic and satellite tracking baselines. For the purpose of intercontinental satellite triangulation, the adoption of geocentric orientation parameters as a means for referring control station co-ordinates to an international geocentred reference figure is recommended.

ACKNOWLEDGMENTS

Astro-geodetic data used in this investigation was provided by courtesy of Mr. A. G. Bomford of the Division of National Mapping.

The 1968 free air geoid values were provided by courtesy of Dr. R. S. Mather, to whom the author is also indebted for supervision and assistance during the preparation of this thesis.

The assistance of several members of the School of Surveying at the University of New South Wales, notably Professor P. V. Angus-Leppan and Messrs G. G. Bennett and A. J. Robinson is gratefully acknowledged.

BIBLIOGRAPHY

ALLMAN, J.S., 1967 Least Squares Adjustment of Observations, a paper presented to Colloquium on Control for Mapping, Univ. of N.S.W.

ATLAS ANTARKTIKI, 1, 1966 Academy of Sciences, U.S.S.R., Moscow and Leningrad.

AYRES, F.M., 1962 Matrices, Schaum.

BARLOW, B.C., 1967a Gravity Meter Calibration Ranges in Australia, *Rep. 122, Bureau of Mineral Resources, Geology and Geophysics.*

BARLOW, B.C., 1967b National Report on Gravity in Australia, January 1963 - December 1966.

BOBROFF, O.J., 1968 Australian Experience with Tellurometer MRA 4, a paper presented to Conference on Electronic Distance Measurement, Univ. of N.S.W.,Nov. 1968.

BOMFORD, A.G., 1963a Small Corrections to Astronomic Observations, *Div. Nat. Mapping, Tech. Rep. 1.*

BOMFORD, A.G., 1963b Woomera Geoid Surveys, *Div. Nat. Mapping, Tech. Rep. 3.*

BOMFORD, A.G., 1963c The Geodetic Adjustment of Australia, Progress to June, 1963, reprinted in *Aust. Surv.*, June, 1964.

BOMFORD, A.G., 1965 Astronomical Observations with the Kern DKM 3a and Wild T 3 Theodolites, *Div. Nat. Mapping, Tech. Rep. 4.*

BOMFORD, A.G., 1967a The Geodetic Adjustment of Australia, 1963 - 1966, *Surv. Rev.* 144, 52-71.

BOMFORD, A.G., 1967b Varycord - A Fortran Program for the Least Squares Adjustment of Horizontal Control Surveys. *Div. Nat. Mapping, Tech. Rep. 6,* Canberra, A.C.T.

BOMFORD, A.G., Private Communication.
1969

BOMFORD, G., Geodesy, Oxford Uni. Press, 2nd Ed.
1962

CLARK, D., Plane and Geodetic Surveying, Vols. I and II, 4th Edit.,
1964 Constable and Co., Ltd.

COOK, A.H., A Note on the Errors involved in the Calculation of
1951 Elevations of the Geoid. *Proc.R.Soc.* A.208, 133-141.

COOK, A.H., A Note on the Geodetic Use of Gravity Measurements,
1962 *Bull. Geod. 63,* March, 1962.

COOK, A.H., On the Determination of the Even Zonal Harmonics in
1965 the External Gravitational Potential of the Earth.
Geophys. J.R. astr. Soc. 10, 181-209.

DE WITTE, L., On the Derivation and the Properties of Stokes'
1965 Gravity Formula, *Geoph. J.* 11, 1966, 453-476.

DIRECTOR OF NATIONAL MAPPING, Main Resolutions Adopted During
1965 Period 1945 - 1965, Canberra, A.C.T. (NMP/65/131).

DIVISION OF NATIONAL MAPPING, National Report to the International
1967 Association of Geodesy, 1963 to 1966, Canberra, A.C.T.

FISCHER, I., An Astro-geodetic World Datum from Geoidal Heights
1960 Based on the Flattening f = 1/298·3, *J. Geoph. Res.*
65, 7, July, 1960, 2067-76.

FISCHER, I., A Revision of the Geoid Map of North America,
1966 *J. Geoph. Res.* 71, 20, Oct. 1966, 4905-8.

FISCHER, I., and SLUTSKY, M., A Preliminary Geoid Chart of
1967 Australia, *Aust. Surv.*, Dec., 1967, 327-331.

FRICKE, W., et.al., Report to the Executive Committee of the Work-
1965 ing Group on the System of Astronomical Constants,
Bull. Geod. 75, 59-67.

FRYER, J.G., 1970 Geodetic Application of Gravimetry, a paper presented to the 13th Annual Survey Congress, Adelaide, April, 1970.

FURBER, T.F., 1898 The Trigonometrical Survey of New South Wales, with mention of similar surveys in other Australian Colonies, *Aust. Assoc. Adv. Sci.* Vol. VII, 176-237.

GAZETTE, 1966 Australian Commonwealth Gazette, 84, 6th Oct. 1966.

HEISKANEN, W.A., and MORITZ, H., 1967 Physical Geodesy, Freeman.

HEISKANEN, W.A., and VENING MEINESZ, F.A., 1958 The Earth and its Gravity Field, McGraw-Hill.

HIRVONEN, R.A., 1956 On the Precision of the Gravimetric Determination of the Geoid. *Trans. A.G.U.* 37, 1-8.

HIRVONEN, R.A., 1960 New Theory of the Gravimetric Geodesy. *Ann. Acad. Scien. Fenn.* A III, 56.

HODGES, D.J., 1969 Errors in Geodimeter Measurements and a Method for Increased Accuracy, a paper presented to 12th Survey Congress, Melbourne, March, 1969.

HUNTER, J. DE GRAAFF, 1966 Earth Shape Studies and Relevant Assumptions, *Bol. de. Uni. Fed. do Parana, Geodesia,* 10, 1966.

I.A.G., 1967 Resolutions Adopted at the General Assembly, International Association of Geodesy, Lucerne, *Bull. Geod.* 86, 367-383.

JOHNSON, H.A., 1964 Geodetic Surveys Through the Australian Sandridges, *Aust. Surv.* Sept. 1964, 157-184.

KAULA, W.M., 1966 Tests and Combination of Satellite Determinations of the Gravity Field with Gravimetry, *J. Geophys. Res.* 71, 5303-5314.

LAMB, H., 1940 Infinitesimal Calculus, Camb. Univ. Press.

LAMBECK, K., 1968a Geodesy and Artificial Earth Satellites, *Aust. Surv.*, June, 1968, 113-121.

LAMBECK, K., 1968b A Hypothetical Application of the Geometric Method of Satellite Geodesy, *Aust. Surv.* Dec., 1968, 281-309.

LAMBERT, B.P., 1962 A Figure of the Earth for Australia, *Aust. Assoc. Adv. Sci.*, reprinted *Aust. Surv.* Sept., 1962, 178-185.

LAMBERT, B.P., 1968 The Johnston Geodetic Survey Station, *Aust. Surv.* 22, 93-96.

LAW, P., 1965 Geography in the Antarctic, The Griffen Taylor Memorial Lecture, July, 1965, Univ. of Sydney, reprinted in the *Aust. Geographer*, March, 1967.

LEE, W.H.K., and KAULA, W.M., 1966 A Spherical Harmonic Analysis of the Earth's Topography. *J. Geoph. Res.* 72, 2, Jan., 1967, 753-758.

MATHER, R.S., 1967 The Extension of the Gravity Field in South Australia. *Oster. z.f. Vermessungswesen 25*, 126-138.

MATHER, R.S. 1968a The Free Air Geoid in South Australia and its Relation to the Equipotential Surfaces of the Earth's Gravitational Field. *Univ. of N.S.W., Unisurv. Rep. 6.*

MATHER, R.S., 1968b The Non-Regularised Geoid and its Relation to the Telluroid and Regularised Geoids, *Univ. of N.S.W., Unisurv. Rep. 11.*

MATHER, R.S., 1968c The Formula for Normal Gravity in Geodetic Calculations, *Surv. Rev.* 150, 341-348.

MATHER, R.S., 1969 The Free Air Geoid for Australia from Gravity Data Available in 1968. *Univ. of N.S.W., Unisurv. Rep. 13.*

MATHER, R.S., 1970a The Australian Geodetic Datum in Earth Space, *Univ. of N.S.W., Unisurv. Rep. 19.*

MATHER, R.S., 1970b The Harmonic Representation of the Disturbing Potential, to be published, possibly *Bull. Geod.*

MATHER, R.S. and FRYER, J.G., 1970a Orientation of the Australian Geodetic Datum, *Aust. Surv.*, 23, 1, March, 1970, 1-10.

MATHER, R.S. and FRYER, J.G., 1970b Geoidal Studies in Australia, *Surv. Rev.*, XX, 156, April, 1970.

MOLODENSKII, M.S., et.al., 1962 Methods for Study of the External Gravitational Field and Figure of the Earth. Israel Program for Scientific Translations.

MORITZ, H., 1965 The Boundary Value Problem of Physical Geodesy, *Ann. Acad. Scien. Fenn.* A III, 83.

MORITZ, H., 1968a On the Use of the Terrain Correction in Solving Molodensky's Problem. *Dept. of Geodetic Science, Ohio, Rep. 108.*

MORITZ, H., 1968b On the Computation of the Deflections of the Vertical, *Bol. de Geof. Teo. ed. Applicata.*, Vol. X, 40, 326-331.

PELLINEN, L.P., 1962 Accounting for Topography in the Calculation of Quasigeoidal Heights and Plumb-line Deflections from Gravity Anomalies, *Bull. Geod. 63,* 57-66.

PELLINEN, L.P., and DEMYANOV, G.V., 1969 Quasigeoidal Heights Accuracy and Possibilities of Known Geocentric Distances Application in Geodetic Satellite Networks Processing, a paper presented to the Joint Symposium re Satellite Triangulation, Paris, February, 1969.

RAPP, R.H., 1968 Comparison of Two Methods for the Combination of Satellite and Gravimetric Data. *Dept. of Geodetic Science, Rep. 113, Ohio State Univ.*

RAPP, R.H., 1969 The Geopotential to (14,14) from a Combination of Satellite and Gravimetric Data, *Bull. Geod.* 91, 47-80.

ROBINSON, A.J., Private Communication.
1968

ST. JOHN, V.P., Gravity Anomalies in New Guinea, Ph.D Thesis, Univ.
1967 of Tasmania.

SAZONOV, A.Z., Accuracy of Elements of Astro-geodetic Network of
1969 the U.S.S.R., a paper presented to the Joint Symposium re Satellite Triangulation, Paris, February, 1969.

SOLLINS, A.D., Tables for the Computation of Deflections of the
1947 Vertical from Gravity Anomalies, *Bull. Geod. 6*, 279-300.

STOKES, G.G., On the Variation of Gravity at the Surface of the
1849 Earth, *Trans. Camb. Phil. Soc., Math. Phys. 2*, 131-171.

VENING MEINESZ, F.A., New Formulas for Systems of Deflections of the
1950 Plumb Line and Laplace's Theorem, also Changes of Deflections of the Plumb Line brought about by a Change of Reference Ellipsoid, *Bull. Geod.* 15, 33-42 and 43-51.

VINCENTY, T., Transformation of Co-ordinates between Geodetic
1965 Systems, *Surv. Rev.* 137, 128-133.

BIOGRAPHICAL NOTES

JOHN FRYER was educated at the University of New South Wales where he graduated in Surveying with first class honours in 1968 and was awarded the University Medal. He was also awarded the N.S.W. Surveyor's Board medal as the most outstanding student in his class. An Australian Commonwealth Government Post-Graduate Scholarship enabled him to commence work in 1968 on the the effect of the geoid on the Australian Geodetic Network. The results of his research have been submitted for consideration in meeting the requirements for the award of a Ph. D. degree.

Mr. Fryer joins the Commonwealth of Australia's Division of National Mapping on completion of his scholarship to participate in various geodetic survey programs. His principal research interests are problems associated with mapping of the geoid from astro-geodetic data and the evaluation of the indirect effect for the free air geoid.

DEPARTMENT OF SURVEYING - UNIVERSITY OF NEW SOUTH WALES

Kensington. N.S.W. 2033.

Reports from the Department of Surveying, School of Civil Engineering.

* 1. The discrimination of radio time signals in Australia.
G.G. BENNETT *(UNICIV Report No. D-1)*

* 2. A comparator for the accurate measurement of differential barometric pressure.
J.S. ALLMAN *(UNICIV Report No. D-3)*

* 3. The establishment of geodetic gravity networks in South Australia.
R.S. MATHER *(UNICIV Report No. R-17)*

4. The extension of the gravity field in South Australia.
R.S. MATHER *(UNICIV Report No. R-19)*

UNISURV REPORTS.

* 5. An analysis of the reliability of barometric elevations
J.S. ALLMAN *(UNISURV Report No. 5)*

* 6. The free air geoid in South Australia and its relation to the equipotential surfaces of the earth's gravitational field.
R.S. MATHER *(UNISURV Report No. 6)*

* 7. Control for Mapping. (Proceedings of Conference, May 1967).
P.V. ANGUS-LEPPAN, Editor. *(UNISURV Report No. 7)*

* 8. The teaching of field astronomy.
G.G. BENNETT and J.G. FREISLICH *(UNISURV Report No. 8)*

* 9. Photogrammetric pointing accuracy as a function of properties of the visual image.
J.C. TRINDER *(UNISURV Report No. 9)*

* 10. An experimental determination of refraction over an icefield.
P.V. ANGUS-LEPPAN *(UNISURV Report No. 10)*

11. The non-regularised geoid and its relation to the telluroid and regularised geoids.
R.S. MATHER *(UNISURV Report No. 11)*

12. The least squares adjustment of gyro-theodolite observations.
G.G. BENNETT *(UNISURV Report No. 12)*

13. The free air geoid for Australia from gravity data available in 1968.
R.S. MATHER *(UNISURV Report No. 13)*

* Out of print

14. Verification of geoidal solutions by the adjustment of control networks using geocentric cartesian coordinate systems.
R.S. MATHER *(UNISURV Report No. 14)*

15. New methods of observation with the Wild GAKI gyro-theodolite.
G.G. BENNETT *(UNISURV Report No. 15)*

16. Theoretical and practical study of a gyroscopic attachment for a theodolite.
G.G. BENNETT *(UNISURV Report No. 16)*

17. Accuracy of monocular pointing to blurred photogrammetric signals.
J.C. TRINDER *(UNISURV Report No. 17)*

18. The computation of three-dimensional cartesian coordinates of terrestrial networks by the use of local astronomic vector systems
A. STOLZ *(UNISURV Report No. 18)*

19. The Australian geodetic datum in earth space.
R.S. MATHER *(UNISURV Report No. 19)*